



# UNIVERSITÀ DEGLI STUDI DI MILANO

Doctorate in Pharmacological, Experimental and Clinical Sciences  
Department of Pharmacological and Biomolecular Sciences  
Cycle XXXI

PhD Thesis

**Understanding the Early Stages of Alzheimer's Disease  
Pathogenesis: CAP2 as a Link Between Spine  
Dysmorphogenesis and the Amyloid Cascade.**

BIO/14

Lina Lorna Josefien Vandermeulen  
Student number: R11497

*Tutor: Prof. Monica Di Luca*  
*Co-Tutor: Prof. Elena Marcello*  
*Coordinator: Prof. Alberico L. Catapano*

Academic Year 2017-2018

# Understanding the Early Stages of Alzheimer’s Disease Pathogenesis: CAP2 as a Link Between Spine Dysmorphogenesis and the Amyloid Cascade.

ABSTRACT .....	5
INTRODUCTION .....	11
<b>1.) ALZHEIMER’S DISEASE .....</b>	<b>12</b>
1.1.) ALZHEIMER’S DISEASE CLINICAL SYMPTOMS AND NEUROPATHOLOGICAL HALLMARKS .....	12
1.2.) ALZHEIMER’S DISEASE PATHOGENESIS: THE AMYLOID CASCADE HYPOTHESIS .....	14
1.3.) ALZHEIMER’S DISEASE AS A SYNAPTOPATHY .....	18
1.3)1. <i>What is a dendritic spine?</i> .....	19
1.3)2. <i>The post synaptic density</i> .....	21
1.3)3. <i>The spinoskeleton</i> .....	26
1.3)4. <i>Synaptic Plasticity</i> .....	28
1.3)5. <i>Synaptic Dysfunction in AD</i> .....	32
1.4.) AD MICE MODELS.....	34
<b>2.) ADAM10.....</b>	<b>37</b>
2.1.) WHAT IS ADAM10?.....	37
2.2.) WHAT ARE THE SUBSTRATES OF ADAM10? .....	39
2.3.) ADAM10 ACTIVITY REGULATION BY INTRACELLULAR TRAFFICKING.....	41
2.4.) ADAM10 IN AD.....	42
<b>3.) CYCLASE-ASSOCIATED PROTEIN FAMILY (CAP).....</b>	<b>43</b>
3.1.) WHAT ARE CAPS?.....	43
3.2.) CAP FUNCTION IN ACTIN DYNAMICS.....	45
3.3.) CAP2.....	49
3.4.) CAP2 IN THE BRAIN.....	50
<b>AIM.....</b>	<b>52</b>
<b>MATERIALS &amp; METHODS.....</b>	<b>57</b>
<b>1.) HUMAN TISSUE.....</b>	<b>58</b>
<b>2.) ANIMALS .....</b>	<b>59</b>
2.1.) PRIMARY HIPPOCAMPAL RAT NEURONS.....	59
2.2.) APPPS1 MICE .....	59
2.3.) CAP2 KO MICE .....	59
<b>3.) PLASMIDS .....</b>	<b>59</b>
<b>4.) CELL CULTURE PREPARATION AND TRANSFECTION. ....</b>	<b>60</b>
<b>5.) IMMUNOCYTOCHEMISTRY.....</b>	<b>60</b>
<b>6.) PROXIMITY LIGATION ASSAY (PLA) .....</b>	<b>61</b>
<b>7.) DIL LABELING FOR SPINE MORPHOLOGY .....</b>	<b>62</b>

8.)	FREE-FLOATING FLUORESCENT IMMUNOHISTOCHEMISTRY (F-IHC)	
	63	
9.)	CELL CULTURE ELECTROPHYSIOLOGY .....	64
10.)	SUBCELLULAR FRACTIONATION AND PURIFICATION OF POST-SYNAPTIC DENSITIES AND TRITON INSOLUBLE POSTSYNAPTIC FRACTIONS	
	64	
11.)	CO-IMMUNOPRECIPITATION ASSAY .....	66
12.)	WESTERN BLOTTING.....	66
13.)	ELISA.....	67
14.)	PRIMARY NEURONAL CULTURE TREATMENT.....	67
14.1.)	AMYLOID BETA.....	67
14.2.)	LONG TERM POTENTIATION .....	68
14.3.)	LONG TERM DEPRESSION.....	68
15.)	CELL-PERMEABLE PEPTIDE TREATMENT.....	68
16.)	ANTIBODY LIST.....	70
17.)	QUANTIFICATION AND STATISTICAL ANALYSIS.....	71
	RESULTS.....	72
1.)	IDENTIFICATION OF THE MOLECULAR DETERMINANTS OF THE CAP2/ADAM10/ACTIN COMPLEXES .....	73
1.1.)	ANALYSIS OF THE REGIONS RESPONSIBLE FOR CAP2/ADAM10 COMPLEX FORMATION.....	73
1.2.)	CAP2 BINDING DOMAIN WITH ACTIN .....	75
1.3.)	THE ACTIN BINDING DOMAIN OF CAP2 IS RELEVANT FOR ADAM10 ENDOCYTOSIS.....	76
2.)	CAP2 AS A NOVEL REGULATOR OF ACTIN DYNAMICS AND SPINE MORPHOLOGY.....	78
2.1.)	CAP2 LOCALIZATION IN THE NEURON.....	78
2.2.)	CAP2 DIMERIZATION MOTIF IS RELEVANT FOR COFILIN ASSOCIATION.....	79
2.3.)	THE LACK OF CAP2 AFFECTS THE SPINE MORPHOLOGY, THE MOLECULAR COMPOSITION OF THE SYNAPSES AND AMYLOID BETA LEVELS <i>IN-VIVO</i> .....	81
3.)	CAP2 AND ACTIVITY-DEPENDENT SYNAPTIC PLASTICITY .....	84
3.1.)	LONG-TERM POTENTIATION TRIGGERS CAP2 DIMERIZATION .....	84
3.2.)	CAP2 ASSOCIATION TO ADAM10 AND ACTIN IS REGULATED BY ACTIVITY-DEPENDENT PLASTICITY.....	87
4.)	AMYLOID B OLIGOMERS AFFECT CAP2 PATHWAY .....	89
4.1.)	CHARACTERIZATION OF Ab1-42 OLIGOMERS EFFECT ON THE SYNAPSE .....	89
4.2.)	Ab OLIGOMERS PROMOTE ADAM10 SYNAPTIC LOCALIZATION WHILE DECREASING CAP2 SYNAPTIC LEVELS.	91
5.)	CAP2 IN ALZHEIMER'S DISEASE .....	95

5.1.)	CAP2 EXPRESSION AND SYNAPTIC LOCALIZATION ARE REDUCED IN AD PATIENTS' HIPPOCAMPI .....	95
5.2.)	CAP2 ASSOCIATION WITH ACTIN IS INCREASED IN AD HIPPOCAMPI .....	97
5.3.)	CAP2 AND ADAM10 SYNAPTIC LEVELS ARE ALTERED IN APP/PS1 MICE HIPPOCAMPI .....	98
5.4.)	CAP2 ASSOCIATION TO ITS BINDING PARTNERS IS ALTERED IN APP/PS1 MICE HIPPOCAMPI.....	101
<b>6.)</b>	<b>POTENTIAL THERAPEUTIC STRATEGIES FOR ALZHEIMER'S DISEASE TARGETING THE CAP2 PATHWAY .....</b>	<b>105</b>
6.1.)	CHARACTERIZATION CAP2 IN APP/PS1 HIPPOCAMPAL NEURONS.....	105
6.2.)	CAP2 OVEREXPRESSION RESCUES PSD-95 LEVELS AND ADAM10 SYNAPTIC LOCALIZATION IN APP/PS1 MICE	107
6.3.)	DEVELOPMENT OF CELL PERMEABLE PEPTIDES TARGETING CAP2/ACTIN INTERACTION .....	109
6.4.)	TESTING CPPs CAPABILITY TO CROSS THE BLOOD-BRAIN BARRIER .....	109
6.5.)	UNCOUPLING CAP2/ACTIN INTERACTION <i>IN VITRO</i> .....	110
6.5)1.	TESTING CPPs EFFICACY.....	110
6.6.)	UNCOUPLING CAP2/ACTIN INTERACTION <i>IN VIVO</i> : ACUTE TREATMENT .....	111
6.6)1.	TESTING CCPs EFFICACY AND SPECIFICITY <i>IN VIVO</i> .....	111
6.7.)	CPPs CAN MODULATE ADAM10 SYNAPTIC LOCALIZATION AND ACTIVITY TOWARDS APP WITHOUT AFFECTING N-CADHERIN SHEDDING.....	113
	<b>DISCUSSION.....</b>	<b>115</b>
	<b>ACKNOWLEDGEMENTS.....</b>	<b>148</b>
	<b>RESEARCH ACTIVITY .....</b>	<b>153</b>



# Abstract

Italian

La malattia di Alzheimer (AD) è caratterizzata da depositi di beta-Amiloide ( $A\beta$ ) e di proteina tau iperfosforilata. L'enzima ADAM10 taglia la Proteina Precursore dell'Amiloide (APP) impedendo la formazione di  $A\beta$ . L'attività e la localizzazione sinaptica di ADAM10 sono modulate da proteine che interagiscono con la coda citoplasmatica di ADAM10. Ciò considerato, abbiamo condotto un "two-hybrid screening" che ha permesso l'identificazione di cyclase-associated protein 2 (CAP2) come nuovo partner di ADAM10. Le CAPs sono proteine che legano l'actina e sono coinvolte in rimodellamento del citoscheletro e trafficking vescicolare in cellule non neuronali. Un'analisi di microarray ha rivelato come in campioni autoptici da pazienti affetti da AD vi sia una riduzione dell'espressione di CAP2. Pertanto, lo scopo del presente progetto è valutare il ruolo del complesso ADAM10/CAP2/actina nella formazione di  $A\beta$  e nella disfunzione sinaptica legata all'AD. I principali risultati di questo progetto indicano che:

- CAP2 è in grado di formare aggregati e di interagire sia con actina che ADAM10
- È nell'ippocampo di topi CAP2 knock-out, i livelli postsinaptici di ADAM10 e della subunità GluN2A del recettore NMDA siano drasticamente ridotti, indicando come possibile causa la mancanza di CAP2. Il complesso CAP2/actina influenza l'endocitosi di ADAM10, perciò la sua modulazione è fondamentale per la localizzazione sinaptica di ADAM10. L'analisi di neuroni ippocampali di topi CAP2 knock-out ha evidenziato un'alterazione della morfologia delle spine dendritiche, indicando come la mancanza di CAP2 possa influenzare la plasticità strutturale dei neuroni. Inoltre abbiamo rilevato un aumento dei livelli di  $A\beta_{1-42}$  nell'ippocampo di topi CAP2 knock-out.
- Per quanto riguarda AD, nei campioni di ippocampo di pazienti affetti da AD, così come nell'ippocampo di un modello murino di AD, è riscontrabile riduzione di CAP2 e la sua localizzazione sinaptica. In aggiunta, il complesso ADAM10/CAP2/actina è alterato in questi stessi campioni.
- CAP2 ha un ruolo importante nei fenomeni di plasticità sinaptica attività-dipendente e nella plasticità aberrante indotta da oligomeri di  $A\beta$ , processi in grado di modificare la localizzazione sinaptica di CAP2 e l'interazione con i suoi partner.

Alla luce di questi risultati, abbiamo disegnato due approcci terapeutici per modulare la via di CAP2. Nel primo caso, abbiamo overespresso CAP2 in un modello in vitro di AD e abbiamo osservato un aumento della localizzazione sinaptica di ADAM10. In secondo luogo, poiché l'interazione CAP2/Actina è aumentata in AD e questo complesso è importante per la localizzazione sinaptica di ADAM10, abbiamo sviluppato dei peptidi permeabili alle cellule (CPP) in grado di interferire con l'interazione CAP2/Actina. Il trattamento con CPP determina un incremento dei livelli sinaptici di ADAM10 e ne aumenta l'attività nei confronti di APP. In conclusione, dal nostro studio emerge come CAP2 sia potenziale target farmacologico per AD.

# Abstract

English

Alzheimer's disease (AD) is pathologically characterized by amyloid beta ( $A\beta$ ) depositions and hyperphosphorylated tau. A disintegrin and metalloproteinase 10 (ADAM10), is responsible for the  $\alpha$ -secretase cleavage of Amyloid Precursor Protein (APP), that prevents  $A\beta$  generation. The synaptic localization and its activity towards APP are modulated by protein partners, which interact with the cytoplasmic tail of ADAM10. Considering this, we performed a two-hybrid screening that identified actin-binding protein "cyclase-associated protein 2" (CAP2) as a novel binding partner of ADAM10. CAPs are implicated in actin cytoskeleton remodelling and vesicle trafficking of non-neuronal cells, and microarray analysis of AD patient hippocampi specimens revealed a down-regulation of CAP2 in AD patients. Therefore, the aim of this project is to evaluate the role of the ADAM10/CAP2/actin complex in the amyloid cascade and in AD-related synaptic dysfunction.

The main results of the project indicate that:

- CAP2 is self-aggregating and interacts with both actin and ADAM10.
- In the hippocampus of CAP2 knockout mice the synaptic levels of ADAM10 and of the NMDA receptor subunit GluN2A are significantly reduced, suggesting that the lack of CAP2 affects their localization. In particular, the CAP2/actin complex is essential for ADAM10 synaptic localization since it is involved in ADAM10 endocytosis. Additionally, we detect an altered spine density and morphology in hippocampal neurons of CAP2 knockout mice, and they show elevated levels of the toxic  $A\beta_{1-42}$  in their hippocampus. These data indicate the relevance of CAP2 in synaptic function and structural plasticity.
- Regarding AD, a reduction in CAP2 protein levels and in its synaptic localization is detected in the hippocampi of AD patients and AD mice. In addition, alterations in the association of CAP2 to actin and ADAM10 are found.
- CAP2 has a role in activity-dependent synaptic plasticity mediated by long-term potentiation, and in aberrant plasticity triggered by  $A\beta$  oligomers, which regulate CAP2 synaptic localization and association to its binding partners.

In light of these results, we designed two potential therapeutic approaches to tackle the CAP2 pathological pathway in AD. First, we overexpressed CAP2 in an in vitro system modeling AD, and we found an increase in ADAM10 synaptic levels after

overexpression of CAP2. Secondly, since the CAP2-actin complex is increased in AD pathogenesis and this complex seems to be important for ADAM10 synaptic localization, we designed a cell-permeable peptide (CPP) to interfere with the CAP2-actin association. The interference by the CPP treatment can affect ADAM10 synaptic levels and increases its activity towards APP.

Overall these data indicate that CAP2 is a potential pharmacological target to increase ADAM10 synaptic localization as a novel AD therapeutic strategy.

# Introduction

## 1.) Alzheimer's Disease

### 1.1.) Alzheimer's disease clinical symptoms and neuropathological hallmarks

Alzheimer's disease (AD) is a progressive neurodegenerative disorder that was initially reported by Alois Alzheimer in 1907<sup>1</sup>. AD is clinically characterized by the gradual loss of memory and cognitive functions, which accounts for the inability to perform daily tasks and learning, eventually leading to dementia and death. The domains that are found to be disturbed include progressive memory impairment, language differences, calculations, orientation and judgment. When two or more of these domains are disrupted AD is considered. The loss in these functions must be of sufficient severity on the normal functioning to diagnose a patient with AD, and still diagnosis is often erratic and final diagnosis can only be confirmed post-mortem with identification of the brain alterations<sup>2</sup>. Additionally, AD is the most prevalent neurodegenerative disorder and the most common form of age-dependent dementia, where AD accounts for approximately 60-70% of the cases of dementia. According to the World Alzheimer Report from 2015, in the global population 46.8 million people suffer from AD or related forms of dementia, where 9.9 million new cases arise every year.

AD is characterized by the accumulation of amyloid beta ( $A\beta$ ) in extracellular senile or neuritic plaques and by hyperphosphorylated tau protein aggregated in intracellular neurofibrillary tangles (NFTs). The plaques and the tangles accumulations in AD start years before the clinical onset of the disease in the so-called preclinical phase of AD<sup>3,4</sup> (Fig. 1).  $A\beta$  peptide is a proteolytic fragment and the product of the cleavage of APP via  $\beta$ -secretase followed by  $\gamma$ -secretase on specific sites<sup>5,6</sup>. The NFTs are accumulations of aggregated hyperphosphorylated tau protein<sup>7</sup>. These two pathological changes are accompanied by inflammation, synaptic dysfunction, progressive loss of neuronal tissue in the brain, starting from the locus coeruleus and then spreads to the hippocampus via the entorhinal cortex<sup>8</sup>. Additionally, synaptic dysfunction is starting after the  $A\beta$  accumulations, but before the Tau-mediated dysfunction (Fig. 1). Where, to conclude, all events together account for the clinical symptoms, like memory loss



and cognitive impairment, which will arise during the mild cognitive impairment phase (MCI), eventually leading to dementia (Fig. 1). Nowadays, the miss-metabolism of the APP gene causing multiple accumulations of the A $\beta$  protein are thought to be the primary driving force of AD development, leading to the “amyloid cascade hypothesis”.

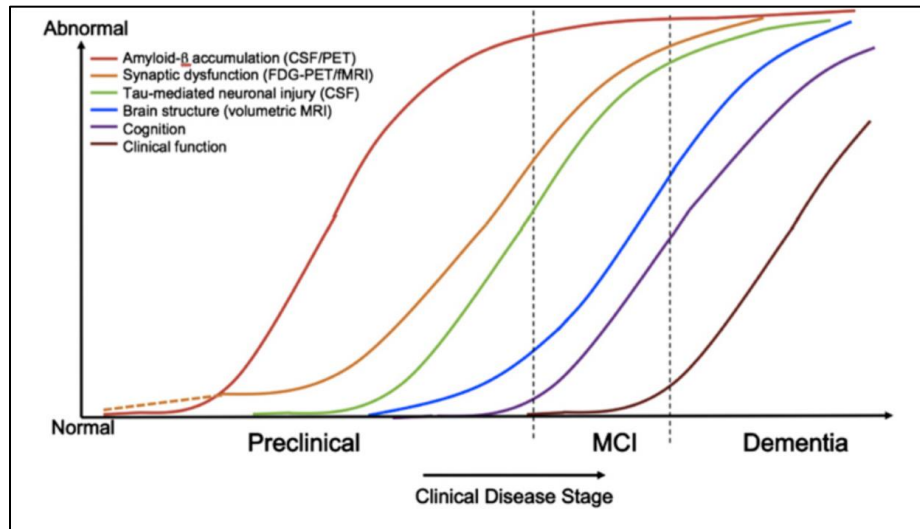


**Figure 1) Dynamic biomarkers of the AD pathological cascade.** A $\beta$  is identified by measuring cerebrospinal fluid (CSF) A $\beta$ 42 or Positron Emission Tomography (PET) amyloid imaging. Tau-mediated neuronal injury and dysfunction is identified by CSF measures of tau or fluorodeoxyglucose-PET. Brain structure is measured by use of structural MRI. MCI=mild cognitive impairment. Obtained from Jack et al. 2010, adjusted by <http://www.acnr.co.uk/2014/06/imaging-presymptomatic-alzheimers-disease/> <sup>9</sup>

There are two forms of AD: the early-onset familial AD (fAD) and the late-onset sporadic variant (sAD). fAD is developed before the age of 65 due to autosomal dominant mutations in the amyloid precursor protein (APP) gene on chromosome 21, presenilin 1 (PSEN1) and presenilin 2 (PSEN2) genes on chromosome 14 and 1 respectively <sup>10</sup>. The fAD form of AD accounts for approximately 5% of the AD cases <sup>11-13</sup>. The more common form of AD is the late-onset AD (sAD), which has an onset after the age of 65, which involves multifactorial risk factors, both genetic and environmental <sup>14</sup>. The most widely recognized genetic risk factor of sAD is the  $\epsilon$ 4 allele of the gene that encodes the apolipoprotein E (ApoE $\epsilon$ 4) <sup>7</sup>. APO $\epsilon$ 4 normally enhances the proteolytic degradation of A $\beta$ , thus increasing its clearance. The APO $\epsilon$ 4 variant however, is not as effective in the degrading of A $\beta$  as the other variants which causes an accumulation of

the protein and its deposition in the form of plaques. When a person carries homozygotic APO $\epsilon$ 4 alleles, the degradation mechanism of A $\beta$  is disrupted and this causes an increase in the A $\beta$  protein levels <sup>15</sup>.

## **1.2.) Alzheimer's disease pathogenesis: the amyloid cascade hypothesis**

The main research outcomes in the field of AD have led to the amyloid cascade hypothesis, which states that A $\beta$  plays a pivotal role in AD pathogenesis. This theory is the most widely accepted in the field <sup>5,16-18</sup>. Additionally, the hypothesis indicates that in AD patients the A $\beta$  accumulations trigger synaptic dysfunction, inflammation, NFTs formation and neuronal loss <sup>4,16,19</sup>. Furthermore, in AD animal models the deposition of A $\beta$  also precedes the tangle formation <sup>20</sup>. This implies that the NFTs formation is a downstream event, as a result of the accumulation of A $\beta$  peptide. The increase in A $\beta$  levels is predominantly caused by an imbalance between the production and clearance of the A $\beta$ -protein <sup>5,16</sup> (Fig. 2). For that reason, the mechanisms balancing the A $\beta$  levels are considered as an essential aspect to keep the brain healthy, whereas when the A $\beta$  concentrations raise, plaques can be formed.

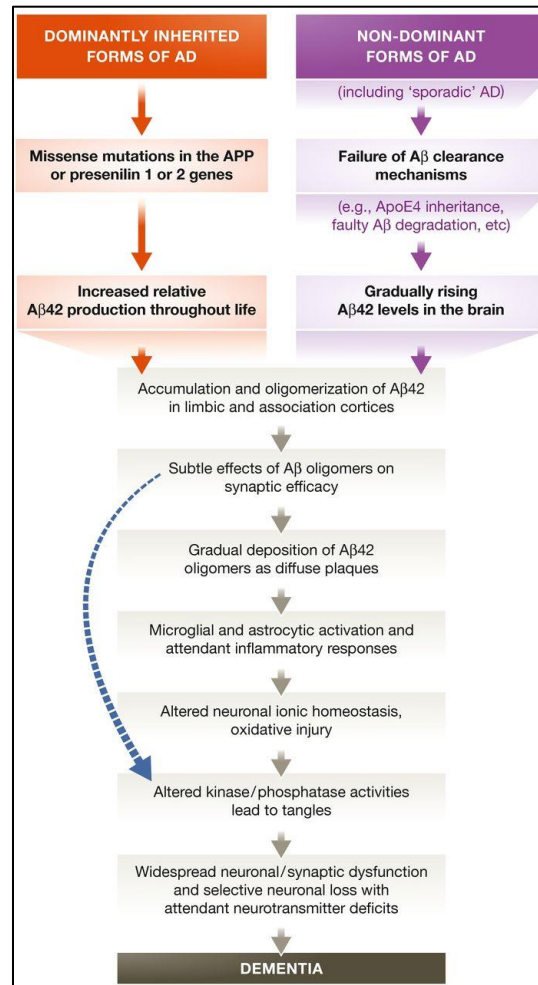
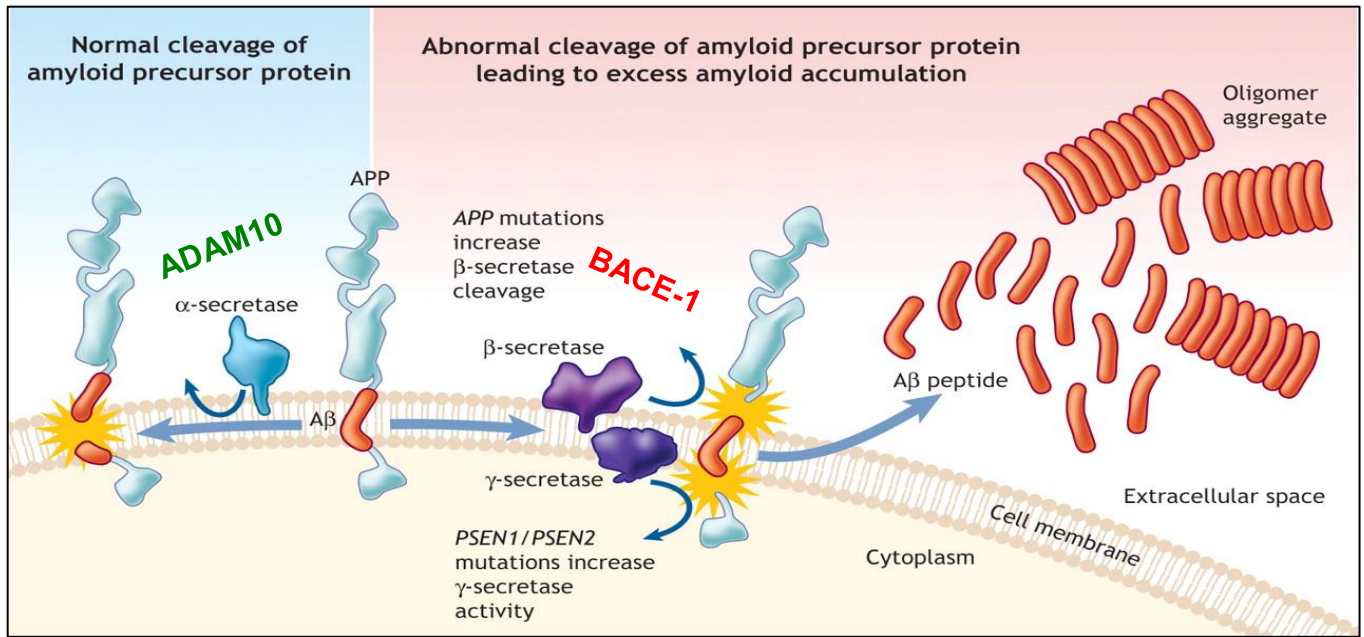


Figure 2) The sequence of major pathogenic events leading to AD proposed by the amyloid cascade hypothesis. Obtained from Selkoe & Hardy 2016<sup>21</sup>.

As described above, Aβ originates from the cleavage of APP by two proteases. The first proteolytic step is the cleavage by the β-secretase, identified as the aspartyl protease β-site APP cleaving enzyme 1 (BACE-1)<sup>6,22,23</sup>. BACE-1 cleaves APP at the N-terminal part of the Aβ domain, thus releasing the C-terminal APP fragment of 99 amino acids (C99), which is then shed by the γ-secretase cleavage, a hetero-tetrameric protease complex of four subunits; (i.e. presenilin, nicastrin, Aph-1 and Pen-2)<sup>24</sup>. Through these cleavages, the sequence of the Aβ peptide will be released in the extracellular space, together with a potential proapoptotic fragment called sAPPβ and the APP intracellular domain (AICD)<sup>25</sup>. Aβ is a 38-42 amino acid long peptide that is hydrophobic and therefore prone to self-aggregate into oligomers and fibrils. The small soluble Aβ

oligomers are the most neurotoxic form that are the cause of the pathological cascade of events causing AD<sup>5,26,27</sup>. The predominant forms of A $\beta$  that are found in AD patients brain tissue are either the 40 or 42 amino acids long structures. The A $\beta$ -42 fragment is found to be the most neurotoxic form<sup>19,28,29</sup> and most likely causes the formation of A $\beta$ -plaques<sup>17</sup>.

Alternatively, APP can be cleaved by the  $\alpha$ -secretase, precluding the formation of A $\beta$ , since the  $\alpha$ -secretase cleavage occurs within the sequence of the A $\beta$ -peptide (Fig. 3). This pathway is also called the non-amyloidogenic pathway, and alongside with the fact that the formation of A $\beta$  peptide is prevented by freeing the C-terminal APP fragment C83, the neurotrophic and neuroprotective sAPP $\alpha$  fragment is released. The C83 fragment is then further cleaved by the  $\gamma$ -secretase, giving rise to the p3 peptide that lacks a part of the A $\beta$  fragment<sup>30-33</sup>. Recent studies demonstrate that, in neuronal cells, this non-amyloidogenic  $\alpha$ -secretase pathway is mediated by 'a disintegrin and metalloproteinase 10' (ADAM10)<sup>34-36</sup>. Several mutations are found in the early onset fAD form. The mutations in the APP gene reduce the  $\alpha$ -secretase cleavage or favor the cleavage by the  $\beta$ -secretase. The other mutations are in the presenilin-1 and presenilin-2 genes (PSEN1 and PSEN2), that are components of the  $\gamma$ -secretase complex. These mutations tend to increase  $\gamma$ -secretase cleavage at position 42 of A $\beta$ , thus increasing the levels of the 42 aminoacid form of the peptide that is more prone to aggregate. This has led to the current view of the A $\beta$  hypothesis that suggests that the soluble oligomers are the key elements which impair synaptic function between neurons. At the same time, the oligomers tend to aggregate into insoluble  $\beta$ -sheet amyloid fibrils, which in their turn can activate a local inflammation response<sup>26</sup>. As time proceeds, these inflammatory oxidative stress responses and biochemical changes will lead to the neuronal death and typical neuritic plaques. Additionally, It has been demonstrated that when A $\beta$  is present at high concentrations in its oligomeric form, it affects glutamatergic synaptic transmission and eventually cause synapse loss<sup>37-40</sup>.



**Figure 3) The amyloid precursor protein (APP) is a transmembrane protein that can undergo a series of proteolytic cleavage steps by secretase enzymes.** When it is cleaved by the  $\alpha$ -secretase (ADAM10) in the middle of the  $\beta$ -amyloid domain ( $A\beta$ ), it is activating the not amyloidogenic pathway, by preventing the production of  $A\beta$ . However, when APP is cleaved by  $\beta$ - (BACE-1) and  $\gamma$ -secretase enzymes, neurotoxic  $A\beta$  peptides are released, which can accumulate into oligomer aggregates and form plaques. Adjusted from Patterson 2008 <sup>41</sup>.

### **1.3.) Alzheimer's disease as a synaptopathy**

The term that is used to define brain disorders that are arising from synaptic dysfunction is 'synaptopathy'. By definition, it includes any sort of perturbation in which aberrant mechanisms contribute to synaptic dysfunction <sup>42</sup>. Since synapses are the most abundant and distinguishing feature of the brain and they are essential for the flow of information throughout the nervous system, it has become evident that synapses are directly disrupted in over one hundred brain disorders. On the one hand, optimal regulation of the activity of synapses is required for a proper brain homeostasis, but on the other hand, subtle but persistent perturbations in the synapse physiology can cause major deficits, which can manifest themselves as brain diseases <sup>43</sup>. During development, but also during adulthood, the adaptations of the number of dendritic spines and their morphology, including synapse formation, maintenance and elimination, allow neuronal circuits to be formed and remodeled. The structural plasticity of spines is tightly related to the functionality of the synapse <sup>44</sup>. It is becoming more evident that synaptic dysfunction is emerging as a major determinant for multiple neurodevelopmental (autism spectrum disorders, Down syndrome and epilepsy) and neurodegenerative disorders, including Parkinson disease and AD, as in these diseases, changes in the number of dendritic spines and their functionality are a key feature (Fig. 4).

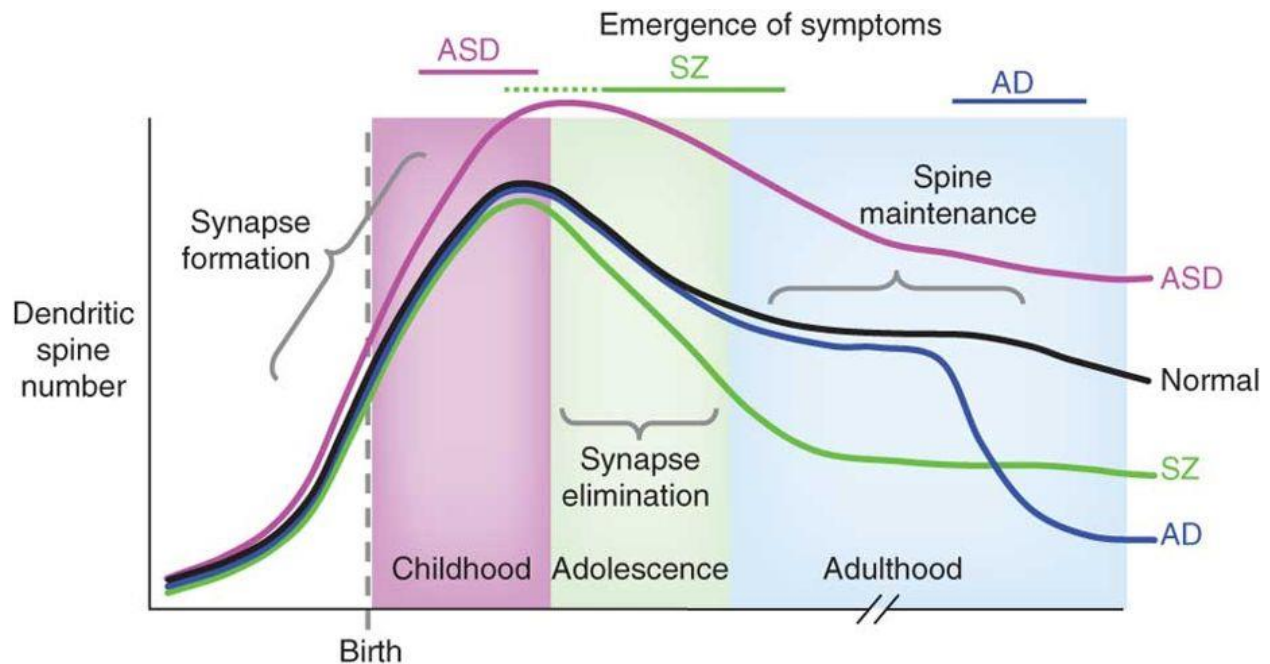


**Figure 4) Putative lifetime trajectory of dendritic spine number in a normal subject (black), in autism spectrum disorder (ASD, pink), in schizophrenia (SZ, green) and in Alzheimer's disease (AD, blue).** Bars across the top are indicating the period of emergence of symptoms and diagnosis. In the normal subjects, spine numbers increase before and after birth; spines are selectively eliminated during childhood and adolescence to adult levels. In ASD, exaggerated spine formation or incomplete pruning may occur in childhood leading to an increased spine number. In schizophrenia, exaggerated spine pruning during late childhood or adolescence may lead to the emergence of symptoms during these periods. In Alzheimer's disease, spines are rapidly lost in late adulthood, suggesting perturbed spine maintenance mechanisms that may underlie cognitive decline. Obtained from Penzes et al. 2011 <sup>44</sup>

### 1.3)1. What is a dendritic spine?

Mammalian neurons communicate through synapses. A synapse is a specialized junction that neurons use to exchange chemical signals with other cells. There are inhibitory and excitatory synapses depending on the neurotransmitter that is released. The neurotransmitter of the excitatory synapse is glutamate, which makes excitatory neurons glutamatergic neurons. The majority of excitatory synapses communicate through contacts between a presynaptic terminal of the axon and postsynaptic sites of dendrites, which receive the input. The post synapses are formed at specialized protrusions called dendritic spines. Dendritic spines are, with their highly complex and dynamic structure, of high importance in plasticity processes and synaptic transmission. In addition, structural or morphological changes of dendritic spines are reflecting the functionality of spines, and the number of spines and their shape are

regulated by both physiological and pathological processes <sup>45</sup>. Therefore, the presence of abnormal dendritic spines has been indicated in several psychiatric and neurological diseases <sup>46</sup>. In the hippocampal CA1 area, these spines have a size of 0,2-2  $\mu\text{m}$  in length, and the spine neck diameter ranges from 0,04-0,5  $\mu\text{m}$ . Additionally, they appear with a density of maximum 10 spines per  $\mu\text{m}$  on the dendritic length of a hippocampal neuron <sup>47,48</sup>. There are multiple spine shapes that vary over a continuum of morphologies from thin to thick-necked, from short to long and from headless to large headed spines. They are characterized according to the classification of Peters and Kaiserman-Abramof into multiple subgroups, namely; stubby, thin and mushroom spines and filopodia <sup>49,50</sup>. The stubby spines are the shortest spine form and they lack a distinctive head/neck configuration. They are seen as the most immature spine form, which is due to the fact that their prevalence is highest during early development and decreases in the adult brain <sup>51</sup>. Thin spines are longer, contain a thin neck, but lack a large bulbous head and have smaller excitatory synapses. Mushroom spines are defined by a large bulbous head with a thin neck and have the largest excitatory synapses. In the mature adult brain over 65% of the spines are thin shaped while 25% of the spines are mushroom shaped <sup>50,51</sup>. Since mushroom spines are thought to have a complete mature shape, they have little range for synaptic strengthening, while newly formed thin spines, that carry immature synapses have a potential for strengthening and play a role in the plasticity of the local circuit. Therefore, mushroom spines can be described as the spines for memory, while thin spines can be the learning spines <sup>52</sup>. The fourth type of spines is the filopodia, which is the smallest structure, described as thin and hair-shaped structures. The immature stubby spines and filopodia take approximately 10% of the spines in the adult brain <sup>50,51,53</sup> (Fig. 5). The function of filopodia is still unknown, but they are the most dynamic spine.



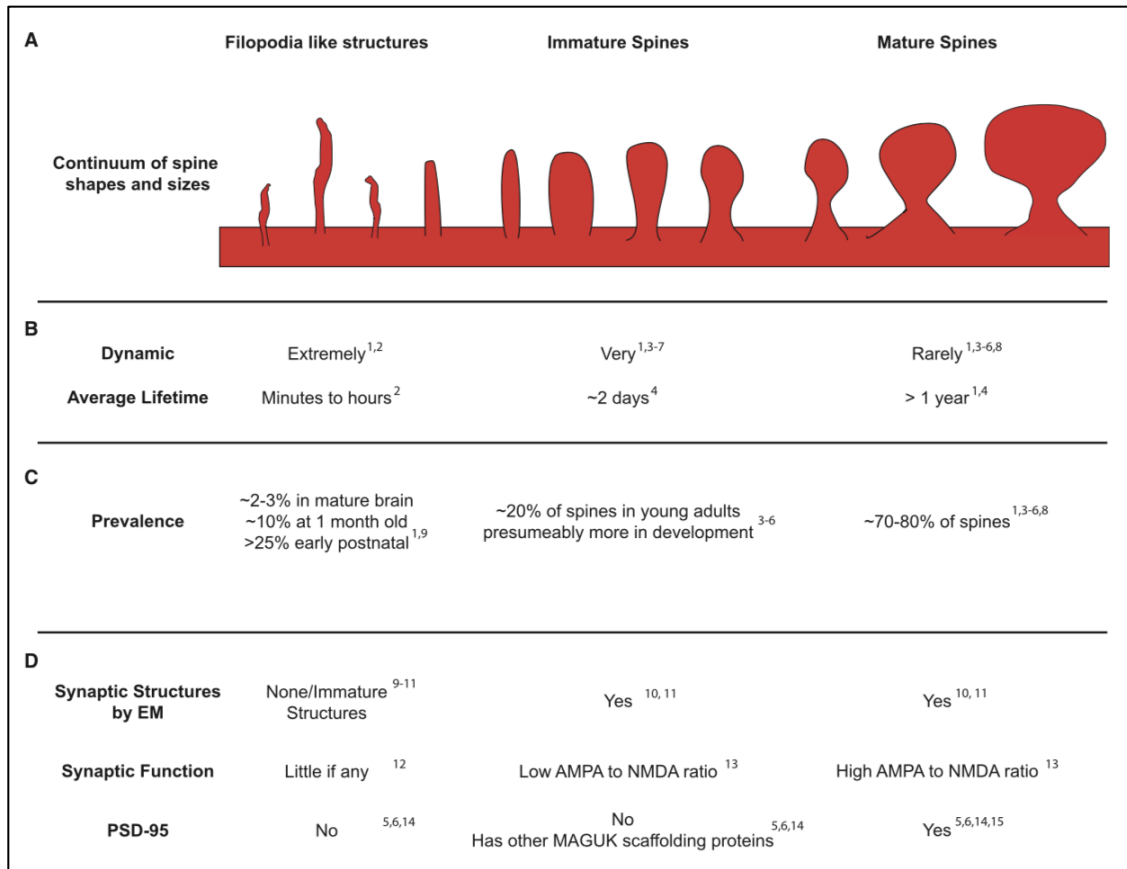


**Figure 5) Spines exist on a continuum of morphologies and related functions from non-functional filopodia-like structures to the large mature spines.** (A) Diagram showing continuum of spine shapes existing on neuronal dendrites. These spines can be grouped into three separate categories, filopodia-like structures, immature spines, and mature spines. Distinguishing between these categories based on morphology is extremely difficult due to the limited resolution of light microscopy, but with some techniques it is possible to distinguish them. (B) The history of a spine can distinguish between these types, where the more mature spine are less dynamic but have a long lifetime. (C) In adults, the majority of spines contain a mature synaptic contact, while 20% are either immature or filopodia like. (D) The three categories of spines are difficult to distinguish based on any one category alone. However, by comparing across several criteria the differences become clearer. Reference keys used in figure: 1) Zuo et al., 2005a; 2) Dunaevsky et al., 1999; 3) Trachtenberg et al., 2002; 4) Holtmaat et al., 2005; 5) Villa et al., 2016; 6) Cane et al., 2014; 7) Majewska and Sur, 2003; (8) Grutzendler et al., 2002; 9) Fiala et al., 1998; 10) Knott et al., 2006; 11) Arellano et al., 2007a; 12) Lohmann et al., 2005; 13) Zito et al., 2009; 14) Lambert et al., 2017; 15) Ehrlich et al., 2007. (Obtained from: Berry & Nedivi 2017<sup>54</sup>)

### 1.3)2. The post synaptic density

In the spine head of excitatory dendritic spines there is a specialized electron-dense web, called the post synaptic density (PSD). In the PSD you can find a high concentration of several hundred proteins, that create a complex structure with a wide range of functions. Some proteins prominently expressed in the PSD are members of the Membrane Associated Guanylate Kinase (MAGUK) or ProSAP/Shank family that

organizes a dense scaffold and creates an interface between clustered membrane-bound receptors and the associated signaling molecules, cell adhesion proteins and an actin-based cytoskeleton. Upon these receptors are the glutamatergic receptors<sup>55,56</sup>. Neuronal activity regulates the morphology and functionality of spines and through this process synaptic transmission and plasticity are controlled<sup>57-59</sup>. Taking advantage of high-resolution electron microscopy and cryo-fixation, it has been shown that a synaptic contact zone is characterized by a presynaptic active zone enriched of synaptic vesicles containing glutamate, a synaptic cleft and a PSD<sup>56,60</sup> (Fig. 6).

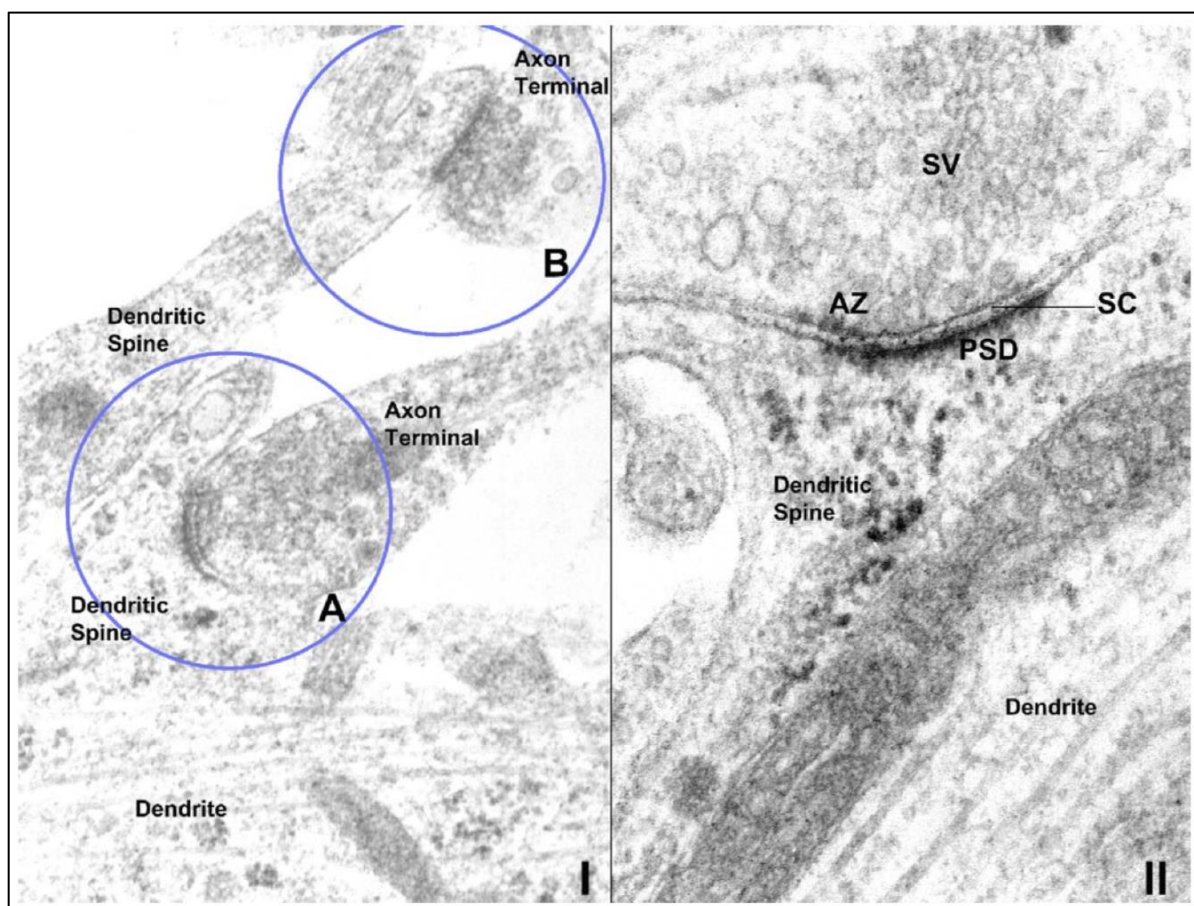


**Figure 6) Ultrastructure of glutamatergic synaptic contacts of hippocampal culture cells.** Hippocampal neurons were fixed 14 days after plating. Left (I) Two type 1 synapses (A, B) with neurotransmitter- filled vesicles lie in the axon terminal. These terminals have the possibility to make contact with protrusions from the dendrite: in this image, one is making a contact with a cup-shaped dendritic spine (A) and the other with a thin spine (B). Right (II) Synaptic ultrastructure at a higher magnification shows the presynaptic axon terminal with vesicles (SV) docked onto the membrane at the active zone region (AZ). The synaptic cleft (SC) is visible between the pre- and postsynaptic membrane. Also the postsynaptic density (PSD) is clearly detectable as an electron-dense thickening of the postsynaptic membrane. The PSD is localized at the tip of a cup- shaped dendritic spine, a small sub compartment of the neuronal dendrite. Scale Synaptic vesicle diameter:50 nm. (Obtained from Boeckers 2006<sup>56</sup>).

## Glutamate Receptors

The surface layer of the PSD is composed mainly by ionotropic and metabotropic glutamate receptors. Glutamate released from pre-synaptic vesicles interacts with the glutamatergic receptors in the PSD. The first class of glutamate receptors is the ionotropic receptors (iGluR) which exerts a fast response, where the second class the metabotropic G-coupled receptors (mGluR) produces a slower effect. There are multiple types of iGluRs, including  $\alpha$ -amino-3-hydroxy-5-methyl-4-isoxazolepropionic receptors (AMPA) and N-methyl-D-aspartate receptors (NMDA). AMPA receptors are heterotetramers that are composed of the subunits GluA1-4<sup>61</sup>. They are the main receptors involved in the fast-excitatory synaptic transmission, permeable for the cations  $\text{Na}^+$  and  $\text{K}^+$ . The 4 subunits of the AMPA receptors have different roles, where AMPA receptors composed of GluA2 subunits have a lower permeability for  $\text{Ca}^{2+}$ , while receptors containing the other subunits are permeable for  $\text{Ca}^{2+}$ <sup>62</sup>. Phosphorylation sites can be found on the C-terminal tail and those are involved in regulating their activity, and therefore synaptic plasticity. The GluA1 subunit is the subunit that has the highest expression in hippocampal neurons<sup>63</sup>.

NMDA receptors have a slower response, since they are activated only when the presynaptic glutamate release is exerting a larger post-synaptic depolarization. This is due to their  $\text{Mg}^{2+}$  block that has to be released to open the channel<sup>64,65</sup>. In addition to the binding to glutamate, this receptor needs to bind glycine for its activation<sup>66</sup>. NMDA receptors have multiple subunits, namely GluN1, GluN2A-D and GluN3, which can form in a heteropentameric or heterotetrameric structure<sup>67</sup>. Where, similar to the AMPA receptors, the composition of the subunits exerts different properties. The binding site with glycine is localized on the GluN1 subunit<sup>61,66,68</sup>, where the glutamate binding site is found on the multiple GluN2 subunits<sup>69</sup>. The main NMDA receptors expressed in the cortex and hippocampus are GluN2A and GluN2B containing NMDA receptors. The two subunits share approximately 70% of amino acid sequence similarity<sup>70</sup>, they have distinct roles in physiological and pathological processes, including in AD<sup>71</sup>. GluN2A subunit has, compared to the GluN2B subunit, lower affinity for glutamate, but converts greater

channel open probabilities, rapid kinetics and higher  $\text{Ca}^{2+}$ -dependent desensitization<sup>72</sup>. The GluN2A subunit has been implicated in promoting cell survival and has neuroprotective properties<sup>73-75</sup>, while calcium influx through GluN2B-containing receptors plays a role in neuronal cell death pathways and neurodegeneration<sup>76-78</sup>. The increased activation of NMDARs through the toxic  $\text{A}\beta$  oligomer accumulations is thought to occur at the early stages of AD<sup>79</sup>, which is mediated through an increased activation of the GluN2B-containing NMDARs<sup>80</sup>. Therefore, the enhancement of the GluN2A-containing receptor activity and the decrease of GluN2B subunit activity has been suggested in order to halt the early  $\text{A}\beta$ -mediated synaptic dysfunction<sup>81,82</sup>.

### **Adhesion Molecules**

The adhesion molecules found in the PSD are involved in the shaping and structure of dendritic spines, where they are also found to be important in the formation of new synapses and spines<sup>83</sup>. Most of those adhesion molecules (i.e. Neuroligin, SALM and N-Cadherin) bind to scaffold protein PSD-95 and to the actin cytoskeleton (Fig. 7). In addition, adhesion molecules are able to form a connection between the pre- and post-synapse. There is a correlation between the activity of these molecules and their ability to induce synapse maturation. This is done by the recruitment or binding of pre- and postsynaptic partners<sup>83</sup>. In this process they are able to give stability to the synapse, which on the other hand, can be modulated by proteolytic cleavage that disrupts the connection between the pre- and post-synapse and destabilizing the spines. The cadherin based homophilic cell adhesion mechanism is also involved in spine morphogenesis, has ability to steer the apposition of the pre- and postsynaptic compartments and regulates synaptic plasticity<sup>84</sup>. The neuron specific cadherin (Neuronal Cadherin/N-Cadherin) is involved in depolarization-induced spine enlargement, through neuronal activity that induces N-Cadherin redistribution at synapses<sup>85</sup>. N-Cadherin is also able to regulate spine morphology through the recruitment in the spine of  $\beta$ -catenin, which can bind the actin cytoskeleton<sup>86</sup>. In addition, N-Cadherin is important to regulate the synaptic levels of the AMPARs, by the interaction between the N-terminal GluA2 subunit domain to N-Cadherin<sup>87,88</sup>. Overall,

the most important function of N-Cadherin is to keep the long term maintenance and stability of dendritic spines<sup>89</sup>.

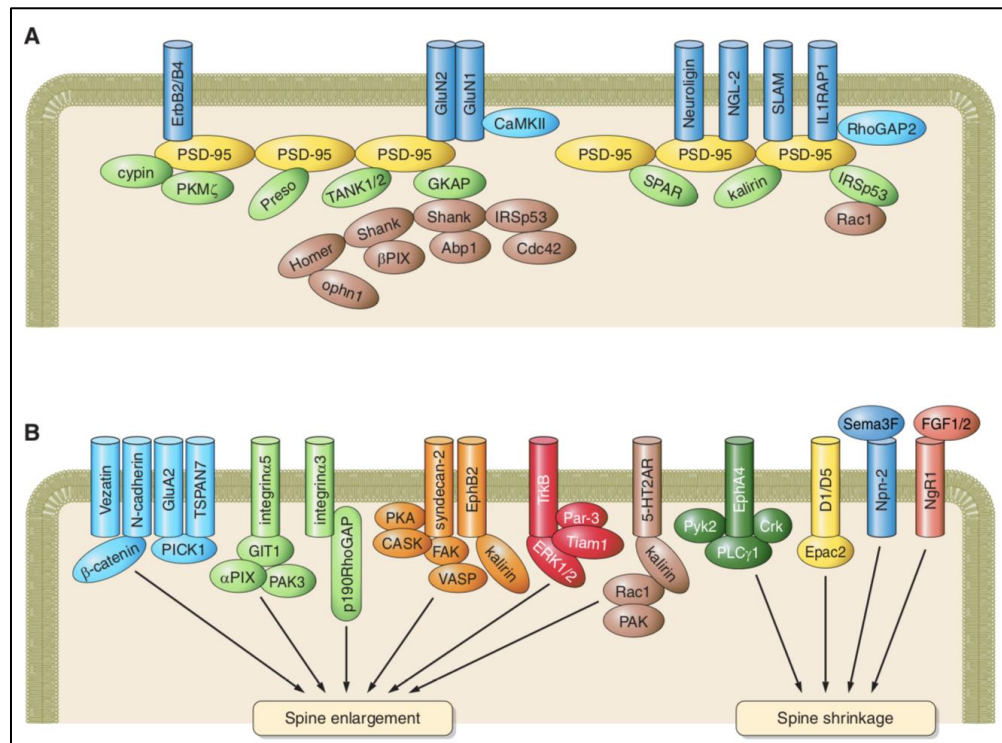


**Figure 7) Synaptic scaffolds and membrane proteins.** The cartoon shows the major PSD-95 associated proteins (A) and synaptic membrane proteins and associated complexes (B) involved in regulating dendritic spine formation. Obtained from Sala & Segal 2014<sup>83</sup>.

### Scaffolding Proteins (MAGUK family)

Underneath this receptor layer the scaffolding proteins like PSD-95, connected to kinases and phosphatases, can be found. The scaffolding proteins are predominantly composed of members of the MAGUK family, which are multidomain proteins that share some structural domains. Proteins belonging to the MAGUK family are PSD-93, PSD-95, synapse-associated protein 102 and 97 (SAP102 and SAP97). They are involved in mediating the glutamate receptor localization at the synapse and anchoring these from the membrane to the cytoskeleton<sup>90</sup>. The structural domains are the three PDZ (PSD95/DLG/ZO1) domains, the Scr homology 3 (SH3) domain and a Guanylate kinase (GK) domain. All members of the MAGUK family are present in the central nervous system, but are expressed in different brain cell compartments<sup>91</sup>. PSD-95 is

highly enriched in the PSD and is the most important scaffolding protein. PSD-95 can form an interaction with the NMDAR subunit cytoplasmic C-terminus, and additionally, PSD-95 also binds to  $\alpha$ -actinin, which can bind the filamentous actin (F-Actin). This scheme is the way how PSD-95 anchors the NMDAR to the cytoskeleton of dendritic spines <sup>92-94</sup>. PSD-95 is also able to couple the NMDAR to an intracellular signaling system which regulates intracellular effects on NMDAR activation processes. The calcium ions, that enter in the postsynaptic compartment through the NMDARs, can bind calmodulin. When activated calmodulin interacts with calcium, it can activate Ca<sup>2+</sup>/calmodulin dependent kinase II (CaMKII). CaMKII is highly enriched in the PSD and one of its target proteins is SAP97. CaMKII-dependent phosphorylation of SAP97 can inhibit the binding with the GluN2A subunit of NMDAR <sup>95</sup>. SAP97 and SAP102 are mainly found in axons and dendrites but also in the cytoplasm and are involved in the trafficking of NMDARs and AMPARs <sup>96,97</sup>. SAP102 is found to be involved in spine morphogenesis and interacts with GluN2B, which mediates the ability to initiate spine formation <sup>98</sup>.

### **1.3)3. The spinoskeleton**

Integrated in the synaptic spines, underneath the PSD, you will find the cytoskeleton, that is mainly composed of filamentous (F)-actin <sup>99</sup>. Most likely, in the more mature spines, actin is involved in stabilizing proteins found in the post synapse <sup>100,101</sup> and in regulating the structure of the spine head which changes as a response to synaptic signaling <sup>102,103</sup>. Actin is highly enriched in all synapses and is present in two distinct forms: the glomerular actin (G-Actin) and F-Actin. The actin cytoskeleton formation is a highly dynamic process which is strictly regulated. The G-Actin is able to polymerize into F-Actin, using ATP-dependent hydrolysis, which forms the polarized F-Actin structure. The F-Actin structure has a barbed end, which is the side where the monomeric G-Actin is added, and the pointed end where actin can depolymerize <sup>104</sup>. The process of polymerization and depolymerization of actin, called treadmilling, is coordinated by the intracellular concentration of G-Actin. When the concentration reaches above 0,1  $\mu$ M, actin polymerization will rise until the G-Actin concentration

decreases again to 0,1  $\mu\text{M}$  and vice versa. This concentration is therefore called the "critical concentration". There are multiple protein families able to bind actin (Actin Binding Proteins; ABP) (Fig. 8) and, thereby, can influence actin dynamics. The capping proteins, gelsolin and Cap Z<sup>105</sup>, are able to interact with the barbed-end of F-Actin which prevents G-Actin addition. The severing of F-Actin is done by another class of proteins, including ADF/cofilin, that breaks up the actin filament and thereby generates new barbed ends for the polymerization process. Proteins able to bind and sequester G-Actin are WASp (Wiskott-Aldrich Syndrome protein, profilin and CAPs (Cyclase Associated Proteins)<sup>106-109</sup>. Profilin acts as a catalyzer for actin polymerization depending on the concentration<sup>110</sup>. ADF/cofilin is able to bind both G- and F-actin and is involved in the actin turnover process. They can depolymerize actin filaments at the pointed ends, while they also produce new barbed ends at the actin filaments. Therefore, the ADF/cofilin complex is necessary for the actin treadmilling<sup>111,112</sup>. Drebrin is a protein that is involved in the regulation of actin polymerization and binds to F-actin<sup>113</sup>. Interestingly, drebrin protein levels are found to be reduced in AD patients<sup>114</sup>. CAPs are multifunctional protein, since they play a role in the adenylate cyclase (AC) activation pathway in non-neuronal cells like yeast, and they interact with actin<sup>115,116</sup>. CAPs are mainly involved in the maintenance of the actin cytoskeleton structure<sup>117</sup>. The actin cytoskeleton in the spine head has a core of stable actin with a slow turnover, and a shell part, which is highly dynamic<sup>103,118,119</sup>. During this process the actin filaments grows in length at the barbed end, while at the pointed end a removal of actin monomers is seen.



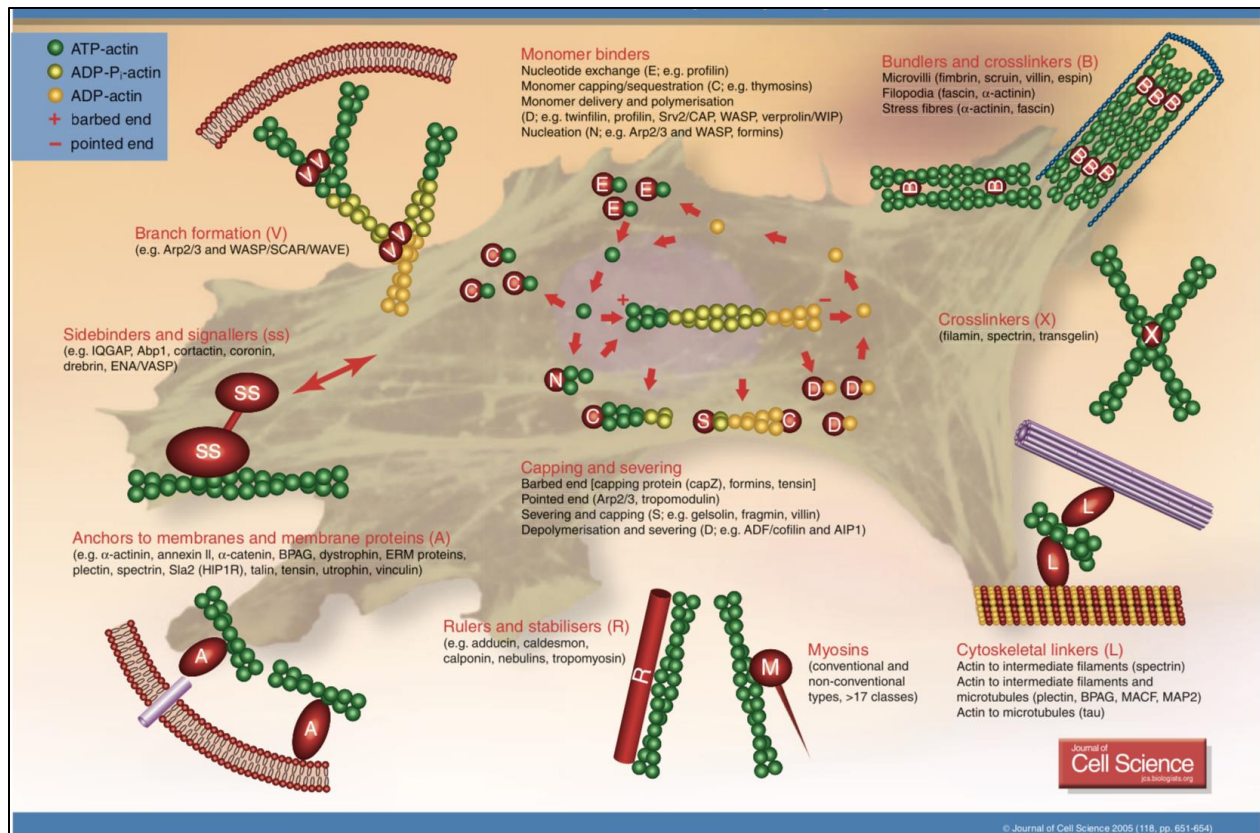


**Figure 8) Actin-Binding Protein.** An overview of protein that bind actin and therefore influence actin dynamics. Obtained from S.J. Winder & K.R. Ayscough 2005 <sup>105</sup>.

### 1.3)4. Synaptic Plasticity

As described above, neurons are capable of communicating with each other through synaptic transmission at the synapses, which are connections between the presynaptic terminal of the axon and postsynaptic side of dendrites. Synaptic plasticity refers to the activity-dependent modification of the synapse and the ability to be modified by experience through the strengthening or weakening of synaptic transmission over time. This is how neurons control how effectively they can communicate with each other <sup>120</sup>. Nowadays, we know that the morphology of the spines and synapses is regulated by the neuronal activity and hereby controls synaptic plasticity. In addition, there is a correlation between the shape of the spines and their functionality, and that this depends on the remodeling of the actin cytoskeleton <sup>121,122</sup>. This was shown by the fact that a larger spine head, includes a larger PSD surface, which leads to a stronger, more functional synapse<sup>58,122</sup> (Fig. 9).



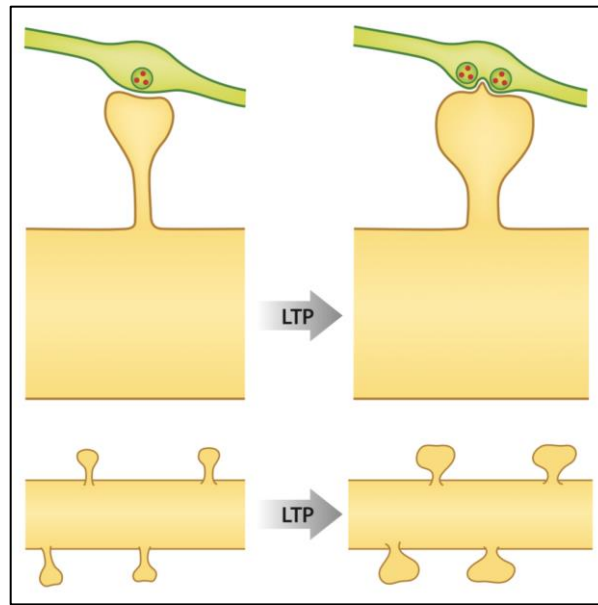


**Figure 9) Changes in spine morphologies during synaptic plasticity.** Representation of the ultrastructural reconstructions during long-term potentiation (LTP) results in larger spine heads and shorter and wider spine necks. Obtained from Yuste 2013 <sup>122</sup>

There are two forms of plasticity, short-term plasticity and long-term plasticity. Short-term plasticity is the form of plasticity that is triggered by the short bursts of activity which cause an increase in calcium in the presynaptic terminals. The increase in presynaptic calcium levels in turn increases the probability of transmitter release by the modification of biochemical processes that cause exocytosis of synaptic vesicles <sup>120</sup>.

Long-term plasticity is the form of plasticity that has long-lasting modifications of synaptic strength. It is believed that memory formation is caused by the strengthening of connections, when the presynaptic activity correlates with the firing of the postsynapse <sup>123</sup>. This is supported by the finding of the excitatory synapses in the hippocampus that are repetitively activated and increase their synaptic strength for hours or even days <sup>124</sup>. Nowadays, we call this event long term potentiation (LTP). LTP is known to have three basic properties: cooperativity, associativity and input-specificity <sup>125</sup>. The term cooperativity indicates that to trigger the initial signal, multiple presynaptic components could be activated simultaneously. In addition, the term associativity means that when there is a strong LTP activation in one subset of synapses it can trigger LTP at another subset of adjacent active synapses in the same cell, only if

both independent sets of synapses were activated within a finite temporal window. Finally, LTP is input-specific, which tells us that an LTP event initiated at one set of synapses, will not occur in the other synapses that are present in the same cell <sup>126</sup>. LTP can arise in different forms and in multiple brain areas, but the most studied form of LTP is at the glutamatergic synapses in the hippocampus. It occurs between the synapses that derive from the CA3 cells (the Schaffer collateral) and the apical dendrites of CA1 pyramidal cells, and is triggered by activation of NMDARs <sup>126</sup>. To induce LTP, glutamate is released from the presynaptic vesicles, it interacts with and thereby activates AMPARs and NMDARs present in dendritic spines. The AMPARs are the main suppliers for the inward current that generates a synaptic response when a cell is in its resting state. As described above, the NMDAR is voltage dependent because of the block of its channel by extracellular  $Mg^{2+}$ , and therefore doesn't contribute much to the basal synaptic transmission in rest. When the cell is depolarized upon LTP induction, the  $Mg^{2+}$  block is released from the channel, and therefore allowing  $Ca^{2+}$  and  $Na^{+}$  to enter in the dendritic spine, increasing their intracellular levels <sup>126</sup> (Fig. 10). The rise of intracellular  $Ca^{2+}$  levels serves as a trigger for the translocation of protein to the synapse, including the AMPARs <sup>127</sup>. These activity-dependent related changes in AMPAR trafficking are necessary for the LTP maintenance. In addition, the intracellular  $Ca^{2+}$  ions activate the kinases PKA, PKC and CAMKII. Moreover, by the change in structure CAMKII is activated and located into the PSD, where it can phosphorylate proteins as AMPAR, NMDAR and PSD95. Upon LTP, the AMPAR subunit GluA1 can be phosphorylated on Ser<sup>831</sup> by either PKC or CAMKII, while Ser<sup>845</sup> can be phosphorylated by PKA <sup>128,129</sup>. The phosphorylation site Ser<sup>831</sup> will show an increased phosphorylation upon LTP <sup>129,130</sup>, where the Ser<sup>845</sup> is important for the activity dependent trafficking of GluA1 in the synapse, where it targets the GluA1 into the synaptic membrane <sup>128,131</sup>. Additionally, dephosphorylation of Ser<sup>845</sup> is implicated in long-term depression (LTD) including a decrease of surface GluA1 in the cell <sup>130,132</sup>.

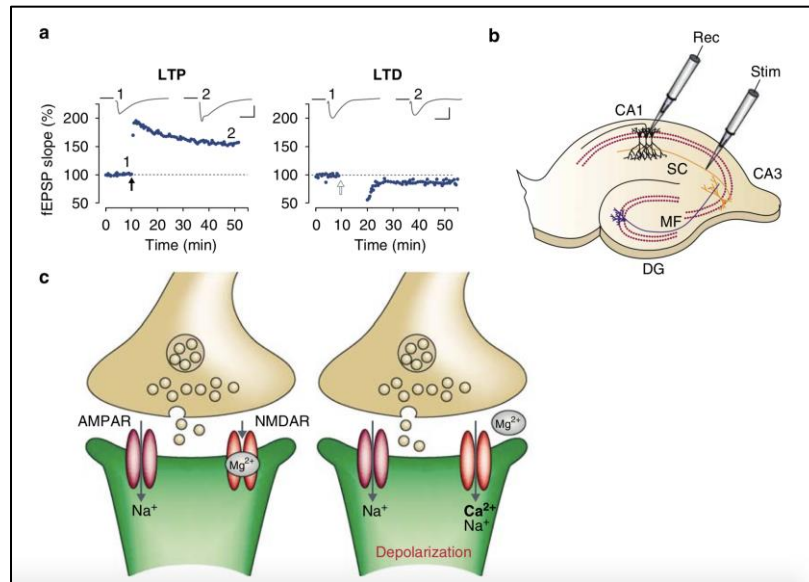


**Figure 10) NMDAR-dependent LTP and LTD at hippocampal CA1 synapses.** A) a sample experiments illustrating LTP and LTD in the CA1 region of the hippocampus. Synaptic strength, defined as the initial slope of the field excitatory postsynaptic potential (fEPSP; normalized to baseline) is plotted as a function of time. The left panel demonstrates LTP elicited by high-frequency tetanic stimulation (100Hz stimulation for 1s; black arrowhead). Right panel illustrates LTD elicited by low-frequency stimulation (5 Hz stimulation for 3 min given twice with a 3 min interval; open arrow). Data traces were taken at the times indicated by the numbers on the graphs (scale bar: 0.5 mV; 10 ms) B) A schematic diagram of the rodent hippocampal slice preparation, demonstrating the CA1 and CA3 regions as well as the dentate gyrus (DG). (SC - Schaffer collateral; MF - mossy fiber). Typical electrode placements for studying synaptic plasticity at Schaffer collateral synapses onto CA1 neurons are indicated (Stim - stimulating electrode; Rec - recording electrode). C) Representative model of synaptic transmission at excitatory synapses. During basal synaptic transmission (left panel), synaptically released glutamate binds both the NMDARs and AMPARs. Na<sup>+</sup> flows through the AMPAR channel but not through the NMDAR channel because of the Mg<sup>2+</sup> block of this channel. Depolarization of the post synaptic cell (right) relieves the Mg<sup>2+</sup> block of the NMDAR channel and allows both Na<sup>+</sup> and Ca<sup>2+</sup> to flow into the dendritic spine. The resultant increase in Ca<sup>2+</sup> in the dendritic spine is necessary for triggering the subsequent events that drive synaptic plasticity. Obtained from Citri & Malenka 2008 <sup>120</sup>

Furthermore, it is shown that upon LTP induction there is an enlargement of the dendritic spine, changing the spine morphology, and that LTP can induce the formation of new spines <sup>133,134</sup>. On top of these changes, LTP is also causing the growth of the PSD itself <sup>135</sup>, and the remodeling of the actin cytoskeleton of the spine <sup>136</sup>. As an opposite event of the LTP there is also LTD <sup>137</sup>, induced by a prolonged low frequency stimulation protocol. Similar to LTP, there are many different forms of LTD in the brain, but the most studied form is the LTD at the excitatory synapses of the hippocampal CA1 pyramidal cells dependent on NMDAR <sup>137,138</sup>. As LTP, LTD is dependent on the intracellular increase of Ca<sup>2+</sup> at the post-synapse and that LTD is

input-specific<sup>138</sup>. While LTP is triggered by high concentration of calcium, to trigger LTD a low concentration of calcium is required. Chemically induced LTD is associated with persistent dephosphorylation of GluA1 at a PKA phosphorylation site Ser<sup>845</sup><sup>130</sup>. This event decreases the open-channel probability of the AMPAR<sup>139</sup>. As during LTP there is an insertion of AMPARs in the post-synapse, LTD is characterized by the removal or endocytosis of AMPARs. This is probably mediated by the dissociation of AMPARs from the PSD followed by clathrin- and dynamin-dependent endocytosis of the AMPARs<sup>140-142</sup>. As written above, dendritic spines are highly enriched with actin, and that the changes in neuronal plasticity correlate with the shape of the spine. This depends on the ability of the fast remodeling of the actin cytoskeleton<sup>143</sup>. During LTP, there is an increase in the F-Actin ratio compared to the G-actin, which increases the size of the spines, where during LTD there is an increased G-Actin concentration that will lead to a smaller spine size<sup>136,144</sup>. Additionally, the link between actin remodeling and synaptic plasticity is shown by the treatment with actin depolymerizing reagents<sup>134,144</sup>.

### **1.3)5. Synaptic Dysfunction in AD**

As highlighted above, besides plaques and tangles, a third hallmark that arises in the early phases of the pathology is synaptic dysfunction and synapse loss, which is known to precede neuronal loss. Already over 100 years ago it was noticed by Ramon y Cajal that dementia resulted from the degeneration of synapses<sup>145</sup>. According to the amyloid cascade hypothesis, this is caused by A $\beta$  oligomers in the brain<sup>146-148</sup>. Synaptic loss is detected in the early stages of AD, before the clinical onset of the disease and it correlates best with the cognitive decline in AD, suggesting that this event is a crucial event in the AD pathogenesis<sup>149-154</sup>. Therefore, it is most likely that synaptic impairment is the basis of the memory loss seen in AD. Moreover, synaptic dysfunction is caused by the impairment of synaptic plasticity and it is seen as the basic process that underlies memory formation<sup>155-157</sup>. The brain alterations that are found at the synaptic levels could be caused by alterations of the expression of pre- and postsynaptic proteins, but the complete mechanism underlying the synaptic dysfunction in AD is not yet

understood<sup>158</sup>. Since both immunohistochemical and biochemical analysis of synaptic protein showed a similar reduction of their expression in the synaptic compartments of AD patients<sup>158</sup> and, additionally, the decrease of synapse density in the early stages of the disease is disproportional with the neuronal loss<sup>149,152,159</sup>, it is thought that the synaptic loss proceeds neuronal degeneration<sup>153,154,160</sup>. Strengthening of synapses by LTP, can lead to an increase in strength of circuit connections, which in turn, are able to store new information. In AD, the A $\beta$  peptide has an inhibitory effect on synaptic transmission<sup>37,161</sup>, by a mechanism that is similar to the one of LTD<sup>38,162</sup>. How the A $\beta$  oligomers effect synaptic plasticity is not fully understood, but most likely they are involved in three different ways. The first mechanism, which is the most important one, involves a toxic gain of function of A $\beta$  by the self-association and novel interactions that will results in impaired synaptic transmission. The other two possibilities state that A $\beta$  has a role in physiological conditions, where reduced A $\beta$  could lead to an abnormal function, and the increased A $\beta$  levels underlie the synaptic dysfunction<sup>163</sup>. These A $\beta$  oligomers target multiple synaptic sites and hereby decrease spine density in organotypic hippocampal slice cultures<sup>40,162,164</sup>, disrupt neurons in culture<sup>165-167</sup> and cause synaptic dysfunction in AD mice models<sup>168,169</sup>. Additionally, A $\beta$  oligomers target also multiple receptors including both acetylcholine and glutamate receptors<sup>40,166,170,171</sup>, which are known sites involved in AD. In particular, they are associated with alterations of the NMDAR subunit GluN2A, which levels are reduced in post-mortem human AD brains<sup>172-174</sup>.

## 1.4.) AD mice models

Multiple genetic animal models for AD are available, predominantly based on the genetic mutations found in the early-onset AD patient group or on the genetic risk factor ApoE $\epsilon$ 4. Unfortunately, no existing model that exhibits all AD characteristics is available, which would involve the development of all clinical and pathological hallmarks of AD, like A $\beta$  plaques, NTFs, synaptic dysfunction, neuronal degeneration and cognitive impairment. Most AD mice models show the cognitive deficits and A $\beta$  plaques, but for instance NTFs are only observed in tau expressing models. Depending on the research aim, it is important to understand which model to use, while for preclinical drug discovery research these models have some clear limitations. This is why the mice models available for AD can be used just as a tool to get a better understanding in the proteins and genes function pathways implicated in AD and to dissect new strategies to target these pathways <sup>175</sup>. Since it is important to understand which model has to be used for the research question that has to be answered, underneath there will be an overview of the most used models.

### hAPP models

First, the animal model that is mostly used is the hAPP mice model which is based on the expression of the human APP gene. This is based on the autosomal dominant APP mutation found in the genetic early onset AD <sup>176</sup>. The animals carrying this mutation will develop the amyloidogenic hallmarks and show memory deficits, but neuronal loss is not found. There are multiple animal models based on the hAPP gene since there are multiple mutations present in AD patients. The most common one is the K670N/M671L Swedish double mutation found at the site where the  $\beta$ -secretase cleaves APP <sup>177</sup>. The mice expressing just the Swedish mutation are called Tg2576, while some other have a combined mutation with the  $\gamma$ -secretase cleavage site (TgCRND8 and J20) or an added mutation inserted in the A $\beta$ -sequence (E693G Arctic mutation) <sup>178</sup>.

## **A $\beta$ models**

Since hAPP mice models will express not just A $\beta$ , but also other cleavage fragments of APP, the A $\beta$  transgenic mouse model was created to be able to isolate the effects of A $\beta$  more specifically. This model is based on the expression of a fusion protein between A $\beta$  and BRI, which is a protein involved in the familial British dementia. This results in A $\beta$  expression upon the expression of the fusion protein<sup>179</sup>. These mice will develop the amyloid accumulations, but don't show cognitive impairments, which makes it questionable whether this mice model is useful in AD<sup>180</sup>.

## **Tau models**

Besides the A $\beta$  accumulations, the other hallmark of AD is the tau pathology. None of the models based on APP or A $\beta$  express any tau pathology. Tau models are mainly based on the human tau expression mutation found in frontotemporal dementia<sup>181,182</sup>, another form of dementia, but importantly to keep in mind is that these mutations are not found in AD pathology directly, although they are important to allow the study of the tau pathology. Models widely used are mice expressing human tau together with hAPP<sup>181-183</sup> and lines that express wild-type human tau<sup>184</sup>. The first model shows motor and behavioral deficits<sup>185</sup>, including A $\beta$  accumulations and tau pathology<sup>181,186,187</sup>.

## **Presenilin & hAPP/presenilin double transgenic models**

Since mutations of the presenilin genes are the most common autosomal dominant mutation found in early onset familial AD, there are mice models based on the PSEN1 gene, encoding presenilin 1. There are many mice models available expressing either one<sup>188-196</sup>, or multiple presenilin mutations<sup>194</sup>. Single mutation mice models show increased levels of A $\beta$ 42 expression without affecting A $\beta$ 40<sup>192</sup>, but additionally they don't express cognitive impairment<sup>197-201</sup>. This is probably due to the differences of the APP/A $\beta$  sequences<sup>202</sup>. Then, there are the double transgenic mice models based on expression of both hAPP and PS1, the APP/PS1 mice lines. The most commonly used one is the hAPP Swedish mutation and PS1 containing the deltaE9 mutation

(APP<sup>swe</sup>/PS1<sup>dE9</sup>), which develop amyloidogenesis and cognitive deficits at 6 months of age<sup>203</sup>.

### **Triple transgenic models**

With a combination of the three mutants, i.e APP, PS1 and tau, the triple transgenic line (3xTg) was bred. In this mouse model, the development of extracellular A $\beta$  plaques are developed before the tangle formation, similar to how the disease progresses in human AD, and in addition, they also develop synaptic dysfunction<sup>20,182</sup>. The advantage of this model is that the main two hallmarks found in AD are simultaneously expressed within one model.



## 2.) ADAM10

### 2.1.) What is ADAM10?

ADAM10 is a member of the “a disintegrin and metalloproteinase” (ADAM) family, which are type 1 membrane protein that have the ability to act as a sheddase towards many substrates when they are properly inserted in the synaptic membrane. Shedding is a process of proteolytic ectodomain release, which is a known mechanism for the regulation of multiple cell surface proteins. The ADAM family members are the most known proteinase family involved in this ectodomain shedding<sup>204</sup>. In the human genome there are 22 known ADAM family members, which are involved in regulating multiple biological processes including, neurite and axon guidance, cell proliferation, cell adhesion and signaling processes. ADAM10 seems to be particularly important, since its involved in neurodevelopment by regulating proteolysis of Notch receptors and in AD by activating the non-amyloidogenic pathway by cleavage of APP<sup>205</sup>.

There is still a lack of functional knowledge about which ADAM10 domain is important for the shedding process, but this is what is known so far. ADAM10 has an extracellular domain with an N-terminal prodomain, the metalloprotease, cysteine-rich and disintegrin domain (figure 11). During maturation the prodomain of ADAM10 is removed, and upon this process ADAM10 becomes catalytically active<sup>205</sup>. The domain structure of ADAMs, with the disintegrin and cysteine-rich domain is the part that is involved in the adhesive, proteolytic and putative signaling activities, since it is necessary for the substrate-recognition<sup>206,207</sup>. Additionally, it was shown that the disintegrin and cysteine-rich sites have self-regulatory functions, where they suppress the metalloproteinase activity when there are no substrates available<sup>208-210</sup>. The cytoplasmic tail of the ADAM family proteins are important for regulation of its activity by the trafficking of the protein into the right cellular location<sup>211-213</sup> (Fig. 11). After the synthesis of ADAMs and the translocation into the endoplasmic reticulum, they are brought to the Golgi apparatus where they undergo further post-translational modifications and where the pro domain will be removed<sup>214</sup>. Upon the maturation, ADAMs are then transferred in a minor degree, into the plasma membrane<sup>215</sup>.

Moreover, ADAM10 is known to be a synaptic protein, being an integral component of the excitatory postsynaptic density, where it is highly enriched <sup>212</sup>. With the functions described above, ADAM10 is involved the modulation of spine morphology and are important for neuronal development. Especially important for this study is the fact that ADAM10 is demonstrated to selectively mediate the non-amyloidogenic  $\alpha$ -secretase pathway in neurons, and thereby preventing the accumulation of A $\beta$ -peptide <sup>34-36</sup>.

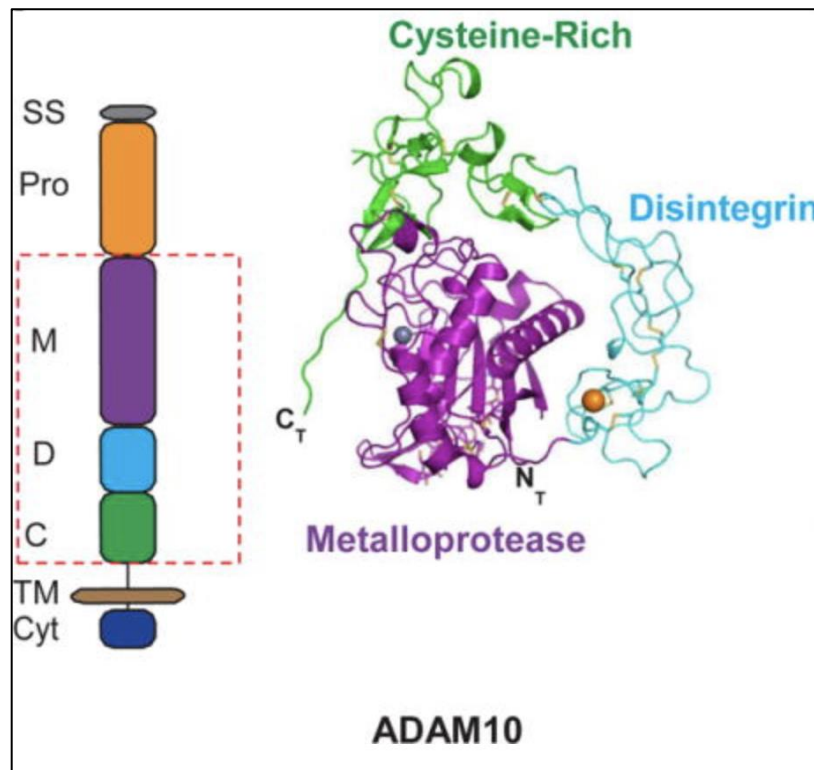


**Figure 11) ADAM10 Structural Overview.** Representation of the architecture and domain organization of ADAM10. Left panel depicts a schematic of the ADAM10 protein colored by domain. SS: signal sequence; Pro: prodomain; M: metalloproteinase; D: disintegrin; C: cysteine-rich; TM: transmembrane; Cyt: cytoplasmic tail. The red box encompasses the portion of the protein visualized in the X-ray structure. The right panel shows the overall architecture of the mature human ADAM10 ectodomain, colored according to the domain schematic in cartoon representation. The catalytic zinc ion is gray, and a bound calcium ion is shown in orange. Cysteine residues engaged in disulfide bonds are shown as sticks. Obtained from Seegar et al 2017 <sup>205</sup>.

## 2.2.) What are the substrates of ADAM10?

There are multiple substrates known of ADAM10 in the central nervous system<sup>216</sup>. The most important substrates of ADAM10 cleavage are ephrins, N-Cadherin, prion protein (PrP), Notch, and APP<sup>204</sup>. The cleavage of ephrin by ADAM10 controls the inactivation of the ephrin/Eph complex, which is important for the axonal growth cone trafficking. This makes ADAM10 important for the axon guidance and its extension in the CNS<sup>217</sup>. ADAM10 cleavage of N-Cadherin is important for the regulation of cell adhesion, the neurite outgrowth and cell migration<sup>218-220</sup>. By the proteolytic cleavage of ADAM10 the soluble extracellular domain is released together with a carboxy-terminal fragment CTF1 that is membrane bound and can be cleaved by the  $\gamma$ -secretase<sup>221,222</sup>. Hereby, ADAM10 can control the coordination of pre- and post-synaptic cell-adhesion, cell proliferation and survival during development and in adult life but also in the case of wound healing. PrP cleavage by ADAM10 is important in the pathology of prion-based disorders of the central nervous system, where ADAM10 activation could be used as a therapeutic option for the breakdown of the toxic PrP domain<sup>223,224</sup>. Notch signaling is a highly conserved process during evolution and is involved in the regulation of cell fates and neurodevelopment<sup>225</sup>. In addition, Notch is required for the maintenance of neuronal stem cells in the adult brain. The cleavage of ADAM10 happens in the extracellular Notch domain<sup>226</sup>, while the intracellular membrane fraction can be cleaved by the  $\gamma$ -secretase. The fragment that is released by this cleavage step is translocated into the nucleus where it serves as a transcription factor<sup>227</sup>, making ADAM10 an important player in the Notch signaling pathway involved in neurodevelopment and neurogenesis.

The most important ADAM10 substrate of our interest is APP. The physiological function of APP is not completely understood although it has been studied broadly. What is known, is that APP has a neurotrophic function supporting the neuritic outgrowth, migration of neurons and neuronal repair<sup>228,229</sup>. Additionally, it has been shown that either the knock down or overexpression of APP affects the number of spines, where mice lacking APP show a two-fold increase of dendritic spines compared to the wild type<sup>230</sup>. Furthermore, APP is shown to be involved in the regulation of the

surface trafficking of the NMDARs in the post-synapse <sup>231</sup>. Since the A $\beta$ -peptide sequence is located in the APP gene, APP is an important target for AD. As written before, the shedding of APP by the  $\beta$ -secretase followed by the  $\gamma$ -secretase leads to the production of the A $\beta$ -peptide. On the other hand, the  $\alpha$ -secretase shedding cleaves APP within the A $\beta$  sequence and therefore prevents its production. There are three main players that show  $\alpha$ -secretase activity, namely ADAM9 (also named metalloprotease/disintegrin/cysteine-rich protein i.e. MDC9), ADAM10 and ADAM17 (also named Tumor Necrosis Factor-alpha converting enzyme i.e. TACE) <sup>34,232,233</sup>. But more importantly, it has been shown that ADAM10 is the main  $\alpha$ -secretase player in neuronal cells <sup>36,234</sup>. This makes ADAM10 an important mediator in the prevention of the A $\beta$ -peptide production in the non-amyloidogenic pathway of APP cleavage.

### **2.3.) ADAM10 activity regulation by intracellular trafficking**

ADAM10, which is highly enriched in the PSD <sup>212</sup>, can only exert activity towards its substrates when its inserted in the plasma membrane. This makes the trafficking of ADAM10 to the synapse an important regulator of its activity. There are multiple proteins involved in the regulation of ADAM10 synaptic localization. One important protein involved in the forward trafficking of ADAM10, and its insertion into the synaptic membrane, is SAP97 <sup>212</sup>. As written above, SAP97 is a member of the MAGUK protein family, and its SH3 domain interacts with the proline-rich C-terminal domain of ADAM10. Upon this interaction, ADAM10 is transferred from the Golgi outposts into the postsynaptic membrane and thereby the ADAM10 can get into close contact with its substrates and its cleavage activity increases. This is mediated by protein kinase C (PKC) phosphorylation site in the SAP97 SH3 domain, that promotes the ADAM10 interaction with SAP97 <sup>235</sup>. Additionally, it was shown that LTD increases ADAM10 levels in the synaptic membrane by fostering the forward trafficking of ADAM10 by SAP97 <sup>213</sup>. SAP97 is also implicated in the synaptic targeting of ionotropic glutamate receptor subunits and NMDAR activation fosters SAP97 to the PSD in primary neurons <sup>95,236</sup>. Where, this short-term activation of NMDARs also increases the ADAM10 levels in this compartment in primary neurons <sup>212</sup>. Furthermore, NMDAR activation upregulates genes encoding for ADAM10 and  $\beta$ -catenin, leading to an increased ADAM10 expression and using either inhibitors or agonist of Wnt/ $\beta$ -catenin signaling abolishes or activates the ADAM10 expression respectively. With the use of ERK inhibitors either the NMDAR and the Wnt-induced ADAM10 expression are blocked. This suggests that the ADAM10 expression is controlled by NMDARs through the Wnt/MAPK signaling pathway <sup>237</sup>. On the other hand, the clathrin adaptor 2 (AP2), a heterotetrameric structure, regulates the clathrin-mediated endocytosis of ADAM10. A specific RQR binding motif on the cytoplasmic tail of ADAM10 that serves as an AP2-binding motif, regulates ADAM10 localization through endocytosis. In addition, LTP is able to decrease ADAM10 synaptic membrane levels via the induction of AP2-mediated endocytosis <sup>213</sup>.

## 2.4.) ADAM10 in AD

As mentioned above, ADAM10 is the main  $\alpha$ -secretase involved in the non-amyloidogenic pathway of AD. In the light of the involvement in AD pathogenesis, specimens of sporadic AD patients, as the cerebrospinal fluid (CSF) and platelets, were investigated, and reduced ADAM10 protein levels were found in platelets of AD patients compared to non-demented control patients. Additionally, the sAPP $\alpha$  levels in the CSF, which give an indication of the ADAM10 activity, are decreased as well <sup>238,239</sup>. On the other hand, the mRNA levels of ADAM10 were increased in the hippocampus and cerebellum of severe late-stage AD patients, which indicate a possible defense mechanism in the later stages of the disease <sup>240</sup>. As written above, the regulated interaction of ADAM10 to SAP97 and AP2 is a physiological pathway that controls the synaptic ADAM10 levels and thereby its activity in the synapse <sup>212,213</sup>. Because of the role of ADAM10 in the A $\beta$  production pathway and synaptic function, the dysregulated balance of either SAP97 or AP2 binding to ADAM10 could have a role in the APP processing in AD. The interactions between ADAM10 to either SAP97 or AP2 are associated with AD pathology, where a decreased association between ADAM10 to SAP97 <sup>241</sup> and an increased binding between ADAM10 to AP2 <sup>213</sup> was found in early-stage AD patient hippocampi. Upon interference with the ADAM10 association to SAP97 with a cell-permeable peptide in mice, increased A $\beta$  levels are found suggesting a similar process found in the initial stages of AD <sup>242</sup>. To conclude, this suggests that the reduced levels of ADAM10 synaptic localization and therefore decreased activity, are probably due to the defect of ADAM10 forward trafficking and endocytosis by SAP97 and AP2.

### 3.) Cyclase-associated protein family (CAP)

#### 3.1.) What are CAPs?

Cyclase-associated protein (CAP) is a protein family involved in the Ras-cAMP signaling pathway activating the adenylate cyclase (AC) and in regulating the cytoskeleton. They were first isolated from *Saccharomyces Cerevisiae*, called *Srv2/CAP*, and yeast that lacks CAP are not capable to grow and show for instance abnormal morphological cell shapes compared to normal cells<sup>116</sup>. Importantly, the interaction with the AC and its regulation is not found in all forms of CAPs, only those present in *Saccharomyces cerevisiae* and *Schizosaccharomyces pombe* show a direct interaction<sup>116,243</sup>. Therefore, CAPs are indicated as bifunctional proteins, able to bind and regulate the actin cytoskeleton and activation of the AC<sup>117</sup>. Furthermore, the deletion of CAP leads to deficiencies in cell morphology, endocytosis, migration and development<sup>244-246</sup> (Fig 12D). CAPs are evolutionary highly conserved protein and there are at least two different CAP homologs identified, CAP1 and CAP2. These genes share 64% amino acid identity in mammals<sup>247,248</sup>. The CAP1 homologue is expressed widely in mammals, except in the skeletal muscle tissue, where CAP2 is mainly expressed in the skeletal muscle, heart, testis and in the brain<sup>245,247</sup>. This indicates more unique roles for CAP2, as for instance that CAP2 is a crucial mediator of the heart and skeletal muscle sarcomere assembly. Recently, it was shown that that CAP1 can rapidly translocate into to the mitochondria, where it induces actin- and cofilin-dependent apoptosis<sup>249</sup>. While CAP2 has been shown to for instance regulate the sarcomere assembly in striated muscles<sup>250</sup>. CAPs are multifunctional protein of 450-550 amino acids and have multiple domains. CAPs are composed of an  $\alpha$ -helix and a  $\beta$ -sheet region at the C-terminal domain and are mainly hydrophilic. The most important domains of CAPs, both structural and functional, identified in *Saccharomyces cerevisiae* are; (1) the N-terminal domain, that is able to physically interact with the AC and hereby can activate the Ras signaling pathway, (2) the C-terminal domain, involved in the actin cytoskeleton rearrangement<sup>243,251</sup> and (3) the central proline rich domain responsible for the association to SH3 domain-containing proteins (Fig. 12). The N-terminal domain (~40 residues) contains an alpha-helical coiled-coil structure<sup>252</sup>, that

is one of the subunit oligomerization motifs in proteins and is the part interacting with the AC in yeast <sup>253</sup>. However, the CAP N-terminal domain of *Dictyostelium* does not exert the same function. The N-terminal domain structure, as revealed by X-ray diffraction <sup>254</sup>, indicates a stable bundle of six antiparallel  $\alpha$ -helices called the helical folded domain (HFD) (Fig. 12B). In yeast, this domain is able to bind to the ADF-cofilin-G-actin complex <sup>255,256</sup> and associates with ADF/cofilin to mediate the F-actin severing <sup>257</sup>. The central domain contains two proline rich areas (P1 and P2). P1 is the most conserved region compared to the P2. There are several binding partners of CAPs that are able to either bind the P1 or P2, including for instance actin-monomer-binding protein profilin <sup>258,259</sup>. In addition, a region was detected that comes behind the SH3 binding domain that is called the Wiscott Aldrich Syndrome protein homology 2 (WH2) domain <sup>260,261</sup>. This domain is able to bind to both ATP- or ADP-G-actin, mediating actin nucleotide exchange <sup>262</sup>. The C-terminal domain of CAP consist mainly out of  $\beta$ -sheets and helices and is called the CARP domain <sup>263</sup> (Fig 12C). The last 27 amino acids of the C-terminal domain is the region where CAPs bind to actin and the last 35 amino acids sequence in this region contains a motif which allows CAPs to form dimers <sup>263-265</sup>. CAPs are able to dimerize and oligomerize, whereas this capacity of CAP has been implicated to have a role in the regulation of the actin cytoskeleton <sup>266</sup>. In yeast, Srv2/CAP (55 kDa) can form together with actin (42 kDa) a high-molecular-weight complex of over 600 kDa <sup>267,268</sup>, containing 6 molecules of each <sup>256,267</sup>. Three regions of CAP are able to self-associate: the coiled-coil region at the N-terminus <sup>256,269</sup>, the HFD domain <sup>254,270,271</sup> and the C-terminal motif <sup>263</sup> (Fig. 12). When the N-terminal coiled-coil region is mutated and thereby dimerization is disrupted, the binding between ADF/cofilin to F-actin is disrupted <sup>256,257</sup>, while the deletion of the C-terminal dimerization motif decreases the strength of the binding to actin <sup>265</sup>. This tells us that the oligomerization of CAP can promote its function in the regulation of actin. Nonetheless, the full function of CAP oligomerization and its role in actin regulation still need to be elucidated.



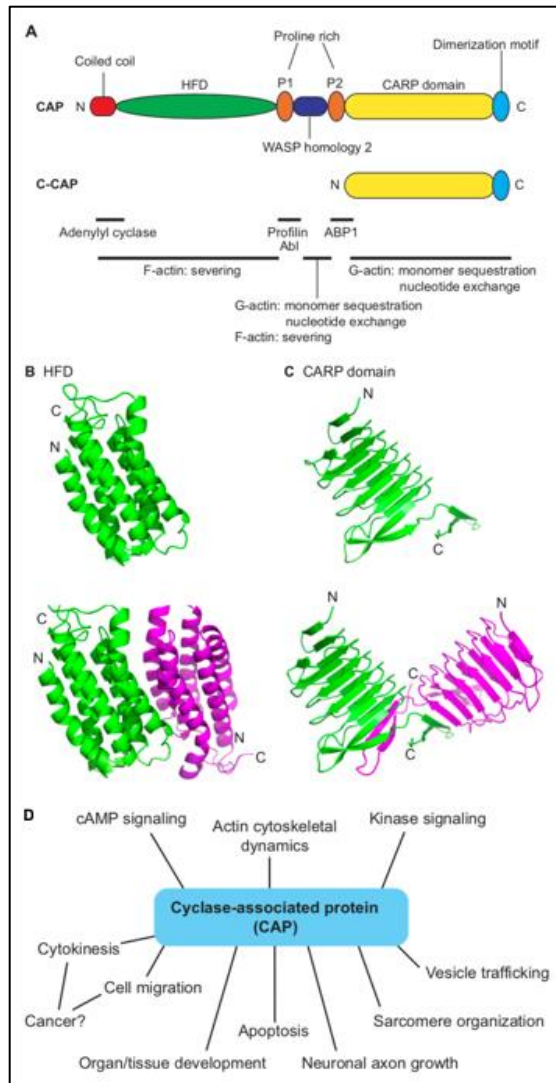


**Figure 12) Structure and biological functions of CAP.** A) The domain organization of CAP and C-CAP (CAP in protozoans). The representative interaction partners and actin-regulatory functions are shown below functional domains. B,C) Ribbon diagram of the structures of the helical folded domain (HFD) (B) and b-sheet/b-helix (CARP) domain C). Structures of monomers (top) and dimers (bottom) are shown. Locations of N- and C-termini are indicated. D) shows the known biological functions of CAPs. Obtained from S. Ono 2013<sup>266</sup>.

### 3.2.) CAP function in actin dynamics

As written above, CAP was first discovered as a component of the Ras-cAMP pathway, but the actin-regulatory function of CAPs are more evolutionarily conserved<sup>116</sup>. Biochemical studies have shown that CAPs have a sequestering role on the actin-monomers (G-actin) and thereby prevent the nucleation of actin and its elongation from the filaments<sup>272</sup>. Although, more recent studies, described below, demonstrated

a more active role of CAPs in promoting actin dynamics, making it necessary to revise the earlier studies.

### **Role of CAP on G-actin: monomer sequestering and nucleotide exchange enhancement**

The binding of CAP and G-actin occurs at a molar ratio of 1:1 and is able to reduce the spontaneous G-actin polymerization, demonstrated from yeast <sup>272</sup> to humans <sup>273</sup>. Furthermore, the results of the role of CAPs on actin are so far controversial, where in yeast it was shown that CAPs have an inhibiting effect on the incorporation of G-actin at both the pointed- and barbed-end of actin <sup>272</sup>, while another study demonstrates that CAP inhibits G-actin incorporation only at the barbed-end <sup>274</sup>. The main difference might be due to the different ratios of CAP and G-actin used. More importantly, CAPs are able to increase the nucleotide exchange rate of actin and thereby influencing actin polymerization. In the treadmilling process of actin, the actin-bound nucleotide exchange occurs mainly at the G-actin, where the hydrolysis of ATP to ADP occurs upon actin polymerization. Freshly depolymerized G-actin monomers are predominantly ADP-bound and when free ATP is available, the G-Actin-ADP can exchange its ADP for ATP, which is necessary for the maintenance of the treadmilling process. In concordance, when there is no free ATP available the treadmilling is prevented <sup>275-279</sup> (Fig. 13). Some other G-actin binding protein, including ADF/cofilin <sup>280</sup> and thymosin  $\beta$ 4 <sup>281</sup> inhibit the nucleotide exchange and prevent the actin from recharging ADP to ATP. Profilin promotes the nucleotide exchange of G-actin catalytically <sup>280,282,283</sup>, in a similar manner as CAP does <sup>255,256,267,284,285</sup> and in the presence of thymosin  $\beta$ 4 <sup>286,287</sup> or ADF/cofilin <sup>288,289</sup>, actin turnover is enhanced (Fig. 13). This similarity between CAPs and profilin was proven by the rescue of the cytoskeletal phenotypes after CAP knock down, by overexpressing profilin <sup>251</sup>. However, profilins are preferentially binding to ATP-G-actin <sup>287</sup>, CAP is competing with ADF/cofilin for the association to ADP-G-Actin <sup>255,274</sup>. The yeast CAP/SRV2 and CAP1 domain in human able to interact with the ADF/cofilin-actin complex was found to be located in the HFD domain and improves the ADF/cofilin-mediated turnover of F-actin <sup>255,256</sup>. More recent studies indicate a

different view, where the HFD domain is not required for this process, but has instead a role in the actin filament severing <sup>257</sup>. The site of CAP that are important for the monomer sequestering and nucleotide exchange activities are located in the WH2 and CARP domains in the C-terminal part of CAP. The C-terminal domain can bind one G-actin molecule <sup>272</sup>, whereas the WH2 and CARP domain can both bind an actin monomer as well <sup>262,273,274,290</sup>. Notably, the CARP domain of CAP is sufficient to induce the nucleotide exchange of ADP-G-actin <sup>290</sup>, whereas WH2 is mandatory to promote this exchange when ADF/cofilin is bound by ADP-G-actin <sup>262,291</sup>. This makes the WH2 domain probably mandatory for the competition of CAP and ADF/cofilin for the binding to G-actin <sup>266</sup> (Fig. 13).

### **Role of CAP on F-actin: filament severing**

Besides the binding to G-actin, CAPs are also able to bind with the filamentous form of actin and it is shown to promote the disassembly of the filaments <sup>255</sup>, which was again demonstrated by the microscopic images showing that CAP increases the severing of F-actin <sup>257,292</sup> (Fig. 13). CAP1 expressed in mammalian tissue is able to sever actin at a basic pH <sup>293-295</sup>, while if CAP1 is bound to ADF/cofilin they can sever F-actin at a bigger pH range <sup>292</sup>. This is why CAP1 or ADF/cofilin are probably a pH-dependent filamentous actin disassembly factors, while if they are forming a complex, they act as pH-independent F-actin severing factors. A genetic study done in yeast shows that the N-terminal HFD domain of CAP is important for this process <sup>257</sup>, however the functional mechanism of how the severing of actin filaments is done is still not known. Additionally, as far as concern, in mammalian CAP2, the severing of F-actin is mediated by the WH2 domain, which can sever F-actin without ADF/cofilin <sup>273</sup>.

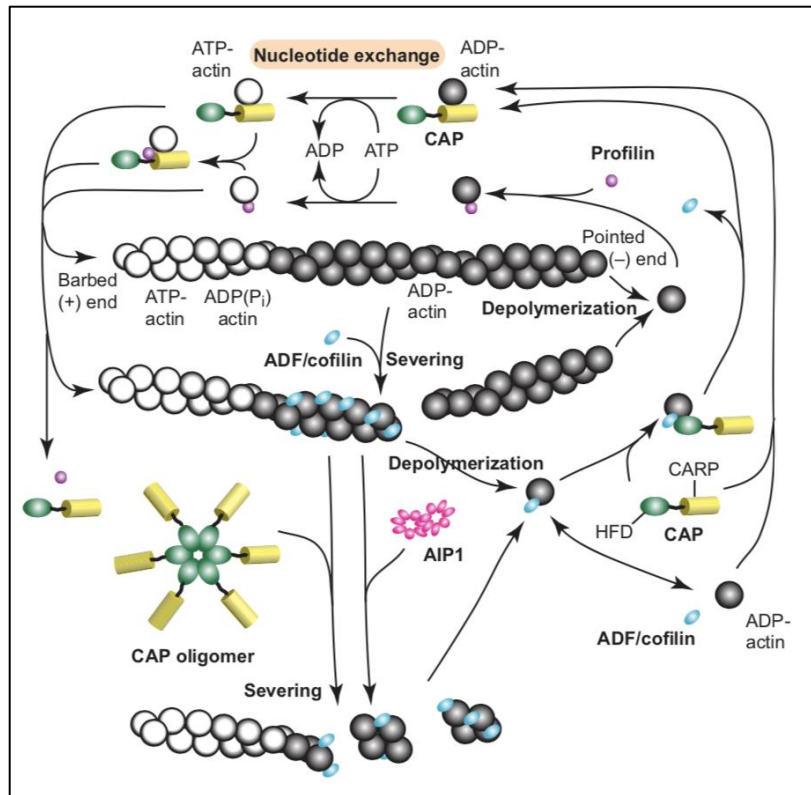


**Figure 13) Regulation of actin filament dynamics by CAP, ADF/cofilin, profilin and AIP1.** CAPs compete with ADF/cofilin for binding to G-actin (right) and promotes its nucleotide exchange (top). CAP can also promote severing of ADF/cofilin-bound actin filaments (bottom). These activities are similar to those exerted by profilin and AIP1. ADF/cofilin cooperatively binds to actin filaments and severs them at the boundary between ADF/cofilin- bound and the bare ends of the filaments. Note that the molecular organization of the CAP oligomer is hypothetical. Also note that CAP binds to actin monomers in an oligomeric form but, for simplicity, only a monomeric CAP is shown as a G-actin-bound form. Obtained from S. Ono 2013<sup>266</sup>

### 3.3.) CAP2

As mentioned above, higher eukaryotes express two different CAP homologs, CAP1 and CAP2, which are closely related. CAP2 is present in a limited amount of tissues, including the brain, which makes this protein an interesting protein with possibly unique roles<sup>246</sup>. While CAP1 is well studied <sup>245,255</sup>, the role of CAP2 is still poorly understood. With the use of a gene-trap model a CAP2 knockout mice was created (CAP2<sup>gt/gt</sup>), which serves as the best characterization of CAP2 so far. In the mice where CAP2 is abolished, a specific phenotype is expressed, including a decreased body weight and of survival, development of cardiomyopathy, disarrayed sarcomeric organization and loss of G-actin sequestering ability <sup>273</sup>. Only a subset of the mice survives, where in the other mice ablation of CAP2 is lethal, but it is unknown how these mice overcome the lethal phenotype <sup>273,296,297</sup>. Another study shows that CAP2 deficient mice have a delayed wound healing response presumably due to alterations in the actin cytoskeleton dynamics in keratinocytes and fibroblast and reveal a role for CAP2 in actin cytoskeleton regulation <sup>298</sup>. Furthermore, it is reported that CAP2 has a role in cancer, with increased levels of CAP2 in renal, brain, colon, bladder and thyroid cancer and a down regulation in breast cancer <sup>246</sup>. The CAP2 gene is localized on chromosome 6 in the 6p22.3 region in humans. A specific interstitial 6p22-24 deletion syndrome in chromosome 6 was reported where patients with this deletion show variable clinical phenotypes including developmental delay with cognitive deficits, brain-, heart- and kidney defects, craniofacial malformations and eye abnormalities <sup>299,300</sup>. Upon a deletion in this region those clinical symptoms are expressed and since CAP2 is expressed in the brain, it is most likely to be involved in the developmental deficits seen in these patients <sup>299</sup>.

### 3.4.) CAP2 in the brain

Given the abundant expression of CAP2 in the brain, the role in regulating actin dynamics, the clinical relevance in the 6p22-24 deletion syndrome and the fact that CAP2 expression is restricted in to only certain tissue, it suggests an important role in the function of the brain, in particular in neurodevelopment and synaptic plasticity regulated by actin dynamics. So far, one study shows a limited characterization of CAP2 in the brain using the same CAP2<sup>gt/gt</sup> mice model described above. Here the function of CAP2 in the brain is characterized as playing a role in synaptic plasticity, spine development and dendritic morphology<sup>301</sup>. CAP2 is expressed in multiple brain areas in embryonic and adult brain, including the hippocampus, cortex, olfactory bulb and cerebellum. No gross alteration in the overall brain morphology and size were seen in the CAP2<sup>gt/gt</sup> mice. In cortical neuronal cultures CAP2 is expressed in the soma, dendrites and its pre- and post-synaptic terminals, using synapsin I and PSD-95 as markers respectively, whereas colocalization with vGLUT1 indicates CAP2 is expressed in excitatory synapses. In these cultures, a colocalization between CAP2 and F-actin stained with TRITC-conjugated-phalloidin is observed. Additionally, the deletion of CAP2 has an impact on the neuronal development. In cultured cortical neurons, the CAP2<sup>gt/gt</sup> neurons show an increase in dendritic spine density with an increase of specifically the mature mushroom type of spines and an increase in the dendritic complexity of the neurons. Furthermore, as CAP2 is a regulator of filamentous actin, the deletion of CAP2 leads to an increase in F-actin content, with a 1.3-fold increase in F/G actin ratio in the whole brain lysate. In addition, a role of CAP2 is suggested in the surface trafficking of GluA1, where decreased levels of surface GluA1 are revealed upon CAP2 deletion and also induction of chemical LTP (cLTP) resulted in reduced surface GluA1 levels in the cortical neurons of CAP2<sup>gt/gt</sup> mice, implicating disrupted synaptic plasticity. Furthermore, CAP2 is able to bind neuronal cofilin through the C-terminal domain and that this interaction is dependent on the phosphorylation of cofilin, where in the mutant brain decreased phosphorylated-cofilin levels were associated with its aberrant localization. These data together delineate a possible role for CAP2 in synaptic plasticity, dendritic complexity, spine density and morphology

and AMPAR trafficking which is most probable mediated by its role in actin and cofilin regulation<sup>301</sup>. Additionally, microarray analysis of hippocampal gene expression of AD patients tissue, reported a downregulation of CAP2 gene<sup>302-304</sup>, indicating a role for CAP2 in AD.

**Aim**



Although AD, the major form of dementia, is emerging as the most prevalent and socially disruptive illness of the aging population, it is currently incurable. AD pathogenesis is multifaceted and difficult to pinpoint, but genetic and cell biological studies led to the amyloid hypothesis, which posits that A $\beta$  plays a pivotal role in AD pathogenesis<sup>5,16</sup>. A $\beta$  originates from the amyloid precursor protein (APP). Two enzymatic steps lead to the formation of A $\beta$ : the  $\beta$ -secretase BACE-1 cleaves APP<sup>6</sup>, followed by the second  $\gamma$ -secretase cleavage. Alternatively, APP can be cleaved by the  $\alpha$ -secretase, which prevents the formation of A $\beta$ , since  $\alpha$ -secretase cleavage occurs within the A $\beta$ -sequence. Recent studies demonstrate that, in neuronal cells, the non-amyloidogenic  $\alpha$ -secretase pathway is selectively mediated by ADAM10<sup>34-36</sup>. Therefore, enhancing ADAM10 cleavage of APP to limit A $\beta$  production might be a potentially effective way of addressing the problem of AD therapy<sup>35</sup>. It has been previously shown that ADAM10 is a synaptic protein, being an integral component of the excitatory postsynaptic density<sup>212</sup>. ADAM10 can be considered a major protease for membrane proteins, in particular of Notch, N-Cadherin and APP, in the central nervous system<sup>305</sup>. Indeed, ADAM10 activity can regulate not only the synaptic morphology but also a variety of neurotransmitter receptor-cell adhesion molecules interactions to strongly influence the degree of functional synaptic connectivity<sup>213,220</sup>. ADAM10 synaptic localization and activity towards APP are modulated by protein partners, which interact with ADAM10 cytoplasmic tail. For example, SAP97 and AP2 are responsible for ADAM10 forward trafficking to the synapse and ADAM10 endocytosis, respectively<sup>212,213</sup>. Notably, such interactions are altered in AD patients at the earliest stages of the disease<sup>241</sup>.

In light of the importance of ADAM10 cytoplasmic domain in the regulation of ADAM10 activity, we performed a two-hybrid screening and have recently identified a protein called cyclase-associated protein 2 (CAP2) as a novel protein partner of ADAM10. CAP2 is a member of the CAP family, which are evolutionary highly conserved multidomain actin-binding proteins involved in several processes as orchestrating changes in actin cytoskeleton such as cell migration, movement and

polarity, linking signaling pathways to elements of the cytoskeleton, vesicle trafficking and endocytosis <sup>117</sup>. Moreover, CAPs are essential for the regulation of the G- and F-actin balance. CAP1 and CAP2 are the two homologues members of the CAP family. CAP1 shows expression in nearly all cells, where CAP2 has a more limited expression, including the brain, indicating unique roles of CAP2 in neuronal cells <sup>245</sup>. Preliminary data show, with both a biochemical and an imaging approach, that CAP2 is confirmed to associate to actin and as a novel binding partner of ADAM10, whereas this interaction occurs along dendrites (Fig. 14A/B).

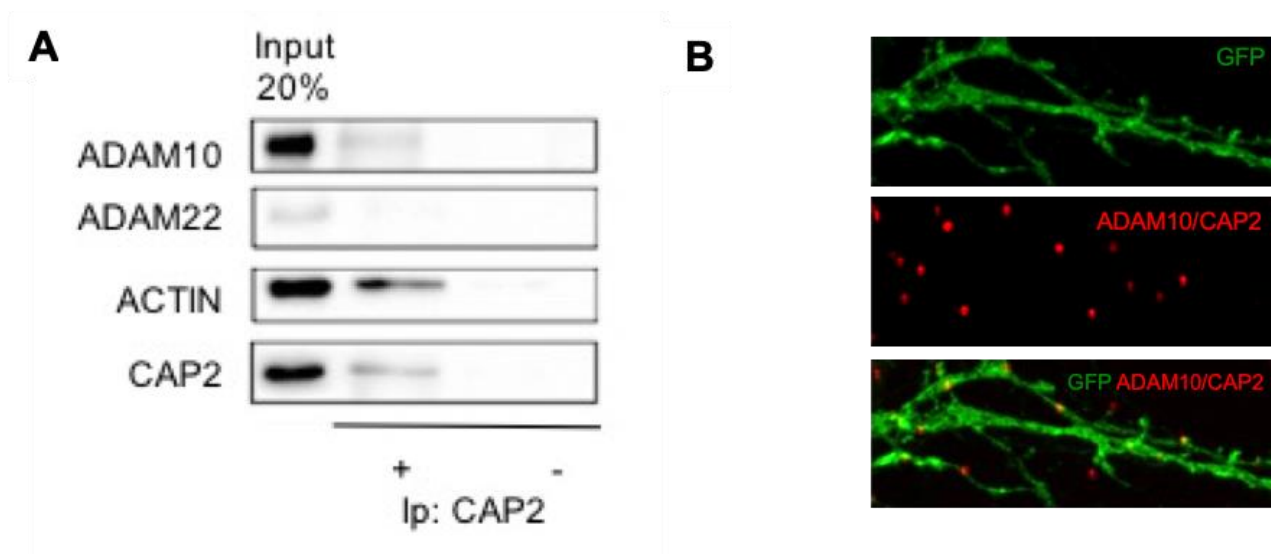


**Figure 14) CAP2 interacts with ADAM10 and Actin in neurons.**

A) Co-immunoprecipitation assay confirms CAP2 as a novel binding partner of ADAM10, but not of ADAM22, another member of the ADAM family. CAP2 is also able to precipitate actin.

B) Proximity Ligation Assays (PLA) show that the binding between CAP2 and ADAM10 is confirmed and the binding is localized along dendrites in primary hippocampal neurons.

These preliminary data suggest an important role for CAP2 in neuronal cells. Since it is a novel binding partner of ADAM10, and might have an influence on the regulation of its synaptic localization, it is important to understand the role of CAP2 in this physiological process and to unravel its role in AD.

Therefore, the aims of my project are:

1. To dissect the binding domains of CAP2 to ADAM10 and actin, and the role of these complexes in ADAM10 synaptic localization
2. To unravel the physiological role of CAP2 in the brain
3. To characterize the ADAM10/CAP2/Actin complex in activity-dependent plasticity phenomena
4. To evaluate ADAM10/CAP2/actin complex role in aberrant plasticity phenomena triggered by A $\beta$  oligomers
5. To analyze ADAM10/CAP2/actin complex in AD patients and animal models at different stages of the disease.
6. To generate therapeutic approaches to interfere selectively with the CAP2 complex formation with actin and ADAM10.

# Materials & Methods

## 1.) Human Tissue

The hippocampus (Hp) from late onset/sporadic AD patients (AD;  $n=6$ , Braak 4/5 level) and age-matched healthy controls (HC;  $n=6$ ) were obtained from the Netherlands Brain Bank. Stringent criteria were used for the selection of human brain tissues employed in this study. HC have no history of psychiatric or neurological disease and no evidence of significant age-related neurodegeneration. For detailed information see table 1.

Subjects	Gender	Age at death, years		PMD, hours		pH CSF		Brain weight, g		Braak level
1 (AD)	M	82		5,15		6,34		1182		5
2 (AD)	F	84		5,55		6,42		1017		5
3 (AD)	F	88		6,45		6,5		1148		5
4 (AD)	F	91		6,25		6,05		1026		4
5 (AD)	M	90		5,55		6,37		1080		4
6 (AD)	M	91		4,1		6,28		1117		4
mean +/- SD		87,67	+/- 3,83	5,51	+/- 0,84	6,33	+/- 0,15	1095	+/- 66,23	
1 (HC)	F	85		6,25		6,6		1080		3
2 (HC)	F	89		6,35		6,73		1139		3
3 (HC)	F	91		4,1		6,58		1052		3
4 (HC)	M	83		5,15		6,6		1372		1
5 (HC)	M	80		4,25		6,59		1429		2
6 (HC)	M	89		6,5		6,23		1185		2
mean +/- SD		86,1667	+/- 4,22	5,43	+/- 1,09	6,56	+/- 0,17	1210	+/- 156,03	

**Table 1:** Demographic and neuropathological characteristics of AD and HC cases.

AD (Alzheimer's Disease); CSF (Cerebrospinal fluid); F (Female); M (Male); PMD (Postmortem delay)

## **2.) Animals**

### **2.1.) Primary hippocampal rat neurons**

Sprague-Dawley rats of 6 weeks, and its E18 embryos were used for the preparation of primary hippocampal neuron cultures. The Institutional Animal Care and Use Committee of the University of Milan and the Italian Ministry of Health (#326/2015) approved all experiments involving neuronal cultures preparation.

### **2.2.) APPPS1 mice**

APP/PS1 mice (double transgenic mice expressing a chimeric mouse/human amyloid precursor protein (Mo/HuAPP695swe) and a mutant human presenilin 1 (PS1-dE9)), directed to CNS neurons were used either wild type or heterozygous. (reference link of the animal model: <https://www.jax.org/strain/005864> and <https://www.alzforum.org/research-models/appswepsen1de9-0>). Animal handling and surgical procedures were carried out with care taken to minimize discomfort and pain and in accordance with ethical regulations and guidelines of the European Communities Council (Directive of 14 November 1986, 86/609/EEC) The Institutional Animal Care and Use Committee of the University of Milan and the Italian Ministry of Health (#497/2015) approved all experiments involving APP/PS1 mice.

### **2.3.) CAP2 KO mice**

CAP2 KO mice tissues were kindly provided by our collaborator Dr. Marco Rust (University of Marburg). All mice used are adult mice between 5 to 6 months of age. For the in-vivo spine morphology all female mice were used, where for biochemical analysis a mix of male and female mice were used.

## **3.) Plasmids**

EGFP CAP2 plasmid was a kind gift from Professor Angelika Noegel (University of Cologne). This plasmid was used to perform a point mutation inserting a stop codon for the codon corresponding to aa 452 using the QuickChange site-directed mutagenesis kit (Stratagene, La Jolla, CA) following the manufacturer's instructions to prepare specific CAP2 mutations. Myc CAP2 plasmid was created using the restriction

enzyme and then used to introduce point mutations inserting a stop codon for the codon corresponding to aa 452 and C32G using the QuikChange site-directed mutagenesis kit (Stratagene, La Jolla, CA) following the manufacturer's instructions. EGFP plasmid was kindly provided by Dr. Maria Passafaro (CNR, Milan, Italy). The TAC-RAR-ADAM10 plasmid was created in our lab previously and used according to previous protocol<sup>306</sup>.

#### **4.) Cell Culture preparation and transfection.**

Hippocampal neuronal primary cultures were prepared from embryonic day 18-19 (E18-E19) rat hippocampi. The cells were plated in DMEM medium containing Horse Serum, Glutamax and Pen/Strep and +/- 16 hours after plating the medium was changed to Neurobasal medium containing B27 supplement, Glutamax and Pen/Strep. Neurons were transfected between DIV7-DIV10 using calcium-phosphate co-precipitation method with 1-2 µg of plasmid DNA. According to their purpose, neurons were treated, lysed or fixed at DIV 14 and then used for immunocytochemistry or PLA assay or for biochemical purposes.

#### **5.) Immunocytochemistry**

For co-localization and morphological studies hippocampal neurons were fixed for 5 minutes with 4% Paraformaldehyde (PFA)-4% sucrose in PBS solution at room temperature and washed with PBS for several times after. Cells were permeabilized with 0.1% Triton X-100 in PBS for 15 min at room temperature and then blocked with 5% BSA in PBS for 30 min at room temperature. Cells were then labelled with primary antibodies at 4 °C in an overnight incubation. Cells were washed and then incubated with secondary antibodies for 1 h at room temperature. After, the cells were washed in PBS and mounted on glass slides with Fluoromount mounting medium (Sigma Aldrich). Cells were chosen randomly for quantification from different coverslips. Fluorescence images were acquired by using Zeiss Confocal LSM510 Meta system or with the Nikon Ti2 A1 system. We obtained the images with sequential acquisition setting at 1024x1024 pixels resolution; for each image two up to eight 0.5µm sections were acquired and a z-projection was obtained<sup>220</sup>.



## 6.) Proximity Ligation Assay (PLA)

Brightfield PLA was essentially performed according to the protocol of the manufacturer. We used snap frozen (by isopentane on dry ice) brain tissue that was sectioned with A Leica CM 3050 cryostat to cut 10 µm thin brain sections which were mounted on Superfrost™ Plus Gold slides (Thermo Fisher Scientific) and stored at -20 °C until use. Before use the brain sections were kept at room temperature for 30 minutes and were fixed for 10 minutes at room temperature in 4 % paraformaldehyde, washed with phosphate buffered saline (PBS) and permeabilized with 0.4 % CHAPSO for another 10 minutes at room temperature. Endogenous peroxidase activity was blocked with hydrogen peroxide solution by 10 minutes incubation at room temperature and the slices were then washed in washing solution A. Unspecific binding sites for antibodies were blocked for 30 minutes with blocking solution at 37 °C and the slices were subsequently incubated with primary antibodies overnight at 4 °C. The following day, secondary probes attached to oligonucleotides were added and, after washing, the oligonucleotides of the bound probes were ligated, amplified and made visual by addition of the detection reagent and substrate solution. After addition of the nuclear stain solution, containing Mayer's haematoxylin, the brain slices were dehydrated in ascending concentrations of ethanol and finally xylene and subsequently mounted. The PLA signals were visualized using a light microscope (Nikon Eclipse E800M). A 40x objective was used when capturing images which were analyzed using the Image J software.

As negative controls for the PLA experiments, we omitted one of the primary antibodies. However, we found that similar amounts of signals appear in the negative controls also when performing PLA without any primary antibodies. Hence, as negative control we decided to exclude primary antibodies altogether. For quantification, PLA signals generated in the negative control samples were subtracted from the signals generated in the interaction samples.

For the PLA on primary hippocampal neurons, we used DIV14 neurons, fixed with 4% PFA for 5 minutes at room temperature. Then the neurons were washed several times

with PBS for 30 minutes at room temperature. Then the neurons were permeabilized with 0,1% Triton X-100 in PBS for 15 minutes at room temperature and then washed several times with PBS for 30 min at room temperature. The blocking was done with the blocking solution from the PLA kit (Sigma), and the cells were incubated over night with the primary antibodies. The next day we proceeded according to the manufacturer's instructions using the fluorescent method. In short, the next morning the neurons were washed for several times with washing solution A for 15 minutes. Then secondary probes attached to oligonucleotides were added and, after washing, the oligonucleotides of the bound probes where ligated, amplified by a fluorescent polymerase that visualizes the PLA signal in the 555nM filter channel of the confocal microscope (Nikon Ti2 A1)

After the instructions we did a fluorescent immunocytochemistry staining of either the GFP filled neurons or a neuronal marker in the 488nM filter channel. The cells were washed with PBS several times for 30 min at room temperature, then incubated for 1 hour with the primary antibody at room temperature, washed again with PBS several times for 30 min, incubated with the secondary antibody for 1 hour, washed again with PBS several times for 30 min and then mounted in Fluoromount medium (Sigma). As negative controls for the PLA experiments in we omitted one of the primary antibodies. However, we found that similar amounts of signals appear in the negative controls also when performing PLA without any primary antibodies. Hence, as negative control we decided to exclude primary antibodies altogether. For quantification, PLA signals generated were counted by hand and normalized on the total length of the dendrites.

## **7.) DIL labeling for spine morphology**

Carbocyanin dye Dil (Invitrogen) was used to label neurons as it is a lipophilic fluorescent molecule. Protocol used for labeling has been previously described<sup>307</sup>. In short, Dil crystals were applied using a thin needle by delicately touching of the region of interest on both sides of a 3mm hippocampal piece prepared after cardiac perfusion with 1.5% PFA in PB 0.1M. Dil crystals were left to diffuse for 1 day in the dark at room temperature, then slices were post-fixated with 4% PFA in 0.1M PB for 45 minutes at

room temperature. 100  $\mu\text{m}$  hippocampal slices were obtained with a vibratome. The first slices containing the Dil crystals was discarded and the rest of the slices were mounted on Superfrost<sup>TM</sup> glass slides (Thermo Fisher) with fluoromount (Sigma) for confocal imaging. A Nikon Ti2 A1 confocal microscope was used and we obtained the images with sequential acquisition setting at 1024x1024 pixels resolution with the 63x objective and the 555nm channel; for each image between 40 and 100 sections of 0.5 $\mu\text{m}$  were acquired and an appropriate z-projection was obtained.

## **8.) Free-floating fluorescent immunohistochemistry (F-IHC)**

Mice were anesthetized and perfused with 4% PFA in PBS (pH 7.2-7.6) in their right atrium for approximately 10 minutes. The brain was removed and placed in post fixation (4% PFA) for 1.5 hours. After post fixation, the brains were washed with 1x PBS and 50 $\mu\text{m}$  coronal brain sections were cut with a vibratome and maintained free-floating in PBS until F-IHC was carried out. For antigen retrieval, sections were treated with a solution of citrate buffer (10mM citric acid and 0.05% Tween, pH 6), which was boiled, and sections were transferred carefully into the solution and cooled off to room temperature. Then, sections were washed multiple times with 1xTBS, and blocked in 4% normal goat serum in 0.1% Triton-X 100 in TBS1x at room temperature for 1 hour. After, sections were incubated with primary antibodies in 0.1% Triton-X 100 solution over night at 4°C. The morning after, the sections were washed with 1x TBS multiple times and incubated with the secondary antibody conjugated with different fluorophores, able to recognize the primary antibodies, at room temperature for 2 hours. After the labelling of the sections with the secondary antibody, the sections were washed multiple times with TBS 1x, and then the nuclei were stained with DAPI for 5 minutes. Then sections were mounted on SuperFrost Plus slides with fluoromount media and protected by a coverslip. Fluorescent images were obtained by the Nikon Ti2 A1 confocal microscope system with a 63x objective and acquisition setting at 1024x1024 pixel resolution.

## 9.) Cell culture electrophysiology

Electrophysiological recordings were performed by our collaborator Flavia Antonucci (University of Milan). In short, hole-cell patch-clamp recordings of mEPSCs were obtained from DIV 15-16 neurons using a Multiclamp700A amplifier (Molecular Devices) and pClamp-10 software (Axon Instruments, Foster City, CA). All the recordings were performed in the voltage-clamp mode. Currents were first sampled at 5 kHz and then filtered at 2-5 kHz. Recording pipettes, tip resistances of 3-5M $\Omega$  were filled with the intracellular solution of the following composition (in mM): 130 potassium gluconate, 10 KCl, 1 EGTA, 10 HEPES, 2 MgCl<sub>2</sub>, 4 MgATP, 0.3 Tris-GTP. In the beginning of the experiment, mEPSCs have been recorded in the external solution [Krebs' Ringer's-HEPES (KRH)] with the following composition (in mM): 125 NaCl, 5 KCl, 1.2 MgSO<sub>4</sub>, 1.2 KH<sub>2</sub>PO<sub>4</sub>, 2 CaCl<sub>2</sub>, 6 glucose, 25 HEPES-NaOH, pH 7.4 in which also TTX (0.5  $\mu$ M), bicuculline (20  $\mu$ M, Tocris, Bristol, UK) and strychnine (1  $\mu$ M, Sigma-Aldrich, Milan, Italy) were included.

To induce chemical LTD, NMDA (20  $\mu$ M) and glycine (20  $\mu$ M, Sigma-Aldrich, Milan, Italy) were applied for 3 minutes at room temperature in Mg<sup>2+</sup>-free KRH containing TTX (0.5  $\mu$ M), bicuculline (20  $\mu$ M) and strychnine (1  $\mu$ M). 30 minutes after this treatment mEPSCs were collected in the starting KRH solution. Synaptic depression has been also induced in cultures by 30 minutes of oA $\beta$ 1-42 (500nM) in Mg<sup>2+</sup>-free KRH containing only TTX (0.5  $\mu$ M), bicuculline (20  $\mu$ M) and strychnine; again following this treatment mEPSCs were recorded in normal KRH and analyzed. Off-line analysis of miniature events was performed by the use of Clampfit- pClamp-10 software.

## 10.) Subcellular Fractionation and purification of post-synaptic densities and Triton insoluble postsynaptic fractions

To isolate PSDs, rat hippocampi (from 15 animals) were rapidly dissected and pooled. Homogenization was carried out by 10 strokes in a Teflon-glass homogenizer in 4ml/gr of ice-cold 0.32M sucrose containing 1mM HEPES, 1mM MgCl<sub>2</sub>, 1mM NaHCO<sub>2</sub>, and 0.1mM phenylmethylsulfonyl fluoride (PMSF) (pH 7.4). Everything was done at 4°C from here. The homogenized tissue was centrifuged at 1,000g for 10 minutes. The

obtained supernatant was centrifuged at 13,000g for 15 minutes to get mitochondrial and synaptosome fractions. The pellet was resuspended in 2.4ml/gr of 0.32M sucrose containing 1mM HEPES, 1mM NaHCO<sub>3</sub> and 0.1mM PMSF, overlaid on a sucrose gradient (0.85-1.0-1.2M) and centrifuged at 82,500g for 2hours. The fraction between the 1.0 and 1.2M sucrose was removed, diluted with an equal volume of 1% Triton X-100 in 0.32M sucrose containing 1mM HEPES for 15 minutes. This solution was centrifuged at 82,500g for 45 minutes. The pellet (containing the PSD1 or triton insoluble fraction (TIF)) was resuspended and layered on a sucrose gradient (1.0-1.5-2.1M) and centrifuged at 100,000g for 2hours. The fraction between 1.5 and 2.1M was removed and diluted in an equal volume of 1% Triton X-100 and 150mM KCl. The final PSD2 fraction was collected after a centrifugation at 100,000g for 45 minutes and stored at -80°C until usage.

TIF, a fraction highly enriched in PSD proteins (including receptors, signaling, scaffolding and cytoskeletal elements) but absent of presynaptic markers, was isolated from human, rat and mice brain tissue (Hippocampus/Cortex/Half brain). To obtain this fraction, samples were homogenized at 4 °C in an ice-cold buffer containing 0.32 M Sucrose, 1 mM HEPES, 1 mM NaF, 0.1 mM PMSF, 1 mM MgCl in the presence of protease inhibitors (*Complete<sup>tm</sup>*, GE Healthcare, Mannheim, Germany) and phosphatase inhibitors (*PhosSTOP<sup>tm</sup>*, Roche Diagnostics GmbH, Mannheim, Germany), using a glass-Teflon homogenizer. Homogenates were then centrifuged at 1,000g for 5 min at 4 °C, to remove the nuclear contamination and white matter. The supernatant was collected and centrifuged at 13,000g for 15 min at 4 °C. The collected pellet (P2 crude membrane fraction) was resuspended in a hypotonic buffer (1mM HEPES with *Complete<sup>tm</sup>*) and centrifuged at 100,000 g for 1h at 4°C. Triton X-100 extraction of the resulting pellet was done for 15 minutes in an extraction buffer (1% Triton X-100, 75 mM KCl and *Complete<sup>tm</sup>*). After extraction, the samples were centrifuged at 100,000 g for 1h at 4°C and TIF were obtained by resuspending the pellet in a 20mM HEPES with *Complete<sup>tm</sup>* buffer using a glass-glass homogenizer.

TIFs from hippocampi of mice or rats were obtained using a shorter protocol without the first 1,000g centrifugation and the first 100,000g centrifugation. Protein content of

the samples was quantified by using the Bradford Bio-Rad (Hercules, CA, USA) protein assay.

### **11.) Co-immunoprecipitation assay**

100 µg of proteins from rat hippocampus or HEK 293/COS 7 homogenate or 50 µg of proteins from rat hippocampus TIF were in RIA buffer containing 200 mM NaCl, 10 mM EDTA, 10 mM Na<sub>2</sub>HPO<sub>4</sub>, 0.5% NP-40, 0.1% SDS and protein A/G- agarose beads (Thermo Fisher) as pre-cleaning procedure. Primary antibodies were added leaving to incubate overnight at 4 °C on a wheel. Protein A/G-agarose beads were added, and incubation was continued for 2 hours at room temperature on a wheel. Beads were collected by gravity or centrifugation (1,200 rpm) and washed three times with RIA buffer before adding sample buffer for SDS-polyacrylamide gel electrophoresis (SDS-PAGE) and the mixture was boiled for 10 min. Beads were pelleted by centrifugation, all supernatants were applied onto 7-8% SDS-PAGE gels.

### **12.) Western Blotting**

The electrophoretically separated protein on 7% to 12% SDS-PAGE gel were transferred on to a nitrocellulose membrane. The transfer was performed in a blotting buffer containing 20% methanol and 1x blotting buffer (Tris 0.025M, Glycine 0.192M at a pH 8.3) for two hours at 240mA. After the transfer procedure, membranes were blocked in iBlock-TBS (Invitrogen, T2015) or 5% milk in TBS for at least 45 minutes and subsequently incubated with primary antibodies overnight at 4 °C in iBlock-TBS or 3% milk-TBS. The next day, membranes were washed in Tris-buffered saline/tween 20 (TBST) for 3 times for at least 10 minutes each wash, at room temperature. Then, membranes were incubated with horseradish peroxidase (HRP)-coupled secondary antibody (Bio-rad Laboratories) for 1 hour at room temperature and washed again 3 times for 10 minutes at room temperature. For detection, Clarity™ Western ECL Substrates (Bio-Rad Laboratories) were used. For chemiluminescence the membranes were exposed to trans-UV (302nm) with Chemidoc MP system (Bio-Rad Laboratories).

### **13.) ELISA**

A Mouse/Rat sAPP-alpha (high-sensitive) ELISA was used to measure the ADAM10 activity on APP in the APP/PS1 wild type animals treated with the CAP2-Actin peptide. We conducted the assay according to the manufacturer's protocol. (Catalog No. JP27419, IBL/Tecan).

A Mouse/Rat A $\beta$ <sub>1-42</sub> (high-sensitive) ELISA was used to measure A $\beta$  levels in CAP2 KO mice compared to wild type animals. The ELISA was performed according to manufacturer's protocol. (Catalog No. RE45721, IBL/Tecan).

### **14.) Primary neuronal culture treatment**

#### **14.1.) Amyloid Beta**

Synthetic A $\beta$  peptide (A $\beta$ <sub>1-42</sub>) and its scramble inverse sequence (A $\beta$ <sub>42-1</sub>) were purchased from Bachem (Bubendorf, Switzerland), and oligomers were prepared according to<sup>308</sup>. In short, the lyophilized powder was dissolved in 1,1,1,3,3,3-Hexafluoro-2Propanol (HFIP, Sigma-Aldrich) at a final concentration of 1 mM. This solution was sonicated for 10 minutes and after it was aliquoted (10 $\mu$ l) in sterile tubes and left over-night under the hood for HFIP evaporation. The day after the tubes were centrifuged in a Speedvac to remove the remaining traces of HFIP or moisture. The resulting peptide was stocked at -20°C. For oligomers preparation itself, the peptides were placed at room temperature for 5 minutes and were then resuspended in DMSO at 5mM final concentration, vortexed for 30 seconds and sonicated for 10 minutes, then they were diluted with cold Neurobasal medium without phenol red to obtain a final concentration of 100  $\mu$ M. The resulting solution was vortexed for 15 seconds and transferred to 4°C for 24 hours before use for the oligomers to form. The quality of the oligomer preparation was controlled by the separation of the protein onto a 13% Tris-Tricine gels and revealed by western blots against the amyloid- $\beta$  peptide (6E10; Covance, CA, USA), or used for a total protein staining using Coomassie staining. To analyse the presence of oligomeric and fibrillar forms, TEM experiments were performed applying 5  $\mu$ l of protein suspension to a glow-discharge coated carbon grid (Cu 300 mesh, Electron Microscopy Sciences, PA, USA) for 1 min and then negatively

stained with 2% Uranyl acetate. Sample was observed with an EFTEM Leo912ab (Zeiss, Germany) operating at 100 KV and digital images were acquired by a CCD camera 1kx1k (Proscan, Germany) and iTEM software (Olympus, Germany). For experimental procedures, primary hippocampal neurons were treated at DIV14 for 30 minutes. A final concentration of 500 nM or 1  $\mu$ M was used. After 30 minutes the cells were fixed or lysed and used for PLA, ICC or biochemical experiments.

#### **14.2.) Long Term Potentiation**

To induce chemical LTP, hippocampal neuronal cultures at DIV14 were incubated in artificial cerebrospinal fluid (ACSF) for 30 minutes at 37°C: 125 mM NaCl, 2.5 mM KCl, 1 mM MgCl<sub>2</sub>, 2 mM CaCl<sub>2</sub>, 33 mM D-glucose, and 25 mM HEPES (pH 7.3), followed by the LTP stimulation by 50  $\mu$ M forskolin, 0.1  $\mu$ M rolipram, and 100  $\mu$ M picrotoxin (Tocris) in ACSF (no MgCl<sub>2</sub>) at 37°C. After 16 minutes of stimulation, neurons were replaced in regular ACSF for 15 minutes at 37°C and then lysed for TIF extraction or fixed for PLA/immunocytochemistry.

#### **14.3.) Long Term Depression**

To induce chemical LTD, hippocampal neuronal cultures at DIV14 were incubated with ACSF as for the LTP, followed by incubation with 50 NMDA  $\mu$ M in ACSF (with MgCl<sub>2</sub>) for 10 minutes at 37°C. Then the neurons were placed back in regular ACSF for 20 minutes at 37°C, and then lysed for TIF extraction or fixed for PLA/immunocytochemistry.

#### **15.) Cell-Permeable peptide treatment**

The cell-permeable peptides were created by fusing the peptides with the HIV Tat-derived peptide, which is a small basic peptide that has been shown to successfully deliver a large variety of cargoes, from small particles to proteins, peptides and nucleic acids. The domain conveying the cell penetrating properties appears to be confined to a small (11 amino acid) stretch of basic amino acids, with the sequence (YGRKKRRQRRR)<sup>309</sup>. On the basis of the interaction domain between CAP2 and Actin we developed 2 different active peptides and the corresponding inactive peptide. The



designed peptides were then produced by Bachem and upon arrival resuspended in sterile dH<sub>2</sub>O with a stock concentration of 1mM.

Neurons from primary cultures were treated at DIV14 at the concentrations of 1 μM or 10 μM in complete neurobasal medium. Treatments were done for 30 minutes at 37°C before the neurons were lysed or fixed for biochemical experiments or ICC. Adult mice (6 months of age) were treated with active or the inactive peptide at a concentration of 3nmol/gram diluted in sterile saline or treated with the vehicle alone. Peptides were administered with intraperitoneal injections. As an acute treatment 1 injection was done and the mice were sacrificed 24hours after the injection. For chronic treatment the mice were given daily injections for 2 weeks, followed by behavioral test and sacrifice. The tissue was used for Dil Labeling/spine morphology and biochemistry/TIF extraction.

## 16.) Antibody list

<b>Antibody</b>	<b>Species</b>	<b>Company</b>
Actin	Rabbit	Sigma-Aldrich
Actin	Mouse	Sigma-Aldrich
ADAM10	Rabbit	Abcam
ADAM10	Rat	R&D
ADAM10	Goat	Santa Cruz
ADAM10	Rabbit	Proscience
AP50	Mouse	BD Bioscience
APP 6E10	Mouse	Millipore
APP C-term	Mouse	Sigma-Aldrich
BACE-1	Rabbit	Cell Signalling
Calnexin	Rabbit	ENZO life sciences
Calreticulum	Rabbit	Thermo Scientific
CAP1	Rabbit	Protein Tech
CAP2	Rabbit	Protein Tech
CAP2	Goat	Santa Cruz
Cofilin	Rabbit	Cell Signalling
Cofilin-Phospho	Rabbit	Cell Signalling
GAPDH	Rabbit	Santa Cruz
GFP	Chicken	Millipore
GluA1	Mouse	Neuromab
GluA1-Phospho s845	Rabbit	Millipore
GluN2A	Rabbit	Sigma-Aldrich
GluN2B	Rabbit	Sigma-Aldrich
GluN2B	Mouse	Neuromab
GM130	Mouse	BD Bioscience
Histone H3	Rabbit	Protein Tech
HSA	Mouse	Sigma-Aldrich
MAP2	Guinea Pig	Synaptic Systems
Myc	Mouse	Roche / Sigma-Aldrich
Myc	Rabbit	Santa Cruz
N-Cadherin	Mouse	BD Bioscience
Notch1	Rabbit	Thermo Scientific
PDI	Mouse	Affinity BioReagents
PSD95	Mouse	Neuromab
SAP97	Mouse	ENZO life sciences
Synaptophysin	Mouse	Synaptic Systems
Tac-RAR (7G7)	Mouse	Gift of Dr. Bonifacino
Tau-Phospho (AT8)	Mouse	Cell Signalling
Tubulin	Mouse	Sigma-Aldrich
$\alpha$ -Adaptin	Mouse	BD Bioscience
$\beta$ -Adaptin	Mouse	BD Bioscience

## 17.) Quantification and statistical analysis

Quantification of Western Blot analysis was performed by means of computer-assisted imaging (ImageLab, Bio-Rad Laboratories). The levels of the proteins were expressed as relative optical density (OD) normalized on actin, tubulin, GAPDH or Calnexin. Levels and values are expressed as mean +/- standard error of the mean (SEM), of at least three independent experiments. Imaging acquired with a brightfield or confocal microscope were analyzed with the use of Fiji / Image J software (National Institute of Health, Bethesda, MD, USA). Colocalization analysis was performed using Zeiss AIM 4.2 software. For colocalization, PLA and morphological analysis, cells were chosen randomly for quantification from 4 different coverslips (2-3 independent experiments), images were acquired using the same settings/exposure times, and at least 10 cells for each condition were analyzed.

Statistical evaluations were performed by using 2-tailed Student *t* test (a *p* value less than 0.05 was considered significant) or, when appropriate, by using one-way ANOVA followed by Tukey or Bonferroni's as a *post hoc* test.

# Results

## **1.) Identification of the molecular determinants of the CAP2/ADAM10/Actin complexes**

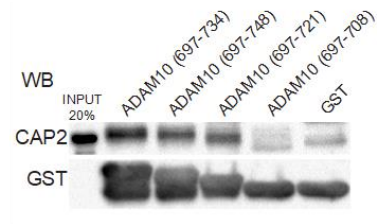
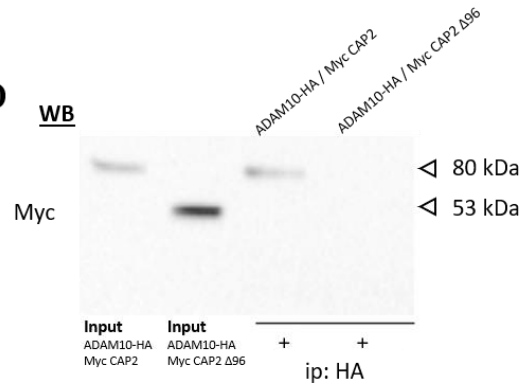
### **1.1.) Analysis of the regions responsible for CAP2/ADAM10 complex formation**

In order to identify the domain of ADAM10 cytoplasmic tail recognized by CAP2, we carried out pulldown assays. Fusion proteins of glutathione-S-transferase (GST) and GST bound to ADAM10 C-terminal domain (GST-ADAM10 Ct) were incubated with rat hippocampus homogenate. GST-ADAM10 Ct was able to specifically pull-down CAP2. Therefore, we tested a series of deletion mutants of GST-ADAM10 Ct, to identify the domain of ADAM10 responsible for the interaction with CAP2. Truncation of the last 41 aa of ADAM10 tail (GST-697-708) abolished binding to CAP2 (Fig. 1A).

To understand which is the CAP2 binding site to ADAM10, multiple deletion mutant of CAP2 were produced to define the binding region with ADAM10. To this aim, we took advantage of a HEK293 cell line with a stable ADAM10-HA transfection and transiently transfected them with either MycCAP2 or the deletion mutant MycCAP2 $\Delta$ 96. Co-immunoprecipitation (Co-IP) experiments revealed that the first 96 aa of the N-terminal part of CAP2 is required for ADAM10 interaction (Fig. 1B/C).

**A**

ADAM10 (697-748) GRKICSVHTPSSNRRKPLPGTLKPPPPQFIQQQRPREYQMGHMTT  
 ADAM10 (697-734) GRKICSVHTPSSNRRKPLPGTLKPPPPQFIQQQRP  
 ADAM10 (697-721) GRKICSVHTPSSNRRKPLPGTL  
 ADAM10 (697-708) GRKICSVHTPSSN

**B****C****D**

**Figure 1) The membrane-proximal proline rich domain of ADAM10 binds the N-terminal region of CAP2.**

**A)** Scheme of representation of ADAM10 mutants.

**B)** Representative Western Blot (WB) of a pull-down assay carried-out with GST- ADAM10 Ct and a series of GST- ADAM10 Ct deletion mutants were incubated with rat hippocampus homogenate. GST- ADAM10 Ct was able to specifically pull-down CAP2, while the lack of the last 41 aa of ADAM10 tail (GST-697-708), abolished CAP2 binding.

**C)** Scheme of a representation of CAP2 mutants.

**D)** ADAM10-HA stable transfected HEK293 cells were transfected with Myc-CAP2 / Myc-CAP2 Δ96 and were lysed and immunoprecipitated (IP) with HA antibody. WB analysis was carried out with an anti Myc. Myc CAP2 is able to bind ADAM10, while CAP2 Δ96 is not able to bind to ADAM10 any longer.

## 1.2.) CAP2 binding domain with actin

Since it was clear that CAP2 binds actin (See Fig. 14 in the aim), the next step was to identify the actin binding region in CAP2 sequence. As it was reported that the CAP2 C-terminal domain is able to bind actin<sup>263-265</sup>, a deletion mutant was created lacking the last 22 aa of CAP2 (CAP2 452Δ). Both with Co-IP and GST-pull down we demonstrate that the CAP2 452Δ mutant is not able to bind to actin (Fig. 2). Additionally, the mutant CAP2 Δ96 is still able to interact with actin, thus demonstrating that ADAM10 and actin do not compete for the binding to CAP2.

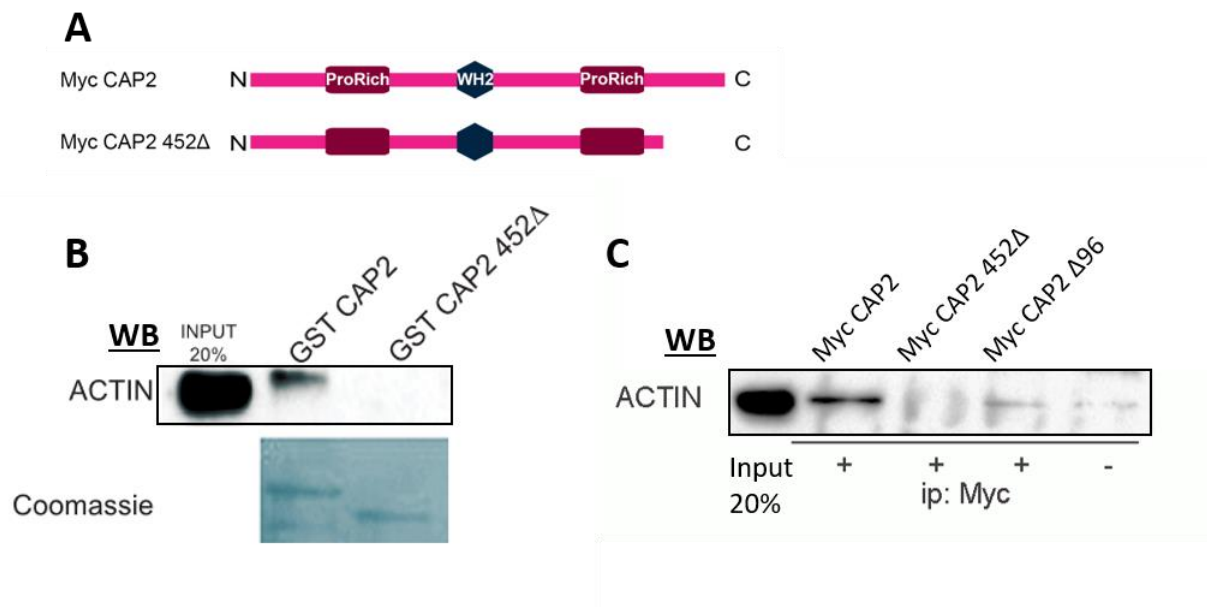


**Figure 2) Actin binds the C-terminal region of CAP2.**

**A)** Scheme of a representation of CAP2 mutants.

**B)** Actin interacts with the C-terminal tail of CAP2. GST CAP2 FL- full length, GST CAP2 Δ452 were incubated in a pull-down assay with rat brain homogenate. WB analysis was performed with actin antibody. GST proteins were stained by Coomassie staining. The deletion of the last 24 aminoacids abolishes actin binding to CAP2, suggesting that this is the sequence responsible for the interaction.

**C)** HEK293 cells were transfected with Myc-CAP2 / Myc-CAP2 452Δ / Myc-CAP2 Δ96 were lysed and immunoprecipitated (IP) with Myc antibody and WB analysis was carried out with an anti actin and Myc. CAP2 and CAP2 Δ96 bind with actin, while the Myc-CAP2 452Δ is not able to bind actin anymore.

### **1.3.) The actin binding domain of CAP2 is relevant for ADAM10 endocytosis**

According to literature the CAP family has an important role in protein trafficking and endocytosis <sup>266</sup>. Moreover, we have previously shown that the cytoplasmic tail of ADAM10 is the biological locus responsible for the regulation of its synaptic localization/shedding activity <sup>212,213,241,242,310</sup>. Thus, we decided to evaluate whether CAP2 affects ADAM10 synaptic localization in primary hippocampal neurons transfected with CAP2 full length (CAP2 FL) or the mutant lacking the actin binding domain (CAP2 452Δ). The quantitative analysis of the co-localization between ADAM10 and PSD-95, showed that CAP2 does not influence ADAM10 synaptic localization, while the mutant without the actin binding domain significantly increases the co-localization degree of ADAM10 with PSD-95 (Fig. 3A/B).

Since the actin binding site of CAP2 affects the levels of surface level of ADAM10 in the synapse, we investigated which mechanism is responsible for the modulation of this process. We decided to evaluate two pathways that are fundamental for ADAM10 localization: the forward trafficking and the endocytic process of the protein <sup>212,213</sup>. We performed an internalization assay in primary hippocampal neurons transfected with TacADAM10-RAR, as previously described <sup>306</sup> and Myc CAP2-FL or the mutant Myc CAP2 452Δ. The mutant of CAP2 significantly impaired the endocytosis rate of ADAM10 while CAP2-FL didn't modulate ADAM10 internalization (Fig. 3C/D). Since the actin cytoskeleton plays an essential role in endocytosis, where actin assembly can create protrusions that encompass extracellular materials <sup>311,312</sup>, these data suggest that CAP2 is involved in ADAM10 endocytosis, probably anchoring the protein to the actin cytoskeleton.



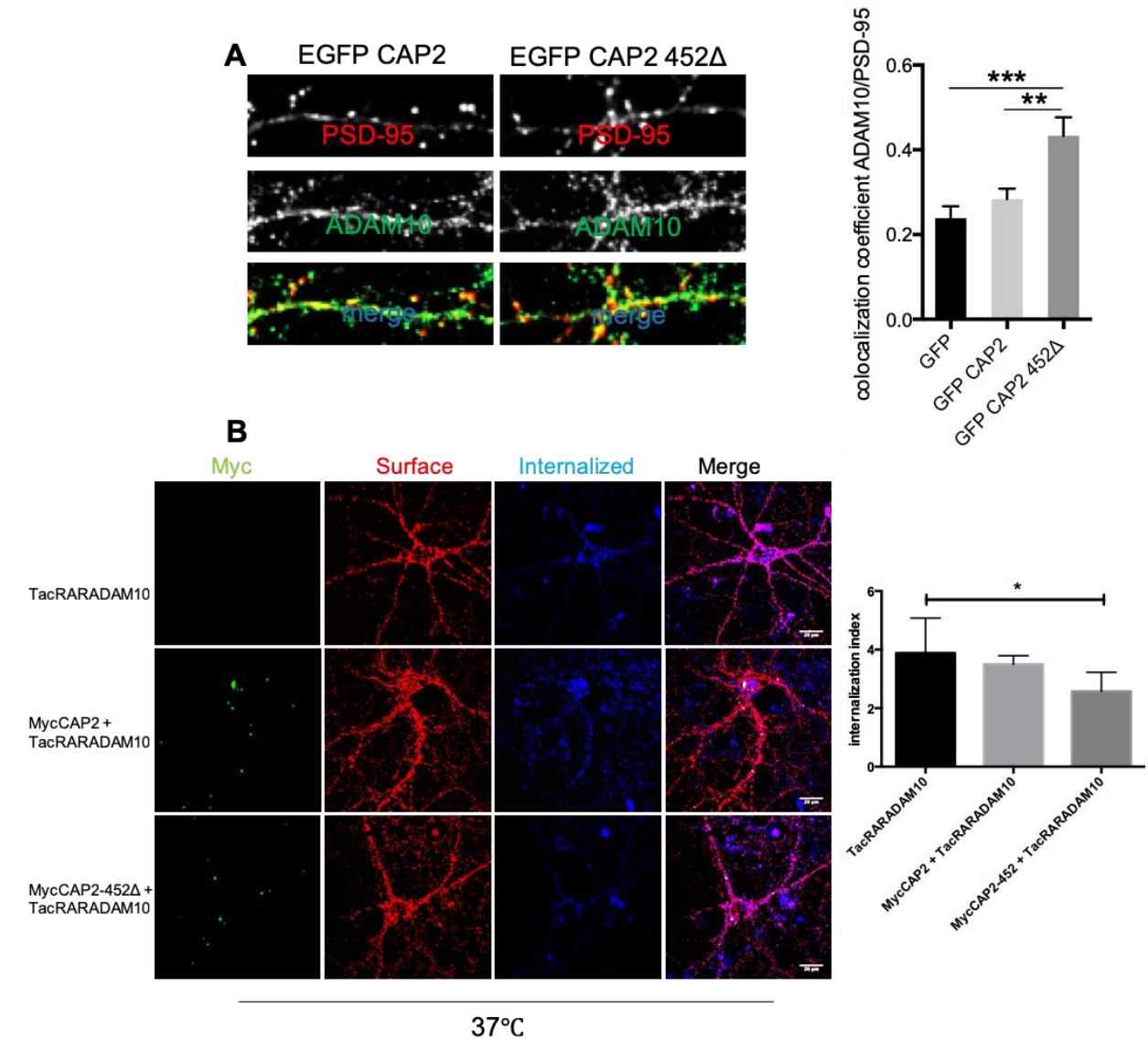


**Figure 3) CAP2 binding to Actin influences ADAM10 synaptic levels**

**A)** Primary hippocampal neurons transfected with EGFP-CAP2 FL or EGFP-CAP2-452Δ (the mutant lacking the actin binding domain), were stained for ADAM10 (green) and PSD-95 (red). Quantification of the colocalization degree was done with a one-way-ANOVA test with a Bonferroni post-hoc test. (GFP, mean = 0.2387 +/- SEM 0.028; GFP CAP2, mean = 0.2839 +/- SEM 0.0245; GFP CAP2-452Δ mean 0.4334 +/- SEM 0.043; GFP vs GFP CAP2-Δ452 \*\*\* $p < 0.001$ ; GFP CAP2 and GFP CAP2Δ452 \*\* $p < 0.01$ ;  $n = 3$ , with at least 6 neurons for each experiment for each condition).

**B)** An internalization assay was performed in primary hippocampal neurons transfected with Tac-RAR-ADAM10 and either Myc-CAP2-FL or Myc-CAP2-452Δ. Representative images of surface (red) and internalized (blue) Tac-RAR-ADAM10 and of CAP2 (green) are shown (scale bar = 20μm). The quantification of the internalization index (the internalized staining on the surface staining) was done with a one-way-ANOVA test with a Tukey post-hoc test. (TAC-RAR-ADAM10, mean +/- SEM; MycCAP2+TAC-RAR-ADAM10 mean +/- SEM; MycCAP2-452Δ +TAC-RAR-ADAM10 mean +/- SEM; TAC-RAR-ADAM10 vs. MycCAP2-452Δ +TAC-RAR-ADAM10 \*  $p < 0.05$ ;  $n = 2$ , with 6 neurons for each experiment for each condition).

## 2.) CAP2 as a novel regulator of actin dynamics and spine morphology

### 2.1.) CAP2 localization in the neuron

Since there is limited information available about the function of CAP2 in the brain and its localization in the cell<sup>301</sup>, we first investigated in which compartment of the neuron CAP2 is expressed. We used rat hippocampal tissue, which was homogenized to purify the PSD fraction. It turned out that CAP2 is present in the PSD, but not as enriched as ADAM10 (Fig. 4A). In addition, we used primary hippocampal neurons which were stained with pre- and post-synaptic markers and CAP2. STED microscopy analysis confirmed that CAP2 does not colocalize with Bassoon (a pre-synaptic marker), but partially colocalizes with PSD-95 (a post-synaptic protein). In addition, CAP2 clearly colocalizes with the F-actin marker phalloidin (Fig. 4B).

Overall, these data suggest that CAP2 is expressed in different compartments of neurons, including the post-synaptic density. In addition, CAP2 fully colocalizes with the filamentous form of actin, confirming it as an actin-binding protein.

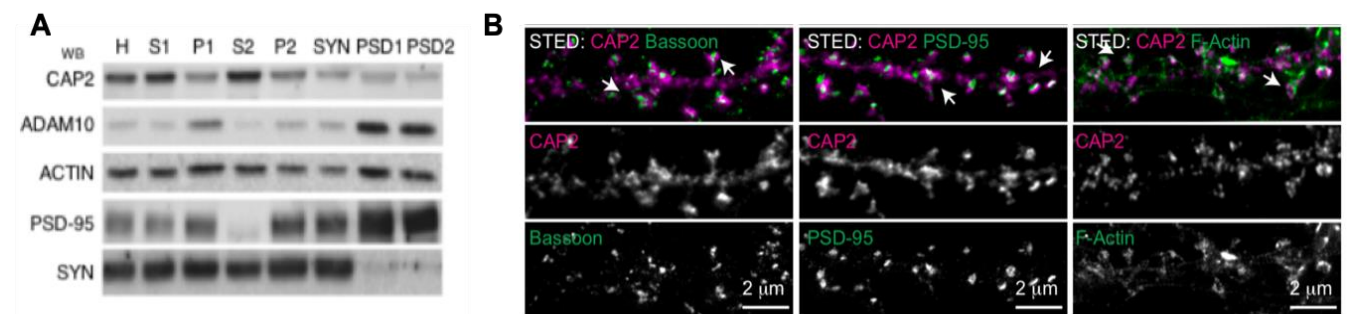


**Figure 4) CAP2 is present in the postsynaptic density compartment, but not enriched**

**A)** Post-synaptic density purified from adult rat hippocampi, CAP2 is present all the fractions but not enriched in PSD as ADAM10. Legend: Homo, Homogenate; S1, Supernatant 1; P1, Pellet 1 (Nuclear fraction); S2, Supernatant 2 (microsomal fraction); P2, Pellet 2; S3, Supernatant fraction; PSD1; PSD2, post- synaptic density.

**B)** Representative staining of CAP2 and synaptic markers. After fixation, neurons were stained with post- and pre-synaptic markers, PSD-95 and Bassoon respectively, to evaluate the localisation of CAP2 at the synapse. CAP2 shows a clear colocalization with F-actin, stained with phalloidin. Scale bar = 2 μm, and arrowhead indicate colocalization.

## 2.2.) CAP2 dimerization motif is relevant for cofilin association

The capability of all CAP protein homologues to self-associate and create multimeric complexes is well documented in the literature <sup>244</sup>. It is believed that, in *Dictyostelium discoideum*, CAP oligomerization is mediated by the first 50 N-terminal residues, other than at C-terminal site, and in particular, a dimerization domain (Di) at the amino terminus has been identified <sup>254</sup>. In agreement, CAP1, the other member of the CAP family, in mammals, could undergo a dimerization through the formation of a disulfide bond that involves the Cys29 residue in the N-terminal region of the protein <sup>313</sup>.

Therefore, first we verified the presence of a disulfide crosslinked CAP2 dimer by loading a lysate of COS-7 cells transfected with Myc CAP2 onto a non-reducing SDS-PAGE. As shown in Fig. 5A, both a band corresponding to Myc CAP2 monomer at 64 kDa and a species of CAP2 with an apparent molecular weight of approximately double the Myc CAP2 monomer (128 kDa) were detected. Remarkably, the Myc CAP2 mutant carrying the mutation of the Cys32 to Gly [Myc CAP2 C32G] is not able to dimerize in one-dimensional non-reducing SDS-PAGE (Fig. 5A).

To strengthen these data, we performed a proximity ligation (PLA) assay in rat hippocampal neurons transfected with EGFP-CAP2 and either Myc CAP2 or Myc CAP2 C32G. In neurons expressing EGFP CAP2 and Myc CAP2, a large number of PLA signals was detected when the two antibodies GFP and Myc were used, indicating that these two CAP2 constructs are in close proximity (<40 nm) to each other along MAP2-positive dendrites (Fig. 5B). In neurons transfected with EGFP CAP2 and the mutant Myc CAP2 C32G the density of PLA signals significantly decreased when compared to cells overexpressing EGFP CAP2 and Myc CAP2 (Fig. 5B). For control experiments, only Myc primary antibody was used and no PLA signal was generated (data not shown). Overall, these findings indicate that the Cys32 is fundamental for the formation of CAP2 dimers and for CAP2 self-association in neurons.

Since CAP2 is known to bind cofilin <sup>255,256</sup>, and possibly enhances the cofilin mediated actin regulation, we used hippocampal neurons transfected with Myc CAP2 or Myc CAP2 C32G to assess the effect of the mutation on CAP2/cofilin association by a PLA experiment. The data show a decreased binding between Myc CAP2 C32G and cofilin

compared to Myc CAP2 - cofilin (Fig. 5C). Therefore, the CAP2 dimer formation, dependent on the Cys32, is relevant for the CAP2/cofilin interaction and we hypothesize that this complex can affect cofilin-mediated activity and the actin treadmilling rate in dendritic spines.

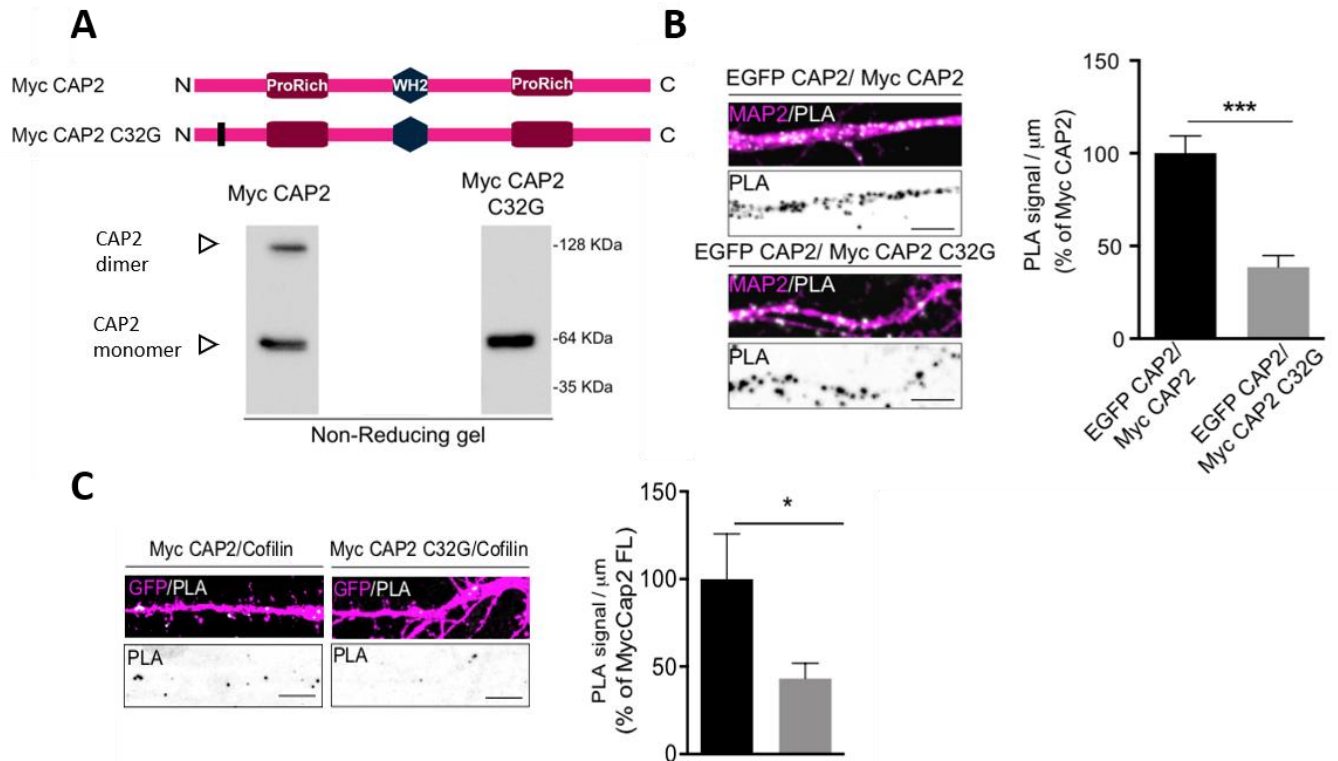


**Figure 5) CAP2 self-association depends on Cys32 and is relevant for the association to cofilin.**

**A)** Representative scheme of CAP2 mutants. Homogenates of cells expressing either the Myc CAP2 or Myc CAP2 C32G mutant were loaded onto a non-denaturing gel; WB analysis was performed with Myc antibody and revealed that the single point mutation Cys32 to Gly avoid the capability to form dimers onto a native-like condition gel (C32G).

**B)** Representative images of a PLA assay carried out in primary hippocampal cultures transfected with EGFP-CAP2 and either Myc-CAP2 or Myc-CAP2 C32G. The quantitative analysis reveals that this mutant decreases the dimerization of CAP2 with approximately 60%. Statistics done with an unpaired two-tailed t-test, (EGFP CAP2+Myc-CAP2 mean = 100 +/- SEM 9.363; EGFP CAP2+Myc-CAP2 C32G mean = 38.64 +/- 6.239; EGFP CAP2+Myc CAP2 vs. EGFP CAP2 + Myc CAP2 C32G \*\*\*P < 0.0001; n = 2, with 8 neurons each condition, per experiment).

**C)** Representative images of a PLA assay carried out in primary hippocampal cultures transfected with Myc CAP2 or Myc CAP2 C32G. The PLA was carried out between a Myc antibody (mouse) and Cofilin antibody (rabbit). The quantitative analysis reveals that the CAP2 mutant decreases the binding to cofilin. Statistics done with an unpaired two-tailed t-test, (Myc CAP2, mean = 100 +/- SEM 25.76; Myc CAP2 C32G mean = 43.20 +/- SEM 8.703; Myc CAP2 vs. Myc CAP2 C32G \*P < 0.05; n = 2, with 5 neurons each condition, per experiment).

### 2.3.) The lack of CAP2 affects the spine morphology, the molecular composition of the synapses and amyloid beta levels *in-vivo*.

To understand more about the physiological role of CAP2, we took advantage of the cortical and hippocampal areas of adult CAP2 Knock-Out mice (CAP2 KO mice) at 5 to 6 months of age, kindly provided by Prof. M. Rust. After the homogenization of the tissue and purification of the Triton-Insoluble Fraction (TIF), which is enriched with post-synaptic proteins, the expression levels of proteins of interest as ADAM10, the post synaptic protein PSD-95 and multiple receptor subunits of the glutamatergic NMDA/AMPA receptors, were measured. No differences in total brain homogenate of both the cortex (data not shown) and hippocampus (Fig. 6A) were detected. However, the synaptic localization of both ADAM10 and GluN2A are significantly decreased in the hippocampal area of CAP2 KO mice when compared to wild-type (WT) mice, without any differences in the cortex (Fig. 6B).

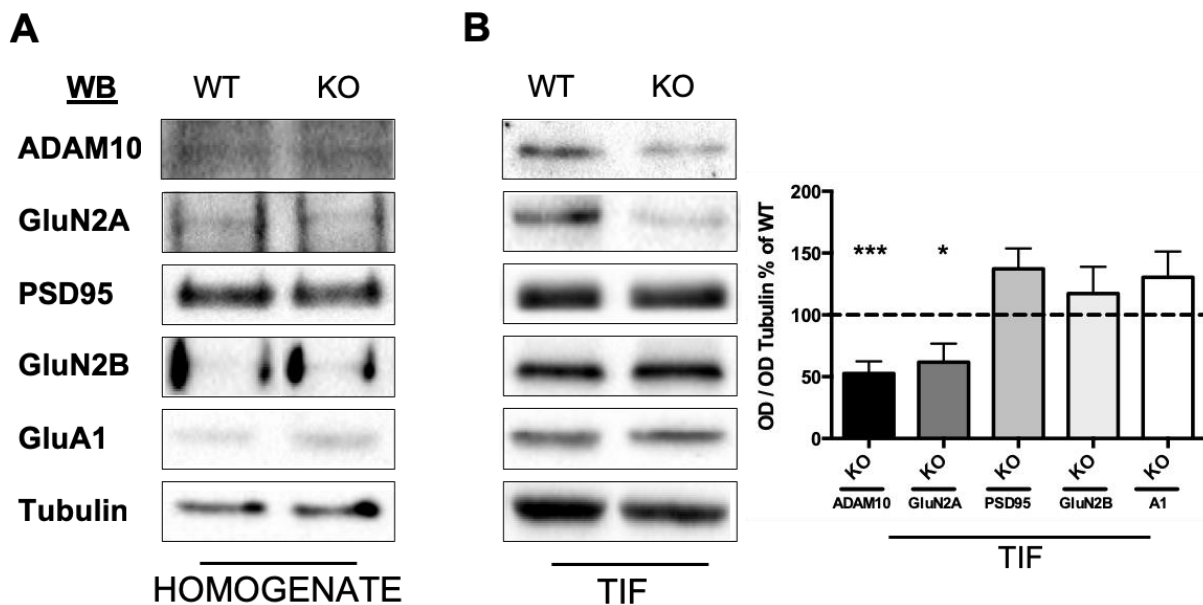


**Figure 6) Characterization of CAP2 KO mice hippocampus.**

**A)** Representative images of WB experiments carried out from the total hippocampal homogenate of CAP2 KO and WT mice.  
**B)** Representative images of WB experiment carried out from the TIF fraction of CAP2 KO and WT mice. On the right the representative graph of the statistical analysis, where the OD of the protein of interest was normalized on Tubulin and shown as a percentage compared to the WT. A two-tailed unpaired t-test was used. (ADAM10 CAP2 KO mean = 52,57 +/- SEM 9, 866; WT vs. KO \*\*\*p<0.001; GluN2A CAP2 KO mice mean = 61.81 +/- SEM 14.8, WT vs. KO \*P<0,05; PSD-95 CAP2 KO mean = 137.3 +/- SEM 16.48, WT vs. KO P = 0.064; GluN2B CAP2 KO mice mean = 117.3 +/- 21.61, WT vs. KO P = 0.45; GluA1 CAP2 KO mean = 130.5 +/- SEM 20.80 WT vs. KO P = 0.19, n = 9 for ADAM10 and GluN2A, for the rest n = 4).

In addition, we analyzed the spine morphology and density of female CAP2 KO mice at the age of 6 months hippocampal neurons ex-vivo. A decrease in the spine density, length and width was found in CAP2 KO mice hippocampal neurons compared with age-matched WT animals. Moreover, an increase of the immature stubby spines was found in the CAP2 KO mice (Fig. 7). Overall, these data suggest that CAP2 is important for the regulation of structural plasticity and the synaptic localization of ADAM10 and GluN2A. In addition, there is a possible role for CAP2 in the development and maturation of synapses, as in CAP2 KO mice the number of the immature stubby spines are increased.

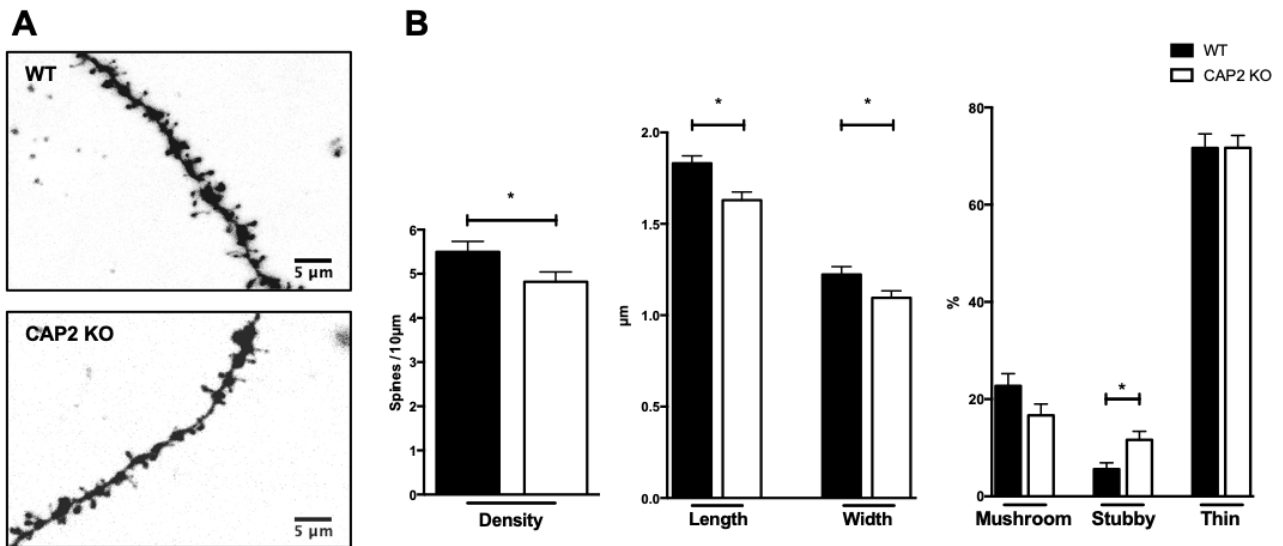


**Figure 7) Spine morphology and density of CAP2 KO mice hippocampal neurons.**

To see if there are differences in the spine morphology and density of hippocampal neurons of CAP2 KO mice, we stained these cells with a fluorescent dye (DiI) and quantified the spine morphology including the density, length and width of the spines.

**A)** Representative image (63x Confocal image, 1024x1024 field) of a hippocampal neuron from a WT and a CAP2 KO. Scalebar = 5 μm.

**B)** Quantification of the spine density, length and width and the classification of the morphology of the spines. For statistical analysis we used a 2-tailed unpaired t-test. Spine density (WT mean = 5.481 +/- SEM 0.2439 & CAP2KO mean = 4.665 +/- SEM 0.22, WT vs. KO \*P<0.05), Length (WT mean = 1.831 +/- SEM 0.041 & CAP2KO mean = 1.629 +/- SEM 0.045, WT vs. KO \*\*P<0.01), Width (WT mean = 1.223 +/- SEM 0.043 & CAP2KO mean = 1.095 +/- SEM 0.039, WT vs. KO \*P < 0,05), Mushroom spines (WT mean = 22.74 +/- SEM 2.51 & CAP2KO mean = 16.68 +/- SEM 2.327, WT vs. KO P = 0.085), Stubby spines (WT mean = 5.595 +/- SEM 1.324 & CAP2KO mean = 11.64 +/- SEM 1.736, WT vs. KO \*\*P<0.01), Thin spines (WT mean = 71.67 +/- SEM 2.886 & CAP2KO mean = 71.68 +/- SEM 2.57, WT vs. KO P = 0.9968) (WT versus KO, n = 2 animals each condition with n = 10 neurons with > 100 spines for each animal)

Finally, taking advantage of an ELISA assay, we looked at the  $A\beta_{1-42}$  levels in the homogenate of the hippocampus of CAP2 KO mice comparing them to the wild type animals. Interestingly, the CAP2 KO mice have elevated  $A\beta_{1-42}$  levels in their hippocampal area (Fig. 8). This indicating that CAP2 is important for the regulation of  $A\beta_{1-42}$  in the hippocampus.

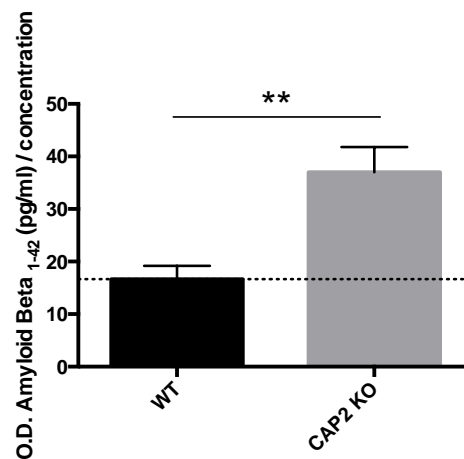


**Figure 8) CAP2 KO mice have elevated amyloid beta levels in the hippocampal area.**

With an ELISA assay we detected  $A\beta_{1-42}$  levels in the hippocampus of CAP2 KO animals compared to matched wild type animals. CAP2 KO mice show higher levels of  $A\beta_{1-42}$  compared to wild-type mice. WT mean = 16.66 pg/ml +/- 2.535 & CAP2 KO mean = 37.02 pg/ml +/- SEM 4.812, WT vs. KO \*\*P<0.01

### **3.) CAP2 and activity-dependent synaptic plasticity**

#### **3.1.) Long-term potentiation triggers CAP2 dimerization**

Given that CAP2 is important in structural plasticity and when CAP2 is abolished this results in an altered spine morphology, the question raised whether CAP2 is involved in physiological plasticity. In addition, given the pivotal role of cofilin-mediated actin dynamics in the structural remodeling of spines during activity-dependent synaptic plasticity phenomena, we tested whether the long-term potentiation (LTP) and the long-term depression (LTD) modulate CAP2 expression and dimerization, and consequently association to cofilin<sup>133</sup>. First, we verified whether LTP regulates CAP2 synaptic availability in the dendritic spines. To this, we induced chemical LTP (cLTP), using a highly validated protocol in hippocampal cultures that results in prolonged NMDA receptor-dependent LTP<sup>213</sup> (Fig. 9A). 30 min after cLTP induction, we purified TIF from control and cLTP-treated hippocampal neurons. Western blot analysis revealed that cLTP elicited an increase in the CAP2 levels in the TIF fraction compared to control neurons (Fig. 9B). Notably, cLTP stimulation caused also a significant increase in CAP2 dimer levels in TIF (Fig. 9C). Then, to evaluate whether these effects could be ascribed to the CAP2 Cys32-dependent dimerization, we analyzed the PLA signal upon cLTP induction in hippocampal neurons transfected with EGFP-CAP2 and either Myc-CAP2 or Myc-CAP2(C32G). The cLTP induction significantly increased PLA signal in neurons transfected with EGFP-CAP2 and Myc-CAP2, confirming the LTP-triggered augment in CAP2 self-association (Fig. 9D). On the other hand, no modifications in PLA signals upon LTP induction were detected when EGFP-CAP2 and Myc-CAP2(C32G) were expressed (Fig 8D). To determine if the increase in CAP2 dimer affects the association to cofilin, we performed PLA assays after cLTP induction. The quantitative analysis revealed a significant increase in the association between endogenous CAP2 and cofilin upon LTP induction (Fig. 9E).



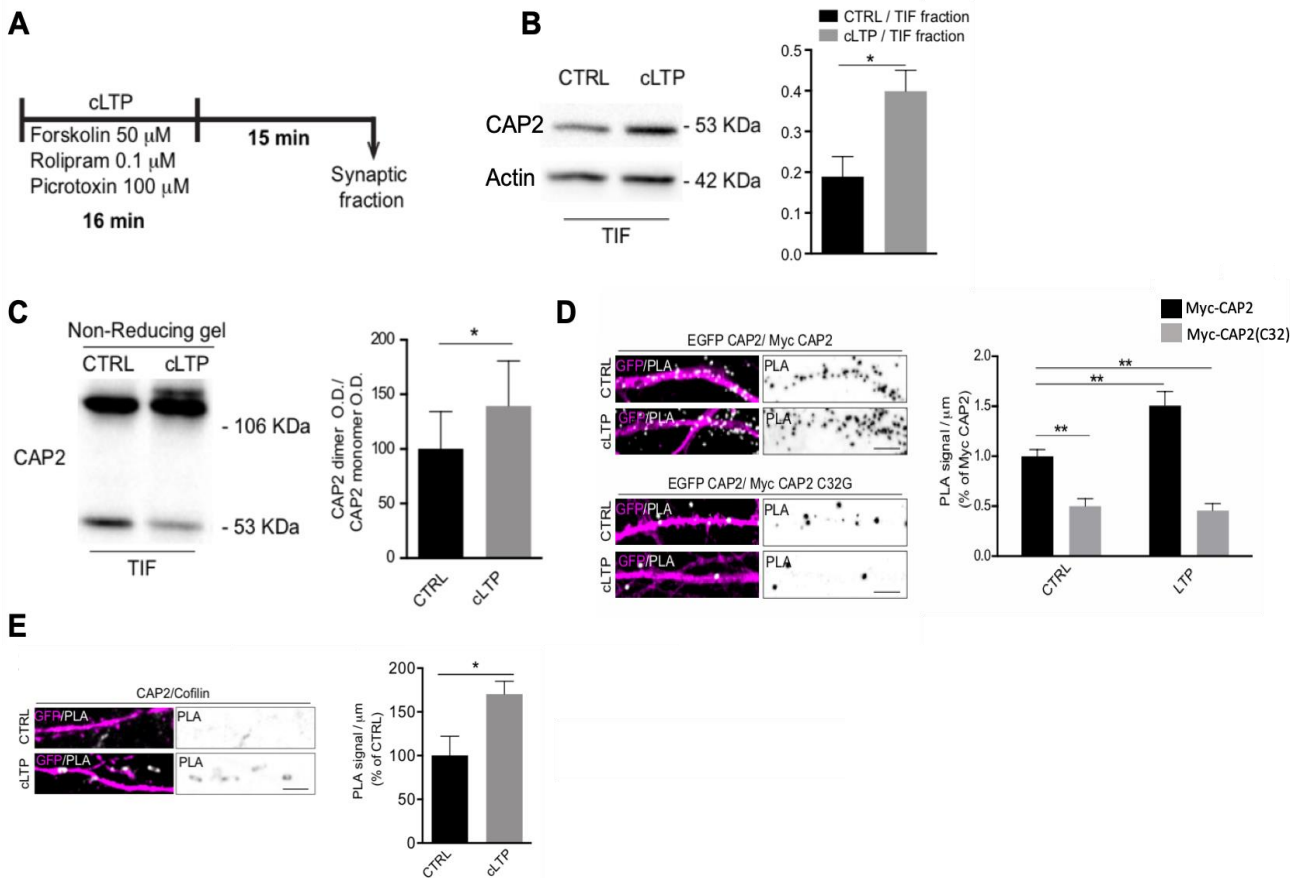


**Figure 9) CAP2 dimerizes and associates upon chemically induced LTP.**

**A)** A schematic overview of the chemical LTP induction protocol in primary hippocampal cultures followed by the TIF purification.

**B)** WB representative images of TIF samples purified from cLTP and control treated cultures. cLTP (15') promotes CAP2 enrichment in the TIF fraction. For statistical analysis we used a 2-tailed unpaired t-test. Ctrl mean = 0.1892 +/- SEM 0.049; cLTP mean = 0.3992 +/- SEM 0.05121, Ctrl vs. cLTP \*P<0.05, n = 5.

**C)** Samples of TIF purification of cLTP and control treated cultures were loaded onto a non-denaturing gel. Western blot analysis performed with CAP2 antibody showed a band corresponding to CAP2 (53 KDa) and another band at 106 KDa corresponding to a CAP2 dimer. TIF purification of control and cLTP-treated neurons. cLTP (15') promotes CAP2 dimerization in the TIF fraction. The ratio dimer/monomers expressed as percentage of control. For statistical analysis we used a 2-tailed unpaired t-test. cLTP mean = 163.3 +/- SEM 27.62; Ctrl vs. cLTP \*P<0.05, n = 8.

**D)** In situ detection of proximity between EGFP CAP2 and MycCAP2 or MycCAP2 C32G (white) along MAP2 (magenta) after cLTP induction; scale bar = 5  $\mu$ m. Data are presented as mean  $\pm$  s.e.m., n = 2 with for each experiment 8 neurons per condition, Myc-CAP2 vs. Myc-CAP2 cLTP \*P< 0.05, statistical analysis done with a 2-way ANOVA with post hoc Tukey test.

**E)** In situ detection of proximity between CAP2 and Cofilin (white) along GFP transfected hippocampal neurons (magenta); scale bar = 20  $\mu$ m. Data are presented as mean  $\pm$  s.e.m., n = 2 with for each experiment 8 neurons per condition, \*P< 0.05, paired Student's t-test.

Then we verified whether LTD has an influence on CAP2 expression and synaptic availability in the spine. We induced cLTD with the classical LTD protocol (Fig. 10A)<sup>314,315</sup>. Data indicate that cLTD induction did not affect CAP2 synaptic localization (Fig. 10B) or its dimer formation, both shown with biochemical (Fig. 10C) and PLA experiments (Fig. 10D). As previously shown, we confirmed a significant difference between the dimer formation between Myc-CAP2 and the Myc-CAP2 C32G mutant (Fig. 5B and 10D).

Therefore, the effect on CAP2 localization and its dimer formation is specifically related to changes triggered by LTP induction, since neither PLA assays or Western Blot analysis of the synaptic fraction revealed any variation in dimer formation after LTD induction.

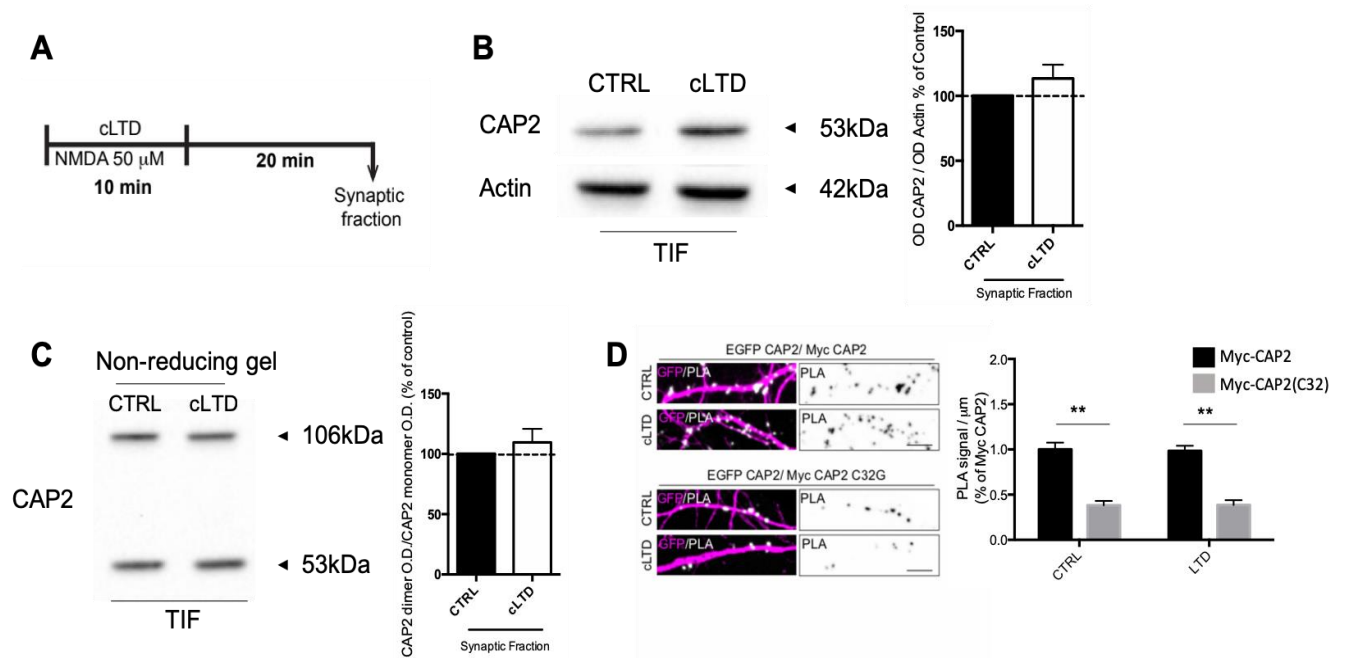


**Figure 10) CAP2 synaptic localization and dimerization are not affected by chemically induced LTD.**

**A)** A schematic overview of the chemical LTD induction protocol in primary hippocampal cultures followed by the TIF purification.

**B)** the WB representative image of the TIF fraction and graph of the analysis (OD CAP2 normalized on OD actin) show no differences of CAP2 localization upon cLTD induction. Statistical analysis done with an unpaired student t-test, data represented as mean  $113.5 \pm \text{SEM } 10.58$ ,  $p = 0.23$ ,  $n = 6$ .

**C)** Representative WB image of a non-reducing gel of the TIF fraction and the graph of the analysis, show no changes in the CAP2 dimer formation upon cLTD induction. Statistical analysis done with an unpaired student t-test, data represented as mean  $109.5 \pm \text{SEM } 11.21$ ,  $p = 0.42$ ,  $n = 6$ .

**D)** PLA experiment of transfected hippocampal cultures with EGFP-CAP2 and either Myc-CAP2 or Myc-CAP2(C32), show again that the CAP2 dimer not influenced by cLTD, neither in the condition where the dimer formation is abolished by the Myc-CAP2(C32) mutant. Of course, there is a significant difference between the dimer formation between the Myc-CAP2 and the Myc-CAP2(C32G) mutant as previously shown. Statistical analysis done with a 2-way ANOVA with a post-hoc Tukey test. Data represent as mean  $\pm \text{SEM}$   $p = 0.99$ .

### 3.2.) CAP2 association to ADAM10 and Actin is regulated by activity-dependent plasticity

To have a complete overview of CAP2 function, we evaluated whether the CAP2 association to its binding partners actin and ADAM10 is affected during the induction of plasticity phenomena in neuronal cells. Firstly, we analysed the PLA signal between CAP2 and ADAM10 upon cLTP or cLTD treatment in primary hippocampal neurons transfected with EGFP as a neuron filler. The cLTP treatment significantly increased the association between CAP2 and ADAM10 (Fig. 11A), while in cLTD conditions we

couldn't detect any changes (Fig. 11C). Then, we analysed the association between CAP2 and actin by co-immunoprecipitation, and we found that the cLTP treatment significantly reduced the association between CAP2 and actin (Fig. 11B), whereas upon cLTD treatment no changes were detectable (Fig. 11D). These results suggest that the binding between CAP2 and its two binding partners is affected only upon cLTP treatment, where cLTD induction does not have any effects on their association.

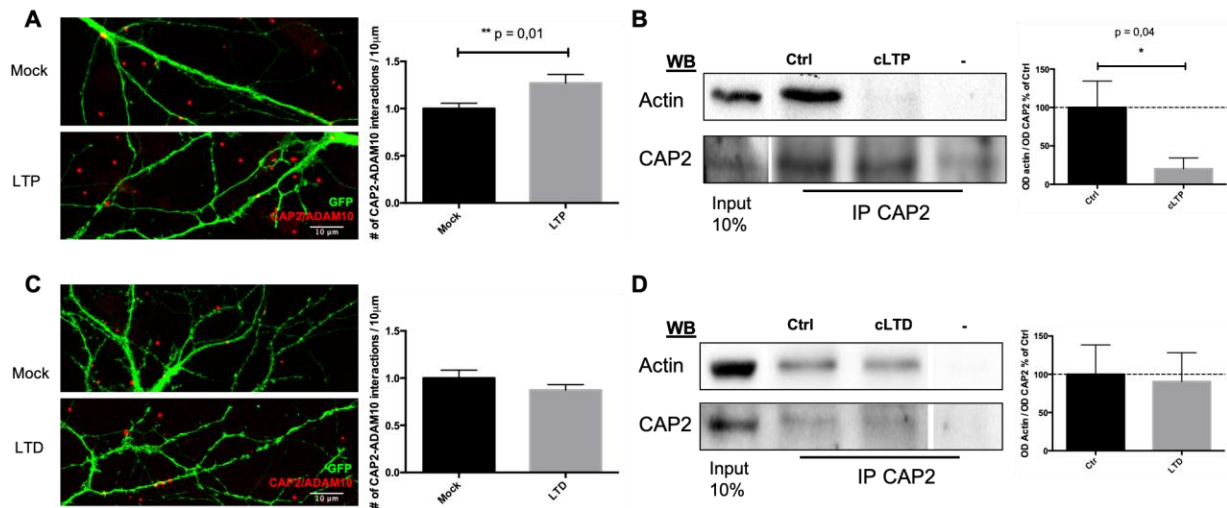


**Figure 11) CAP2 interaction with binding partners ADAM10 and actin in physiological plasticity.**

**A)** Representative images of PLA between CAP2-ADAM10 in EGFP-transfected primary hippocampal neurons upon chemically induced LTP. The quantification shows an increased interaction between CAP2 and ADAM10. Quantifications done by unpaired 2-tailed t-test. Data shown as # of PLA signal normalized on total dendritic length. (Mock mean = 1.00 +/- SEM 0.057, cLTP mean = 1.270 +/- SEM 0.0909, Ctrl vs. cLTP \*\* P < 0.01. n = 14 from 2 individual culture preparations.

**B)** Co-IP between CAP2 and actin in primary hippocampal neurons upon chemically induced LTP. Representative western blot image and quantification, where there is a decreased interaction between CAP2 and Actin. Quantification done by unpaired 2-tailed t-test. Data shown as O.D. Actin / O.D. CAP2 normalized on Ctrl. (Ctrl mean = 100 +/- SEM 34.45, cLTP mean = 20.33 +/- SEM 14.05, Ctrl vs. cLTP \*P<0.05, n=10.

**C)** Representative images of PLA between CAP2-ADAM10 in EGFP-transfected primary hippocampal neurons upon chemically induced LTD. The quantification shows an no altered interaction between CAP2 and ADAM10. Quantifications done by unpaired 2-tailed t-test. Data shown as # of PLA signal normalized on total dendritic length. (Mock mean = 1.00 +/- SEM 0.085, cLTD mean = 0.874 +/- SEM 0.0566, Ctrl vs. cLTD P = 0.23. n = 14 from 2 individual culture preparations.

**D)** Co-IP between CAP2 and actin in primary hippocampal neurons upon chemically induced LTD. Representative western blot image and quantification, where there is a no altered interaction between CAP2 and Actin. Quantification done by unpaired 2-tailed t-test. Data shown as O.D. Actin / O.D. CAP2 normalized on Ctrl. (Ctrl mean 100 +/- SEM 38.41, cLTD mean = 90.53 +/- SEM 37.64, Ctrl vs. cLTD P=0.86, n=6.

## 4.) Amyloid $\beta$ oligomers affect CAP2 pathway

### 4.1.) Characterization of A $\beta$ 1-42 oligomers effect on the synapse

Since we found that CAP2 is involved in plasticity phenomena, we wondered whether CAP2 and the interactions with its partners can be a target of the aberrant plasticity triggered by the toxic soluble A $\beta$  oligomers (oA $\beta$ <sub>1-42</sub>) in AD pathogenesis. To this aim, we treated primary hippocampal neurons with oA $\beta$ <sub>1-42</sub>. (Fig.12). In order to set-up a reliable *in-vitro* model to obtain the effect of oA $\beta$ <sub>1-42</sub> on CAP2 and ADAM10 expression and synaptic localization we fully characterized of our experimental conditions.

First, the oA $\beta$ <sub>1-42</sub> preparation was controlled by different considerations. As a negative control we used a peptide consisting the reverse sequence of A $\beta$  (A $\beta$ <sub>42-1</sub>). With Western Blot analysis, with an antibody detecting the N-terminus of A $\beta$  (6E10 antibody), we show that our oA $\beta$ <sub>1-42</sub> preparation resulted in a spectrum of oligomeric A $\beta$  species, from 4 kDa to 16 kDa (Fig. 12A). Where, as expected, no signal was detected in A $\beta$ <sub>42-1</sub> samples. Transmission electron microscopy (TEM) analysis, performed in collaboration with the laboratory of Nadia Santo (University of Milan), of oA $\beta$ <sub>1-42</sub> confirmed the presence of globular, oligomeric structures, while we did not observe fibrillar or protofibrillar species (Fig. 12B). In addition, consistent with previous results<sup>161,162,316</sup>, we noticed that when oA $\beta$ <sub>1-42</sub> species at a concentration of 500nM were applied to hippocampal neurons for 24 hours, this resulted in a significant reduction in spine density compared to non-treated cultures (CTRL) or to cells exposed to A $\beta$ <sub>42-1</sub> (Fig. 12C). Moreover, this concentration of oA $\beta$ <sub>1-42</sub> didn't increase the mortality of the cells after 24h of treatment, differently from the higher concentrations like 1 $\mu$ M, 5 $\mu$ M and 10 $\mu$ M (Fig. 12D). oA $\beta$ <sub>1-42</sub> species have been previously shown to facilitate synaptic depression of neurons in acute slices<sup>38,40</sup>. Accordingly, in collaboration with the laboratory of Flavia Antonucci (University of Milan), we found that hippocampal cultures exposed to oA $\beta$ <sub>1-42</sub> for 30 min showed a global synaptic depression, indicated by the electrophysiological recordings of mEPSCs (Fig. 12E), as well as upon the stimulation of the classical LTD protocol (20 $\mu$ M NMDA and 20 $\mu$ M glycine for 3min, chemical-LTD; Fig. 12E;<sup>314,315</sup>). Moreover, as shown in figure 12F, the treatment with

our oA $\beta_{1-42}$  preparation (500nM, 30 min) induced a significant dephosphorylation of the phosphorylation-site serine 845 of the GluA1 subunit of AMPARs, without any significant alteration in the total GluA1 synaptic levels, confirming that this concentration can elicit synaptic depression<sup>317</sup>. In addition, we did not detect any changes in the total or synaptic levels of multiple NMDAR subunits and in PSD-95 (Fig. 12F). These results suggest that our oA $\beta_{1-42}$  preparation is able to trigger synaptic depression-like phenomena, affecting specifically the AMPA mediated conductance.

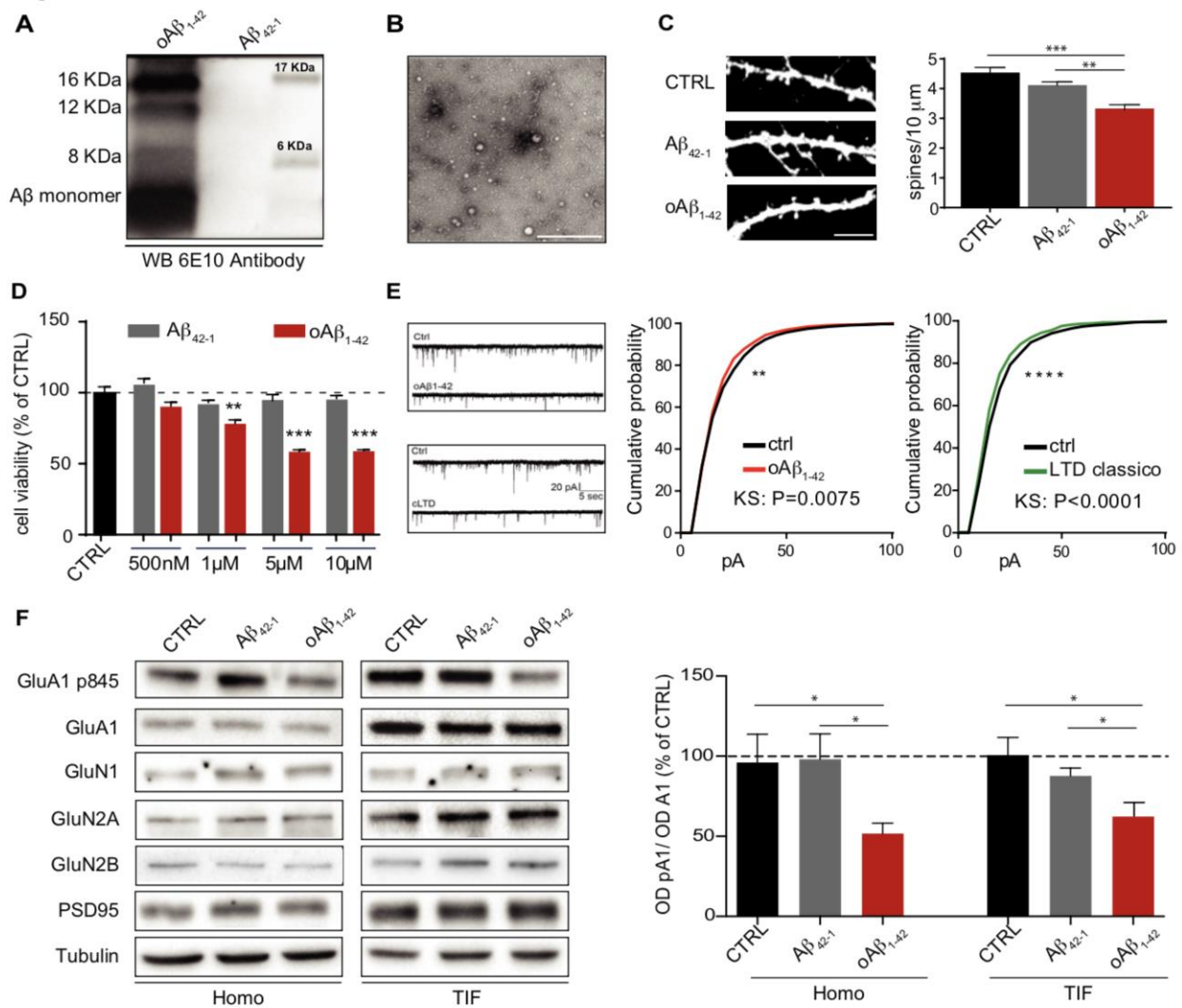


**Figure 12) A $\beta$  oligomers characterization and effects on the synapses.**

**A)** Western blot analysis of oA $\beta_{1-42}$ . The image shows the presence of oligomers formation up to 16kDa.

**B)** TEM revealed globular but not fibrillar structures for oA $\beta_{1-42}$  preparation, scale bar 500 nm.

**C)** Representative confocal images of GFP-transfected primary hippocampal neurons. The analysis shows that oA $\beta_{1-42}$  (500 nM, 24 hr) reduces spine density (CTRL  $4.58 \pm 0.18$ ; A $\beta_{42-1}$   $4.15 \pm 0.12$ ; oA $\beta_{1-42}$   $3.36 \pm 0.18$  (\*\*  $p < 0.01$ , \*\*\*  $p < 0.001$ ; one-way ANOVA,  $n=34-45$ ).

**D)** MTT test shows that exposure to oA $\beta$ <sub>1-42</sub> for 24 hr induces cell death starting from a concentration of 1  $\mu$ M (\*\*  $p < 0.01$ , \*\*\*  $p < 0.001$  one-way ANOVA, oA $\beta$ <sub>1-42</sub> vs CTRL,  $n = 4$ ). Scale bar 5  $\mu$ m.

**E)** Representative traces of mEPSCs collected in hippocampal neurons before and after oA $\beta$ <sub>1-42</sub> exposure (upper panel) and before and after chemical LTD (lower panel). At least 21 neurons before and after each treatment (oA $\beta$ <sub>1-42</sub> or cLTD) have been analyzed and the related analysis of mEPSC amplitudes, here shown as cumulative probability, includes these  $n$  of excitatory events: 1550 (before oA $\beta$ <sub>1-42</sub>, black line) vs 970 (after oA $\beta$ <sub>1-42</sub>, red line), CTRL vs oA $\beta$ <sub>1-42</sub>  $p = 0.0075$ ; 2100 (before cLTD, black line) vs 1970 (after cLTD, green line), CTRL vs LTD  $p < 0.0001$ .

**F)** Western blot analysis of synaptic proteins levels in total homogenate (HOMO) and synaptic fraction (TIF) upon oA $\beta$ <sub>1-42</sub> treatment (500 nM, 30 min). The quantification shows that oA $\beta$ <sub>1-42</sub> incubation for 30 min induces a decrease of GluA1 phosphorylation at 845-residue (GluA1p845/GluA1, HOMO: CTRL  $96.06 \pm 17.65\%$ , A $\beta$ <sub>42-1</sub>  $98.04 \pm 15.88\%$ , oA $\beta$ <sub>1-42</sub>  $51.68 \pm 6.52\%$ ; TIF: CTRL  $100.7 \pm 11.01\%$ , A $\beta$ <sub>42-1</sub>  $87.67 \pm 4.88\%$ , oA $\beta$ <sub>1-42</sub>  $62.26 \pm 8.58\%$ , \* $p < 0.05$  CTRL vs oA $\beta$ <sub>1-42</sub>, A $\beta$ <sub>42-1</sub> vs oA $\beta$ <sub>1-42</sub>, one-way ANOVA,  $n = 7-10$ ). oA $\beta$ <sub>1-42</sub> exposure doesn't induce significant changes of GluA1, NMDA receptors subunits and PSD-95 expression and synaptic localization.

## **4.2.) A $\beta$ oligomers promote ADAM10 synaptic localization while decreasing CAP2 synaptic levels.**

Given that ADAM10 and CAP2 synaptic localization are regulated by synaptic plasticity<sup>213</sup>, do oA $\beta$ <sub>1-42</sub> modify ADAM10 and CAP2 synaptic levels? To address this, we exposed hippocampal neuronal cultures to oA $\beta$ <sub>1-42</sub> (500 nM, 30 min). As shown in Fig 13A, the bath application of oA $\beta$ <sub>1-42</sub> increases the colocalization of ADAM10 with PSD-95, a postsynaptic marker, along the dendrites when comparing them to untreated or A $\beta$ <sub>42-1</sub>-treated cells. To further confirm these results, we used a biochemical approach, where we purified the TIF. ADAM10 levels were significantly increased in the TIF upon oA $\beta$ <sub>1-42</sub> treatment (Fig. 13B), indicating that oA $\beta$ <sub>1-42</sub> is able to induce ADAM10 synaptic localization. On the contrary, CAP2 synaptic levels were decreased upon oA $\beta$ <sub>1-42</sub> treatment, revealing that also CAP2 is a target of oA $\beta$ <sub>1-42</sub> (Fig 13B). As previously shown, LTD induction fosters the SAP97-mediated ADAM10 forward trafficking to the synaptic membrane<sup>213</sup>. However, upon oA $\beta$ <sub>1-42</sub> treatment, no significant alterations of SAP97 synaptic localization were found (Fig. 13B). Moreover, no changes of the synaptic levels of  $\beta$ 2-adaptin, one of the subunits of the AP2 complex that is responsible for ADAM10 endocytosis<sup>213</sup>, was observed (Fig. 13B).

Additionally, since we detected an altered CAP2 dimer formation in the physiological induced cLTP, we addressed whether the acute treatment with oA $\beta$ <sub>1-42</sub> influences the CAP2 dimerization. Neither the CAP2 dimerization expression nor the localization of the dimer are altered upon the oA $\beta$ <sub>1-42</sub> treatment, since there is a high variability among

the samples (Fig. 13C). Finally, to determine the cellular mechanism which is underlying the oA $\beta_{1-42}$ -induced upregulation of ADAM10 synaptic availability, we analyzed the association of ADAM10 to its binding partners SAP97 and AP2. As displayed in figure 13D, the oA $\beta_{1-42}$  treatment is not able to modify the interaction with SAP97, while a significant decrease in the interaction with  $\beta$ 2-adaptin, is found. These results demonstrate that the acute exposure to oA $\beta_{1-42}$  is able to affect ADAM10 synaptic localization, due to the decreased ADAM10 endocytosis rather than to an increase of forward trafficking.

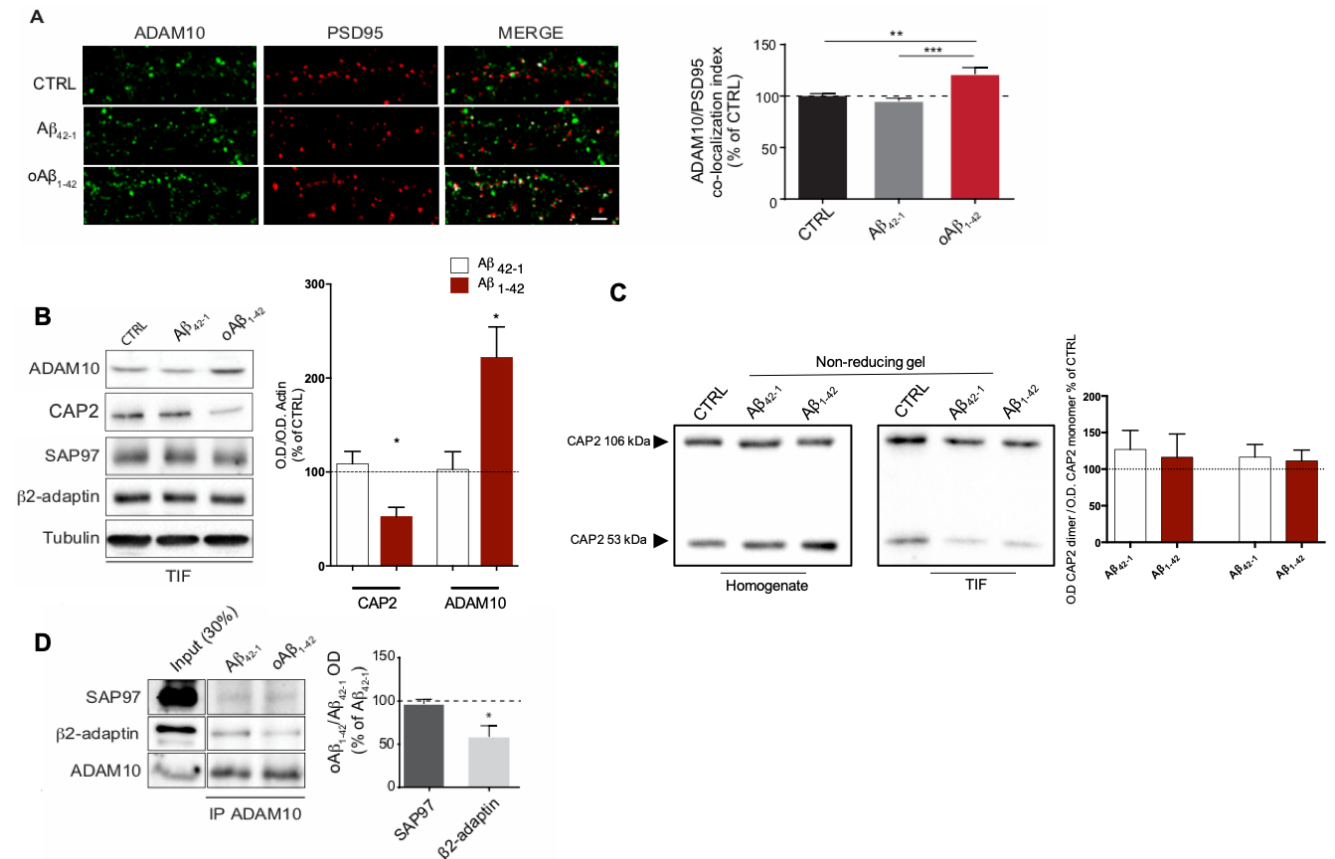


**Figure 13** oA $\beta_{1-42}$  treatment increases ADAM10 synaptic localization, impairing its endocytosis and decreases CAP2 synaptic localization

**A)** Confocal images of primary hippocampal neurons stained with PSD-95 (red) and ADAM10 (green). Cells were untreated (CTRL) or incubated for 30 min with either oA $\beta_{1-42}$  or A $\beta_{42-1}$  (500 nM). The challenge with oA $\beta_{1-42}$  increases the ADAM10/PSD-95 co-localization index (CTRL 100 ± 2.48%, A $\beta_{42-1}$  95.59 ± 2.69%, oA $\beta_{1-42}$  123.1 ± 5.86% \* $p$  < 0.05, \*\* $p$  < 0,01 Kruskal-Wallis one-way analysis on variance,  $n$ =30). Scale bar 5  $\mu$ m.

**B)** Representative images of western blot analysis of ADAM10 and CAP2 in the TIF of primary hippocampal neurons. The quantitative analysis shows that oA $\beta_{1-42}$  increase ADAM10 synaptic localization (CTRL 100 ± 16.55%, A $\beta_{42-1}$  102.7 ± 18.9%, oA $\beta_{1-42}$  222 ± 32.46% \* $p$  < 0,05 one-way ANOVA,  $n$ =3). The quantitative analysis shows that oA $\beta_{1-42}$  decreases CAP2 synaptic localization (CTRL 100 ± 15.37%, A $\beta_{42-1}$  108.8 ± 13.05%, oA $\beta_{1-42}$  52.53 ± 9.966% \* $p$  = 0.014 one-way ANOVA,  $n$ =9).



**C)** Representative western blot of the homogenate and TIF fraction of primary neurons treated with oA $\beta_{42-1}$ , A $\beta_{1-42}$  or CTRL without treatment loaded on a non-reducing gel revealing no differences in the CAP2 dimer upon oA $\beta_{1-42}$  treatment. Statistical analysis is done by a one-way ANOVA with a Tukey post-hoc test. Homogenate: CTRL mean = 100 +/- 16.29, A $\beta_{1-42}$  mean = 126.9 +/- SEM 26.01, oA $\beta_{1-42}$  mean = 116.2 +/- SEM 31.84, P = 0.71, TIF: CTRL mean = 100 +/- 14.24 A $\beta_{1-42}$  mean = 116.4 +/- SEM 17.28, oA $\beta_{1-42}$  mean = 111.3 +/- SEM 14.81. P = 0.73, n = 7.

**D)** Representative images of co-immunoprecipitation between ADAM10 and either SAP97 or  $\beta$ 2-Adaptin. The quantitative analysis shows that oA $\beta_{1-42}$  treatment reduces the interaction with  $\beta$ 2-Adaptin without affecting the interaction with SAP97 (SAP97 96.95  $\pm$  5.26%,  $\beta$ 2-Adaptin 57.39  $\pm$  17.81%, \* p < 0.05 t-test oA $\beta_{1-42}$  vs A $\beta_{42-1}$ , n=3).

Since we previously shown that the actin-binding domain of CAP2 is relevant for ADAM10 endocytosis (Fig. 3), we looked at the CAP2 association with ADAM10 and actin, to see whether those are affected by oA $\beta_{1-42}$  treatment. To assess the interaction between CAP2 and ADAM10 we used primary hippocampal neurons transfected at DIV7 with EGFP, and at DIV14 treated with oA $\beta_{1-42}$ . With the use of PLA, we detected a decreased association between CAP2 and ADAM10 upon the treatment with (Fig. 14A). Additionally, to investigate whether also the binding between CAP2 and actin is altered, we lysed the DIV14 primary rat neurons after oA $\beta_{1-42}$  treatment, and with a Co-IP we identified an increase of the CAP2 and actin interaction (Fig. 14B). Overall, these data show that the CAP2 complex formation with both ADAM10 and actin are affected by oA $\beta_{1-42}$ , and are therefore a target of the early hallmarks of AD. The decreased CAP2/ADAM10 complex formation and the increased CAP2/actin complex, show the opposite effect as what we saw during cLTP induction, probably due to the opposite effects of oA $\beta_{1-42}$  inducing cLTD like phenomena. Since the cLTD did not have any effect on the CAP2 binding formation to ADAM10 and actin, these are possibly during the more severe effects of the oA $\beta_{1-42}$ .

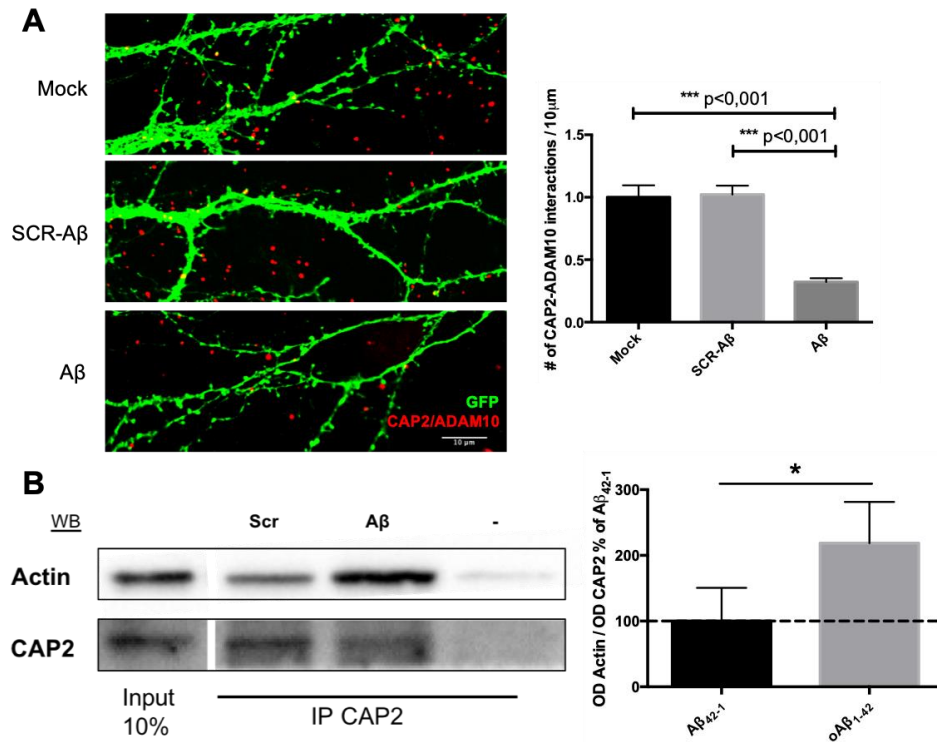


**Figure 14) CAP2 interaction with ADAM10 and Actin is altered upon Aβ oligomer treatment in primary hippocampal neurons.**

**A)** Representative image of the PLA with an anti-rabbit CAP2 antibody and an anti-goat ADAM10 antibody reveals a decrease in their interaction upon the treatment with Aβ oligomer. Quantification of the PLA by counting the # of interactions normalized on the dendritic length by a one-way ANOVA followed by post-hoc Tukey test. Mock mean = 0.1615 +/- SEM 0.0155, Scramble AB<sub>42-1</sub> mean = 0.1650 +/- SEM 0.0115, oAB<sub>1-42</sub> mean = 0.052 +/- SEM 0.00479, Mock vs. oAB<sub>1-42</sub> \*\*\*P <0.0001, Scramble AB<sub>41-1</sub> \*\*\*P<0.0001, n = 10 neurons of 2 individual neuronal culture preparations.

**B)** Representative image of the Co-IP between anti-rabbit CAP2 and anti-mouse actin shows an increased interaction upon the acute oAβ<sub>1-42</sub> treatment compared to scrambled treatment. For the quantification of the Co-IP, raw O.D. Actin / O.D. CAP2 values were normalized on the AB<sub>42-1</sub>. AB<sub>42-1</sub> Scramble mean = 100 +/- SEM 50.62, oAB<sub>1-42</sub> mean = 218.6 +/- SEM 62.77, AB<sub>42-1</sub> vs. oAB<sub>1-42</sub>, P<0.05, n = 6.

## 5.) CAP2 in Alzheimer's Disease

### 5.1.) CAP2 expression and synaptic localization are reduced in AD patients' hippocampi

In order to understand the possible role of CAP2 in AD pathogenesis, we took advantage of human hippocampal specimens provided by the Netherland Brain Bank. CAP2 was characterized in these hippocampal brain samples, comparing AD patients fulfilling Braak 4 and 5 stages with age-matched healthy controls (HC) (see table 1 for patient characteristics in material and methods). In order to avoid protein degradation, AD samples were paired to HC samples by braak stage, age and sex and processed at the same time. To analyze CAP2 expression and localization in these samples, we homogenized the hippocampal brain specimen and purified the TIF fraction. We verified that the TIF has an enrichment of a post-synaptic marker, while presynaptic proteins are absent (Fig. 15).

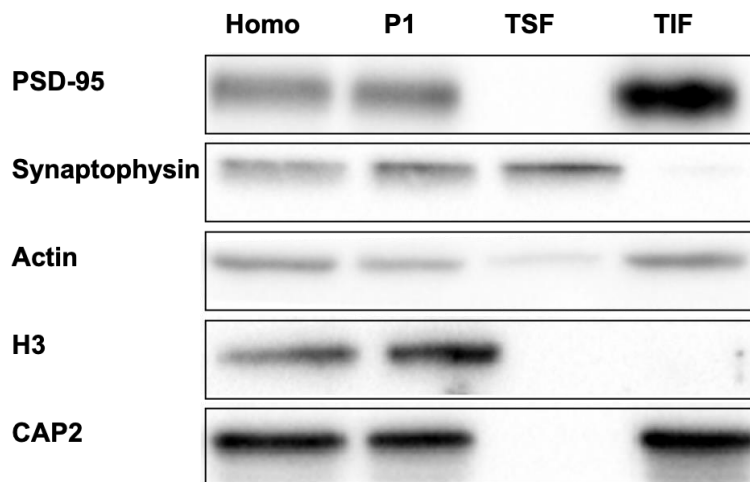


**Figure 15) Validation of the TIF preparation.** Representative images of the different fractions collected during the TIF preparation. Homo = Homogenate. P1 = Nuclei-associated fraction. TSF = Triton-soluble fraction (extra-synaptic). TIF = Triton-insoluble fraction (synaptic fraction). CAP2 is present in the TIF. The PSD95 (marker of post synaptic protein, is enriched in the TIF fraction and absent in the TSF. Synaptophysin (marker for the pre-synaptic protein) is not present in the TIF fraction, but in the TSF. H3 (nuclear marker) is present in the P1 (nuclear) fraction.

The results show a significant down regulation of CAP2 protein levels in the total homogenate (Fig. 16A) and in the TIF fraction (Fig. 16B) of human hippocampal brain samples of AD patients when compared to HC. ADAM10 expression is not modified in these AD patients due to high variability (Fig. 16A) as previously demonstrated <sup>241</sup>. Since we observed that CAP2 dimerization is a partner of cofilin, we looked at the differences of the dimer in the AD patients. Remarkably, the dimer of CAP2 levels were reduced in the synaptic compartment, but not in the total homogenate of AD patients compared to HC (Fig. 16C/D). These data indicate that CAP2 is involved in the AD pathogenesis, and that the synaptic localization of the dimerization of CAP2 is affected in AD patients.

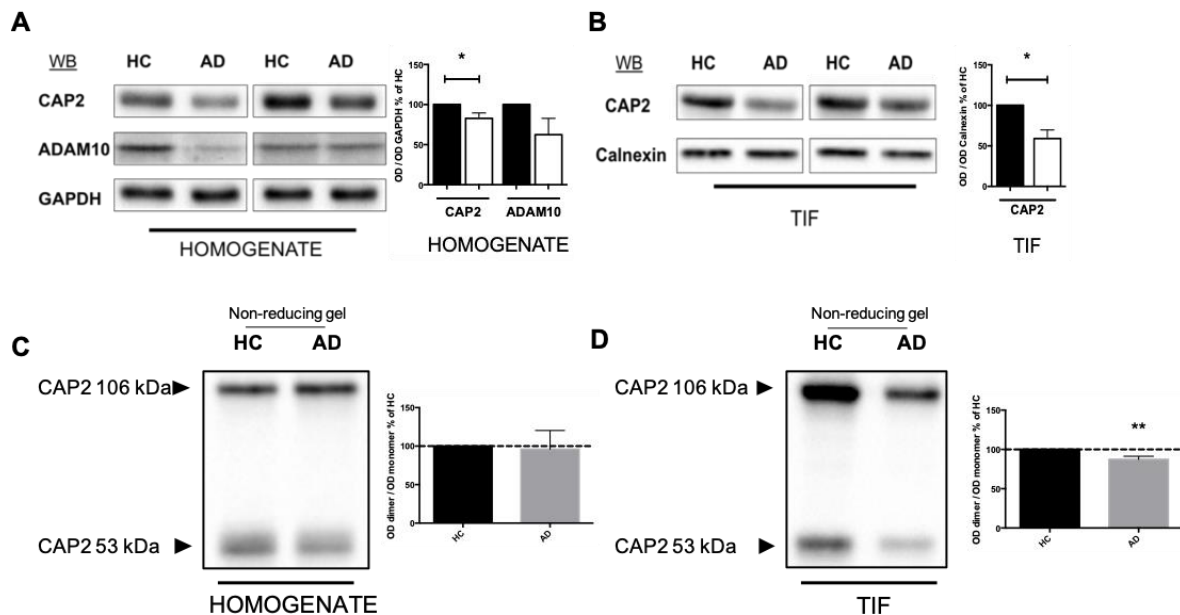


**Figure 16) CAP2 protein levels and localization are reduced in AD patients with a lower CAP2 dimer availability in the synaptic fraction.**

**A)** Representative WB showing the expression of CAP2 in hippocampal samples of human brain material in the homogenate. Quantification of O.D. is normalized on loading control GAPDH O.D. For the statistical analysis, we used a 2-tailed paired t-test. CAP2; AD mean = 82.8 +/- SEM 6.69, HC vs. AD \*P<0.05, n = 6. ADAM10; AD mean = 62.32 +/- SEM 20.47, HC. Vs. AD P=0.125.

**B)** Representative WB of the TIF fraction of CAP2 in hippocampal samples of human brain material of HC and AD patients. Quantification of CAP2 O.D. is normalized on loading control Calnexin O.D. For statistical analysis, we used a 2-tailed paired t-test. CAP2; AD mean = 59.04 +/- SEM 10.59, HC vs. AD \*\*P<0.01, n = 6.

**C)** Representative WB showing the dimerization of CAP2 in the homogenate of hippocampal samples of human brain material. Quantification of O.D. CAP2 dimer is normalized on the O.D. CAP2 monomer. For the statistical analysis, we used a 2-tailed paired t-test. CAP2; AD mean = 95.96 +/- SEM 24.37, HC vs. AD P=0.87, n = 6.

**D)** Representative WB showing the dimerization of CAP2 in the TIF of hippocampal samples of human brain material. Quantification of O.D. CAP2 dimer is normalized on the O.D. CAP2 monomer. For the statistical analysis, we used a 2-tailed paired t-test. CAP2; AD mean = 87.26 +/- SEM 4.06, HC vs. AD \*\*P<0.01, n = 6.

## 5.2.) CAP2 association with actin is increased in AD hippocampi

To understand whether the interaction between CAP2 and its binding partners is altered in AD hippocampal tissue compared to HC, Co-IP assays between CAP2 and ADAM10 or CAP2 and Actin were performed. Co-IP experiments using an ADAM10 antibody first show that CAP2 co-precipitates with ADAM10, but there are no significant changes in AD patients compared to age-matched HC (Fig. 17). The second Co-IP experiment in which a CAP2 antibody was used, as expected, show that actin co-precipitates with CAP2. Remarkably, the association between CAP2 and actin is increased in AD patients compared to age-matched HC (Fig. 18). Overall, these results suggest that the complex formation of CAP2 and actin is a novel target in AD pathogenesis.

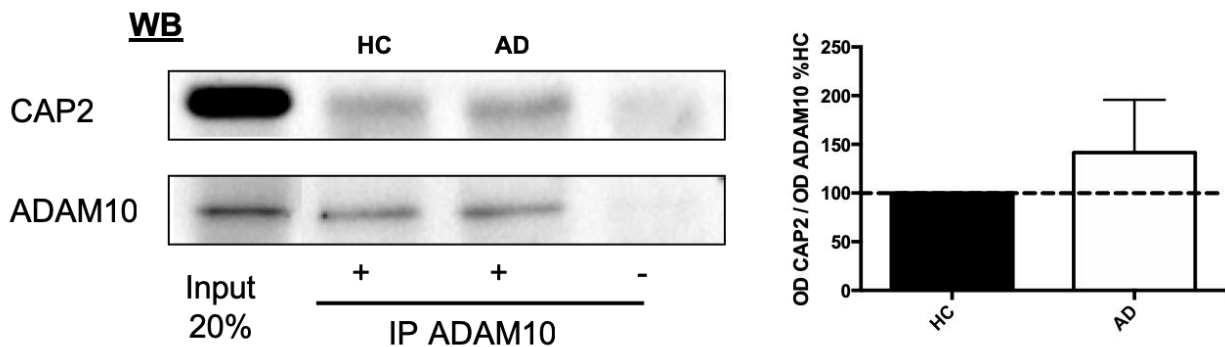


**Figure 17) ADAM10/CAP2 association is not changed in AD hippocampi.**

Human homogenate IP with an anti-rabbit ADAM10 antibody reveals the presence of CAP2 in the immune-complex. IP ADAM10 was detected by WB with a rat anti-ADAM10 antibody, and CAP2 with a goat anti-CAP2 antibody. ADAM10/CAP2 association is not changed between both groups. For statistical analysis we used an unpaired student t-test and quantification of the immunoprecipitated CAP2 O.D normalized on ADAM10 O.D. AD mean = 141.5 +/- SEM 54.24, AD vs. HC P=0.46, n = 6).

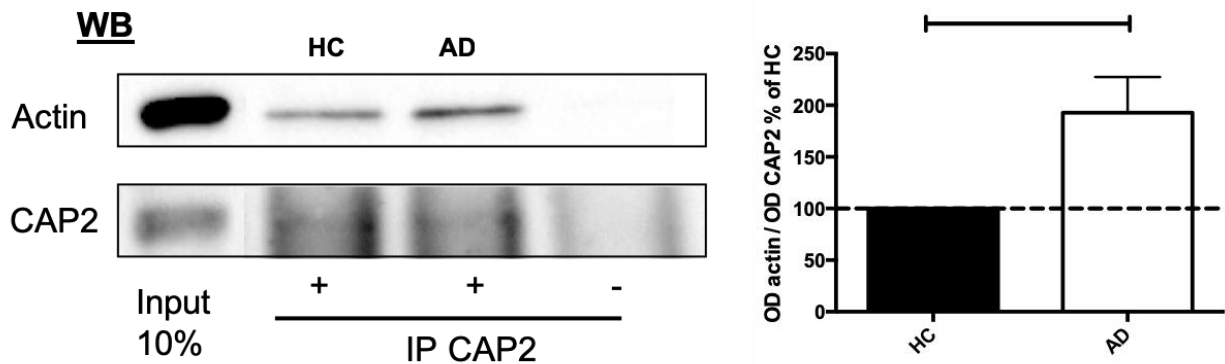


**Figure 18) CAP2/Actin association is increased in AD hippocampi.**

Human homogenate IP with an anti-rabbit CAP2 antibody reveals the presence of Actin in the immune-complex. IP CAP2 was detected by WB with a goat anti-CAP2 antibody, and Actin with a mouse anti-mouse antibody. CAP2/Actin association is increased between both groups. For statistical analysis we used an unpaired student t-test and did the quantification of the immunoprecipitated Actin O.D. normalized on CAP2 O.D. AD mean=192.8 +/- SEM 34.55, AD vs. HC \*P<0.05, n = 6).

### 5.3.) CAP2 and ADAM10 synaptic levels are altered in APP/PS1 mice hippocampi

To unravel the complete mechanism and assess the role of CAP2 in AD, we took advantage of an AD mice model. The AD mice model used in this project are the APP/PS1 double transgenic mice, expressing a chimeric mouse/human amyloid precursor protein (Mo/HuAPP695swe) and a mutant human presenilin 1 (PS1-dE9), directed to CNS neurons<sup>203</sup>. This mouse model shows early synaptic loss and plaque accumulations before the age of 6 months, neuronal loss starting from 9 months on and then cognitive deficits after 12 months of age (Fig. 19).

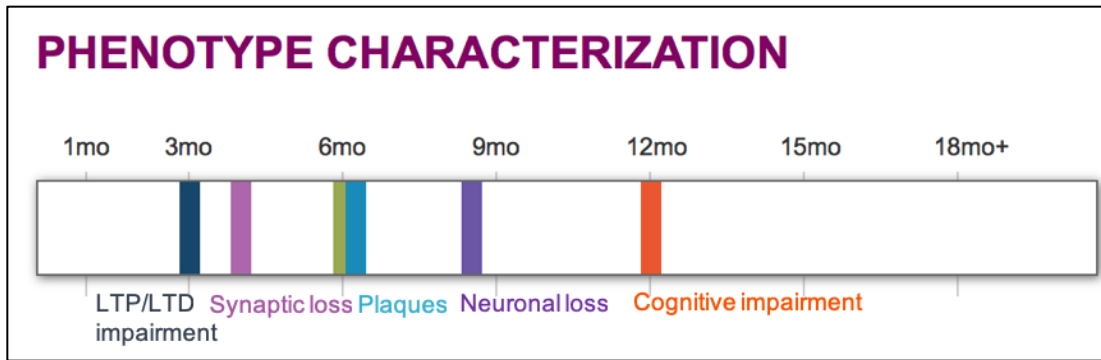


**Figure 19) Phenotype APP/PS1 mice**

APP/PS1 double transgenic mice. Representative image of the phenotype characterization of the APP/PS1 mice expressing (Mo/HuAPP695swe - PS1dE9). Synaptic loss is found around the age of 3 months, with accumulations of amyloid plaques at 6 months, at 9 months neuronal loss is seen where cognitive impairment starts around 12 months of age. (Obtained and modified from <https://www.alzforum.org/research-models/appswepsen1de9-0>)

At the early stages of the disease (6 months of age), these animals show plaque accumulation and synaptic dysfunction, while there are no strong cognitive deficits detectable yet. In the hippocampus of APP/PS1 mice, a decrease in CAP2 and PSD-95 expression was detected (Fig. 20A/C), and in the synaptic fraction, reduced localization of CAP2, PSD-95 and ADAM10 were detected (Fig. 20B/D).

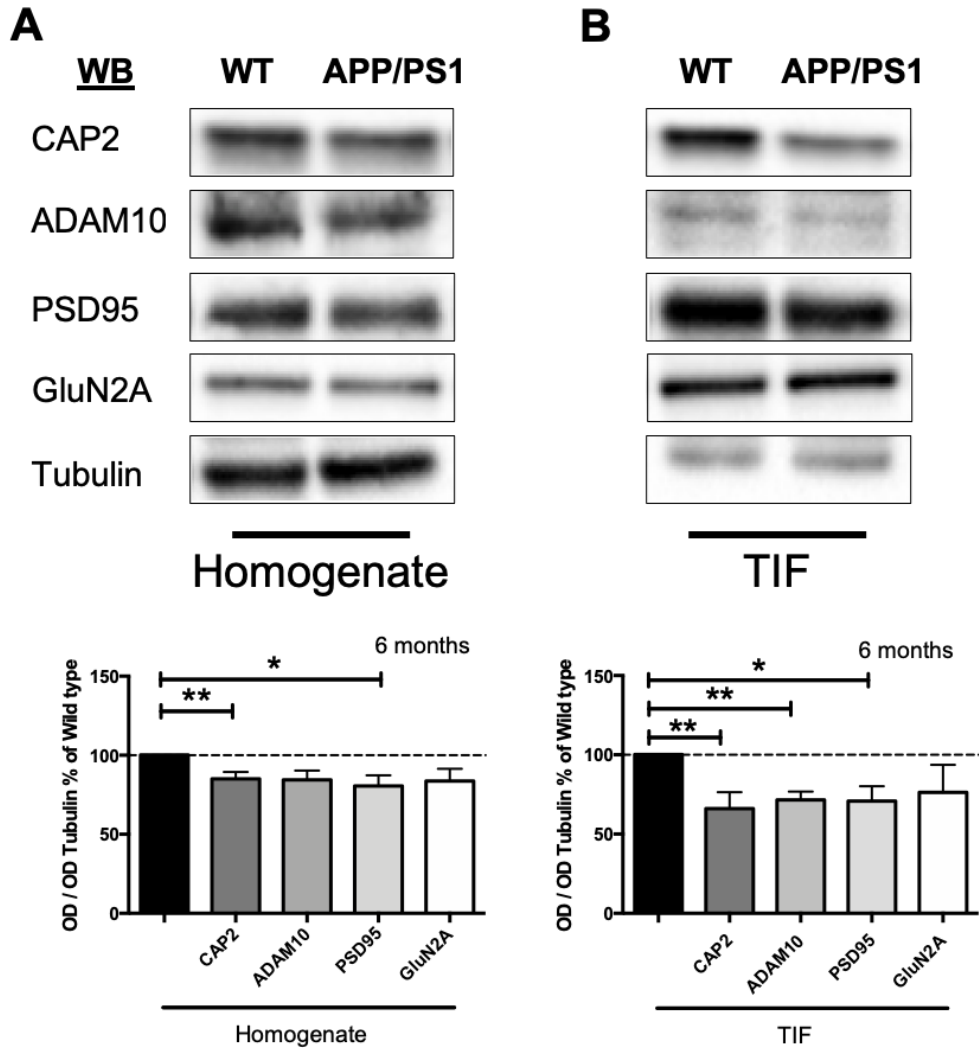


**Figure 20) CAP2 and ADAM10 are altered in APP/PS1 mice hippocampal brain tissue at 6 months of age.**

**A)** Representative WB of the homogenate of hippocampal tissue of 6 months old mice. For statistical analysis we used an unpaired student t-test for all protein individually. We normalized the O.D. of the protein on the O.D. of housekeeping protein Tubulin, and normalized on the WT. (CAP2, APP/PS1 mean = 85.01 +/- SEM 4.286, APP/PS1 vs. WT \*\*P < 0.01, ADAM10, APP-PS1 mean = 84.49 +/- SEM 5.821, P = 0.18, PSD-95, APP/PS1 mean = 80.59 +/- SEM 6.755, P < 0.05, GluN2A, APP/PS1 mean = 83.64 +/- SEM 7.86, P = 0.07, n = 6.)

**B)** Representative WB of the TIF fraction of hippocampal tissue of 6 months old mice. For statistical analysis we used an unpaired student t-test for all protein individually. We normalized the OD of the protein on the OD of housekeeping protein Tubulin, and normalized on the WT.

(CAP2, APP/PS1 mean = 66.07 +/- SEM 10.36, APP/PS1 vs. WT \*\*P < 0.01, ADAM10, APP/PS1 mean = 71.51 +/- SEM 5.264, \*\*\*P < 0.001, PSD-95, APP/PS1 mean = 70.78 +/- SEM 9.408, \*\*P < 0.01, GluN2A, APP/PS1 mean = 76.37 +/- SEM 17.29, p = 0.2, n = 6)

Additionally, since the CAP2 levels are reduced in APP/PS1 mice at 6 months of age, we verified the dimerization of CAP2. No alterations in the expression of the dimer are



found, but the availability of the dimer in the synaptic TIF fraction is decreased (Fig 21). Indicating again a role of the CAP2 dimer in AD, in concordance with the results from the AD patients.

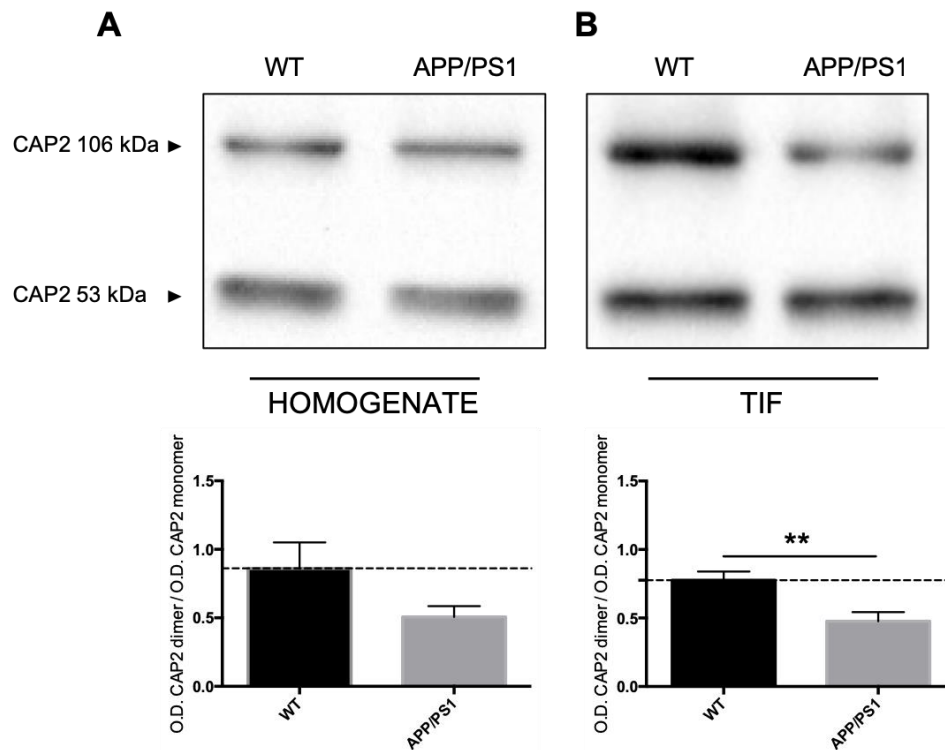


**Figure 21) Availability of CAP2 dimer in synaptic membrane decreased in APP/PS1 mice at 6 months of age.**

**A)** Representative WB of the dimer of CAP2 in the homogenate of the hippocampus of APP/PS1 mice at 6 months of age compared to wild type animals. Underneath the statistical analysis done by an unpaired t-test. Shown as the ratio of O.D. CAP2 dimer on the O.D. CAP2 monomer. (WT mean = 0.8612 +/- SEM 0.1901, APP/PS1 mean = 0.5073 +/- SEM 0.0778, WT vs. APP/PS1 P = 0.128, n = 6)

**B)** Representative WB of the dimer of CAP2 in the TIF fraction of the hippocampus of APP/PS1 mice at 6 months of age compared to wild type animals. Underneath the statistical analysis done by an unpaired t-test. Shown as the ratio of O.D. CAP2 dimer on the O.D. CAP2 monomer. (WT mean = 0.7755 +/- SEM 0.06339, APP/PS1 mean = 0.4765 +/- SEM 0.06695. WT vs. APP/PS1 \*\*P < 0.01, n = 6).

#### 5.4.) CAP2 association to its binding partners is altered in APP/PS1 mice hippocampi

To unravel whether the interaction between CAP2 and its binding partners ADAM10 and actin is altered in the brain of APP/PS1 mice, we analyzed the ADAM10/CAP2 and

CAP2/Actin complex levels in different stages of the disease. Surprisingly, the interaction between CAP2 and ADAM10 is altered only in the early stages of the disease, at 6 months, in the hippocampus of APP/PS1 mice compared with wild type (WT), while at later stages of the disease (12 and 15 months), the binding is brought back to normal levels. This might be due to an overcompensating mechanism during the later stages of the disease, indicating that the binding between CAP2 and ADAM10 is important in the early stages of AD (Fig. 22).

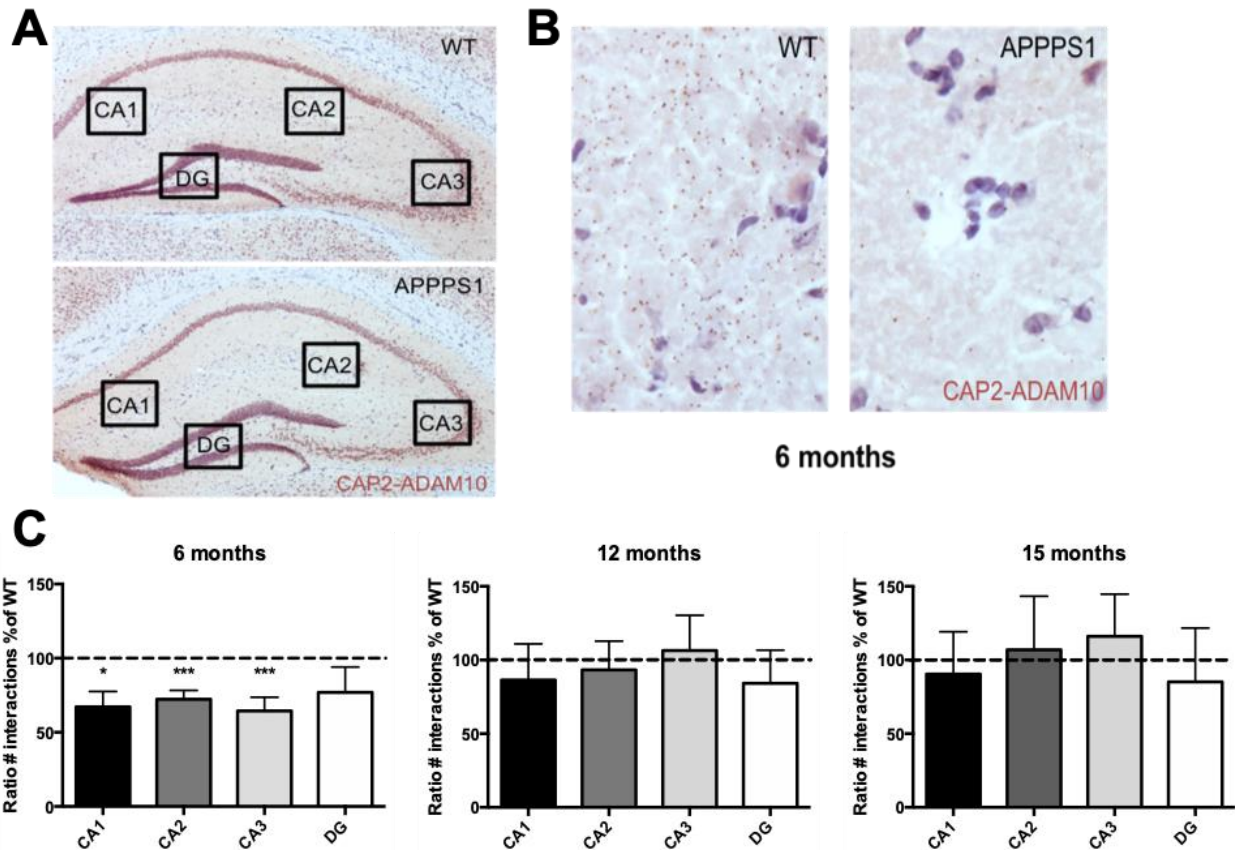


**Figure 22) CAP2/ADAM10 binding is altered in the early stages of disease.**

**A)** A representative image of a brightfield PLA assay between CAP2 and ADAM10 in APP/PS1 hippocampal slices of APP/PS1 mice and WT mice.

**B)** A representative zoomed in image of the PLA signal (brown) in the CA1 area at 6 months of age.

**C)** Quantification of the PLA signal (# of dots normalized on the # of dots in the negative control and the ratio taken on the WT) by an unpaired 2-tailed t-test, where a decreased association between CAP2 and ADAM10 is detected only at 6 months of age, which is rescued at later age (12 and 15 months). 6months: CA1 area mean = 74.72 +/- SEM 12.08, WT vs. APP/PS1 \*P<0.05, CA2 area mean = 72.35 +/- SEM 5.925, \*\*\*P < 0.0001, CA3 area mean = 64.42 +/- SEM 9.269, \*\*\*P<0.001. n = 12 individual PLA assays on sections of n = 4 animals each condition.

In addition, to find out whether the binding between CAP2 and actin is affected in APP/PS1 mice at different stages of the disease, we performed a Co-IP assay, precipitating CAP2 and revealing actin by western blot in the hippocampal tissue of APP/PS1 mice compared to WT at different stages of the disease. We found that in both the early stages of the disease (at 6 months of age) and at later stages of the disease (at 12 months of age), the CAP2 association to actin is increased (Fig. 22). These data are consistent with the data obtained in the AD patients hippocampi and in neuronal cultures treated with A $\beta$  oligomers, indicating that the binding between

CAP2 and actin is involved in AD pathogenesis, and might serve as a potential pharmacological target.

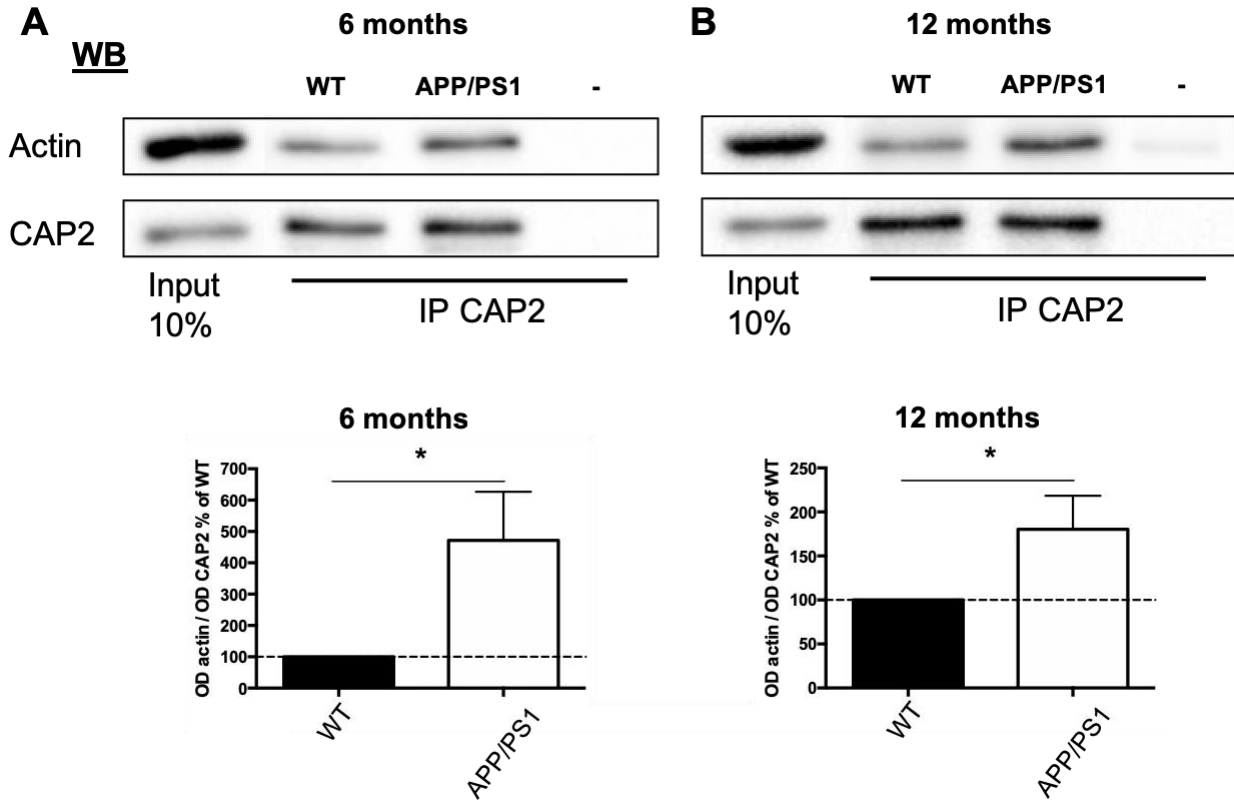


**Figure 23) CAP2/actin binding in multiple stages of disease.**

**A)** Homogenates from hippocampi of WT and APP/PS1 mice, at 6 months of age, were IP with rabbit anti-CAP2 antibody and Actin co-precipitation was revealed. The CAP2/Actin association is increased in APP/PS1 mice compared to WT. For statistical analysis we used an unpaired student t-test and did the quantification of the immunoprecipitated Actin O.D. normalized on CAP2 O.D. and normalized on the WT levels. APP/PS1 mean = 471.5 +/- SEM 155.5, WT vs. APP/PS1 \*P<0.05, n = 10).

**B)** Homogenates from hippocampi of WT and TG mice, at 12 months of age, were IP with rabbit anti-CAP2 antibody and Actin co-precipitation was revealed. The CAP2/actin association is increased in APP/PS1 mice compared to WT. For statistical analysis we used an unpaired student t-test and did the quantification of the immunoprecipitated Actin O.D. normalized on CAP2 O.D. and normalized on the WT levels. APP/PS1 mean = 180.3 +/- SEM 38.10, WT vs. APP/PS1 \*P < 0.05, n = 6).

## **6.) Potential therapeutic strategies for Alzheimer's Disease targeting the CAP2 pathway**

### **6.1.) Characterization CAP2 in APP/PS1 hippocampal neurons**

Our results show that CAP2 is altered in both AD patients and APP-PS1 mice. In particular, CAP2 protein levels are significantly reduced in AD, thus leading to a decrease in CAP2 dimer in the synapses. Therefore, we designed a potential therapeutic strategy aimed at the restoring of CAP2 levels in an AD model.

To this aim, we set up a primary hippocampal neuronal model, obtained from WT and APP/PS1 mice. First, we characterized our model assessing human A $\beta$  levels in the medium by ELISA and the expression and localization of multiple proteins of our interest as CAP2, ADAM10, GluN2A and PSD-95. In the cultures of APP/PS1 mice, we found 1.21 pg/ml of A $\beta$  in the medium taken at DIV14, suggesting that our cultures produce human A $\beta$  and release it into their medium, and thereby confirming the use of this model. We couldn't detect decreased expression levels of CAP2 in the homogenate of these neurons, like in the tissue homogenate, but in concordance with the tissue there is a decrease in PSD-95 expression level, suggesting a decrease in spine density. In addition, in the TIF fraction, we found a decrease of ADAM10 synaptic availability (Fig. 24). Taken together, these data indicate that this model is suitable to further explore whether CAP2 could rescue these deficits.

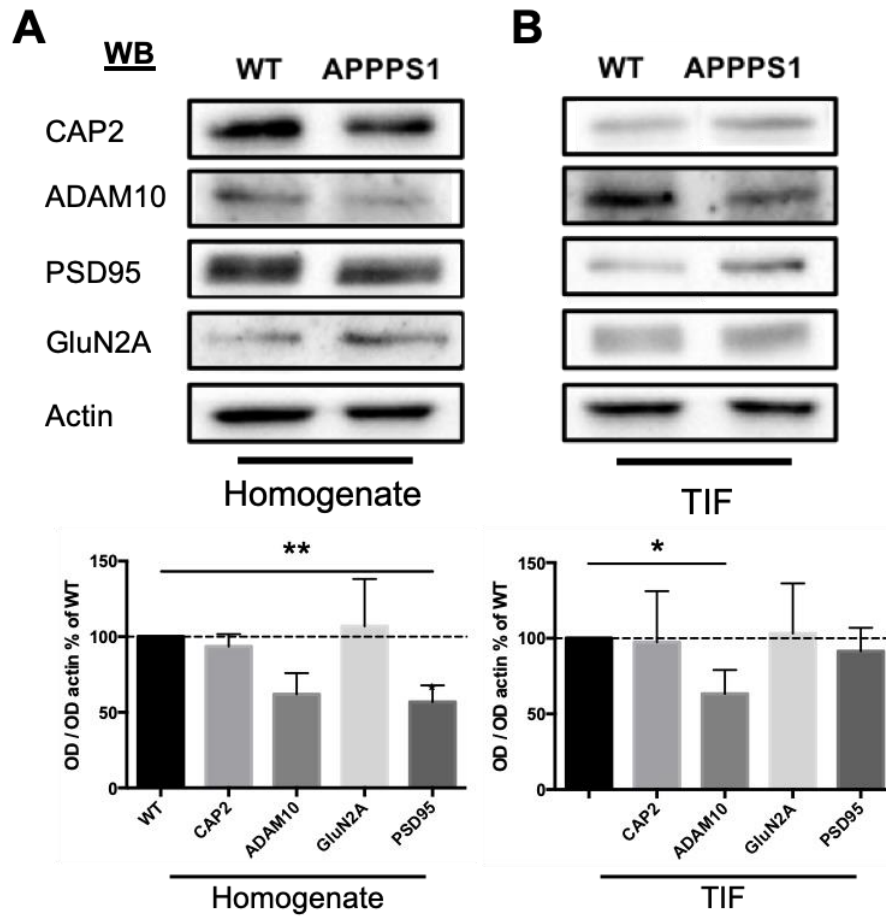


**Figure 24) Characterization of APP/PS1 primary hippocampal neurons.**

In order to understand whether we could use the primary hippocampal neurons of APP/PS1 mice as an *in vitro* model, we characterized the p0 cultures after homogenizing them at DIV14 and extracting the TIF fraction.

**A)** Representative WB image of the homogenate of wild type cultures compared to APP/PS1 cultures. Underneath is shown the statistical analysis which was done by paired t-test, CAP2  $P = 0.44$  mean = 93.54 +/- SEM 8.13, ADAM10  $P = 0.41$  mean = 80.89 +/- SEM 22.43, PSD-95  $P = 0.002$  mean = 56.8 +/- SEM 10.99, GluN2A  $P = 0.82$  mean = 106.88 +/- SEM 31.25.

**B)** Representative B image of the TIF fraction of wild type cultures compared to APP/PS1 cultures. Underneath is shown the statistical analysis which was done by paired t-test, CAP2  $P = 0.94$  mean = 102.01 +/- SEM 27.85, ADAM10  $P = 0.02$  mean = 63.27 +/- SEM 14.40, PSD-95  $P = 0.51$  mean = 91.3 +/- SEM 12.69, GluN2A  $P = 0.91$  mean = 96.87 +/- SEM 27.74.  $n = 8$  for the homogenate and  $n = 6$  for the TIF.

## **6.2.) CAP2 overexpression rescues PSD-95 levels and ADAM10 synaptic localization in APP/PS1 mice**

Since we found a reduction of PSD-95 expression and ADAM10 synaptic localization in the primary hippocampal neurons of APP/PS1 mice, we investigated whether the overexpression of CAP2 could restore these levels. For this we transduced primary hippocampal neurons of both wild type or APP/PS1 P0 mice at DIV10 with a lentiviral vector expressing CAP2, under the control of a neuronal promoter. Results show that we successfully increased the levels of CAP2 by the viral overexpression of CAP2 (Fig. 25A). Then, we show that the overexpression of CAP2 is able to restore the PSD-95 levels that were decreased in the APP/PS1 mice cultures (Fig. 25A) and significantly increase the ADAM10 synaptic availability (Fig. 25B). These data suggest that CAP2 is important for the function of synapses, because of its importance for the regulation of the main scaffolding protein of the postsynaptic compartment (i.e. PSD-95) and by its function in the promotion of ADAM10 in the synaptic membrane, and thereby possibly its activity.

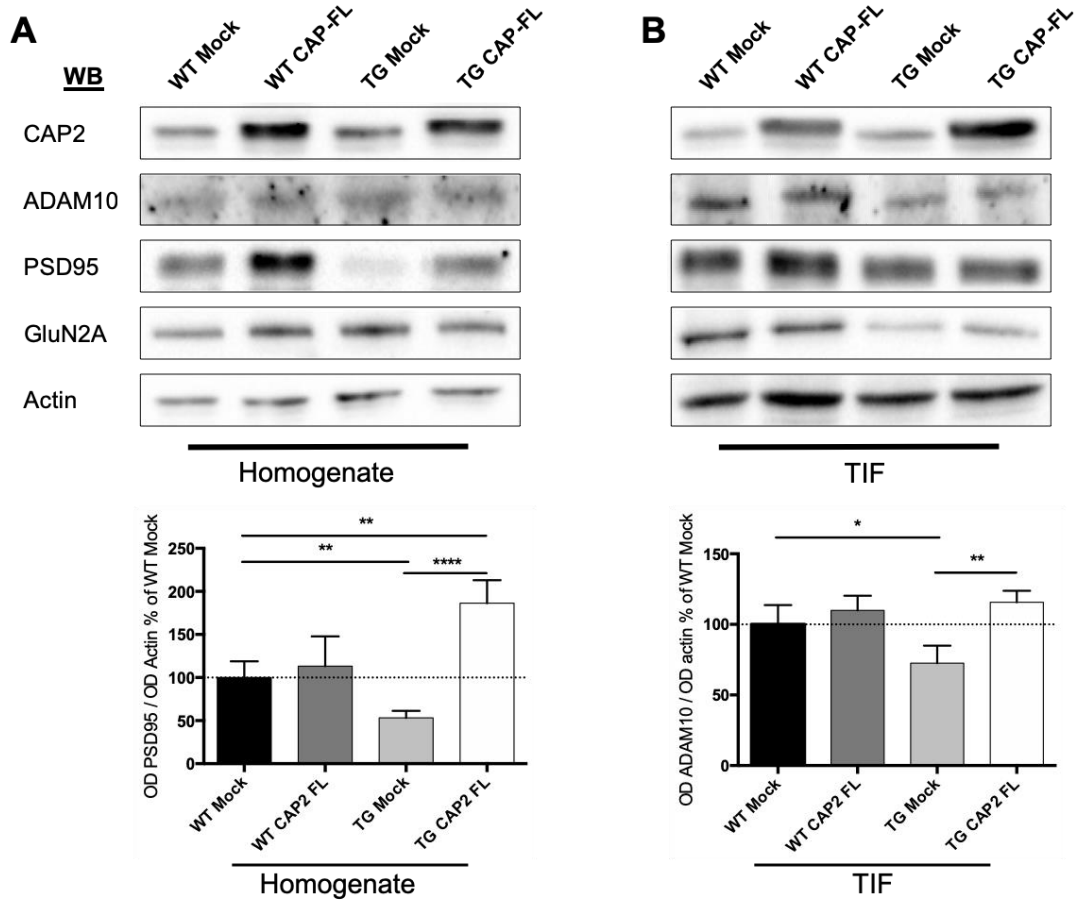


**Figure 25) Overexpression of CAP2 in APP/PS1 P0 primary hippocampal mice neurons rescues PSD-95 expression and ADAM10 synaptic localization.**

To verify whether CAP2 overexpression affect the synaptic molecular composition in APP/PS1 mice cultures, we overexpressed CAP2-FL in DIV10 cultures prepared from WT and APP/PS1 mice and homogenized the cells at DIV14 followed by a TIF purification.

**A)** Representative WB image of the homogenate of wild type cultures compared to APP/PS1 cultures either with or without overexpression of CAP2-FL. Underneath is shown the statistical analysis which was done by one-way ANOVA followed by post-hoc Fisher LSD, the data is shown as O.D. PSD-95 normalized on O.D. of housekeeping protein actin and normalized on the WT Mock. PSD-95 (WT mock mean = 100 +/- SEM 18.91, WT CAP2-FL mean = 113.1 +/- SEM 34.77, TG mock mean = 53.17 +/- 8.204, TG CAP2-FL mean = 186.3 +/- SEM 26.68, \*\* p < 0.01 WT mock vs. TG mock, \*\*\*\* p < 0.01 TG mock vs. TG CAP2-FL, \*\*\* p < 0.001 WT mock vs. TG CAP2-FL. n = 4.)

**B)** Representative WB image of the TIF of wild type cultures compared to APP/PS1 cultures either with or without overexpression of CAP2-FL. Underneath is shown the statistical analysis which was done by one-way ANOVA followed by post-hoc Fisher LSD, the data is shown as O.D. ADAM10 normalized on O.D. of housekeeping protein actin and normalized on the WT Mock. ADAM10 (WT mock mean = 100 +/- SEM 13.69, WT CAP2-FL mean = 109.9 +/- SEM 10.4, TG mock mean = 72.61 +/- 12.33, TG CAP2-FL mean = 115.7 +/- SEM 8.206, \* p < 0.05 WT mock vs. TG mock, \*\* p < 0.01 TG mock vs. TG CAP2-FL. n = 4.)



### **6.3.) Development of cell permeable peptides targeting CAP2/Actin Interaction**

The interaction between CAP2 and actin is increased in AD patients, APP/PS1 mice and upon  $\alpha\text{A}\beta_{1-42}$  treatment. In addition, we showed that the actin-binding domain of CAP2 is important for ADAM10 endocytosis, and thereby, can regulate its synaptic levels.

In light of these data, the interaction between CAP2 and actin could represent an interesting target to restore a pathological alteration in AD. To this aim, in collaboration with Dr. Di Marino (Università Politecnica della Marche), we designed two active cell-permeable peptides (CPPs) (Pep A and Pep B) and an inactive CPP (Inactive) as a control. The CPPs are constituted by a HIV-trans activating protein sequence (TAT - YGRKKRRQRRR), which gives them the capability to cross biological membranes, including the blood-brain barrier (BBB), and the sequence that mimics the actin binding domain of CAP2. Therefore, the peptides can compete with the CAP2 binding to actin.

### **6.4.) Testing CPPs capability to cross the blood-brain barrier**

The mammalian brain is protected by the BBB, which is a highly selective barrier that separates the brain extracellular fluids with the circulating blood. Since the BBB is so selective in allowing permeabilization, we verified the ability of our CPPs to cross the BBB. To assess this, we administered wild-type animals (C57BL/6) with intraperitoneal injections of saline, used as a negative control, and our inactive and active peptides at a dose of 3nmol/g. 24hours after, the animals were sacrificed by perfusion with 4% PFA, and 50 $\mu\text{m}$  coronal brain sections were sliced with the vibratome. Then, we used the brain sections for immunofluorescent labelling, to verify the capability of the CPPs to cross the BBB and enter the brain. For immunofluorescent labelling, we used a neuronal marker (MAP2) in green, a nuclear marker (DAPI) in blue, and an antibody against the TAT sequence inserted in our CPPs (TAT) in red. The TAT protein was only visible in the animals treated with our inactive and active CPPs (Fig. 26). The TAT signal was present in neuronal cells with a distribution from nuclei to their dendrites. In the

animals treated with saline solution no red signal was detected, indicating that the TAT antibody specifically detects the TAT signal of the CPPs.

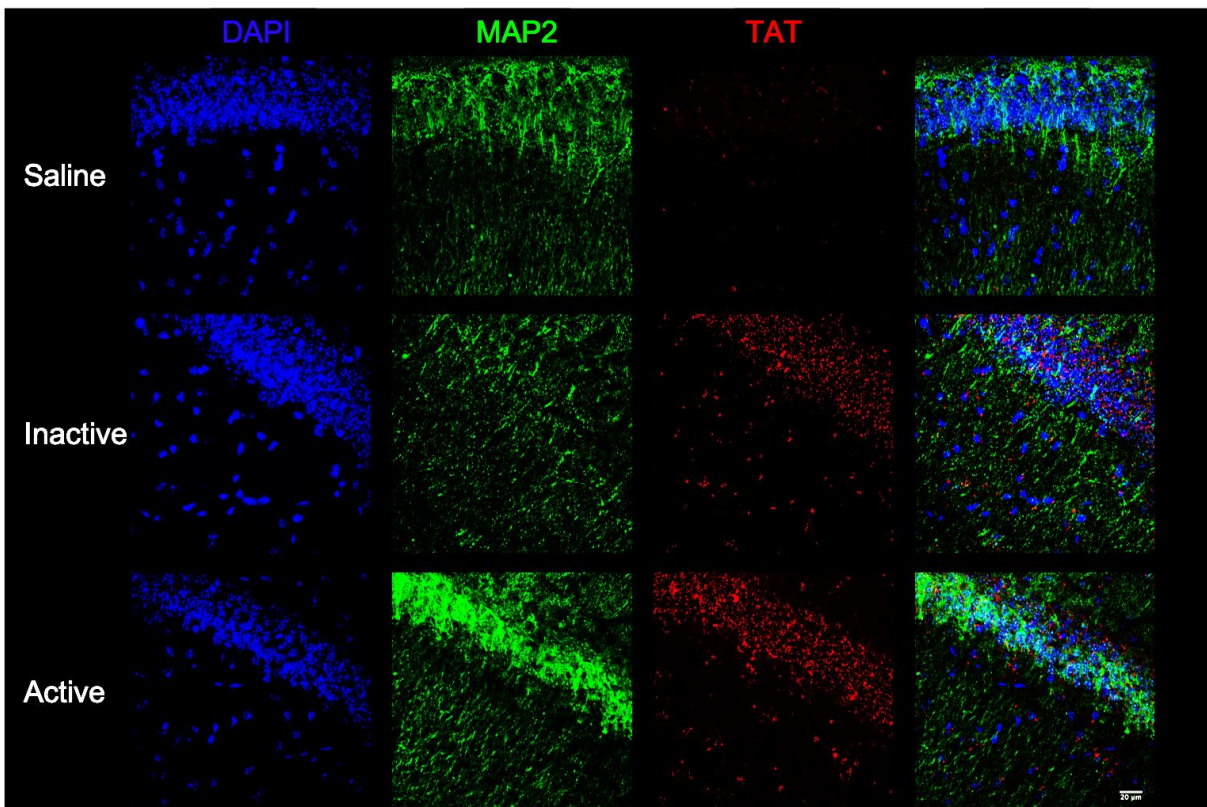


**Figure 26)** the inactive and active CPPs can cross the blood-brain-barrier. Wild type mice were treated with an acute treatment with saline or the inactive and active CPPs with 3nmol/mg. 24 hours after the injection, the animals were sacrificed, and the brain sectioned for IHC purposes. We stained 50 $\mu$ m sections for DAPI (nuclear marker), MAP2 (neuronal marker) and TAT (marker recognizing TAT sequence of our peptide). In the saline treated mice, we couldn't detect the TAT sequence, but in the Inactive and Active treated mice we detected the TAT signal, confirming that our CPPs can cross the blood-brain-barrier. Scale bar = 20 $\mu$ m.

## 6.5.) Uncoupling CAP2/Actin interaction *in vitro*

### 6.5)1. Testing CPPs efficacy

In order to understand which one of the two designed CPPs has the highest efficacy to uncouple CAP2 from actin, we performed *in vitro* tests. We used a GST-Pull-down assay, where we incubated a mouse brain homogenate with a GST-fusion protein for CAP2 and added either the active or inactive CPPs at the concentration of 1 $\mu$ M or 10  $\mu$ M for 30 minutes. Then the levels of actin were revealed by western blot (Fig. 27A). This showed that the CPP with the highest efficacy was Pep B (Fig. 27A). As a second

model, we used primary hippocampal neurons which we treated with the active or inactive CPPs at the concentration of 1  $\mu$ M or 10  $\mu$ M for 30 minutes. As shown in figure 27B, Co-IP assays revealed that again the Pep B seems to be the peptide with the highest efficacy.

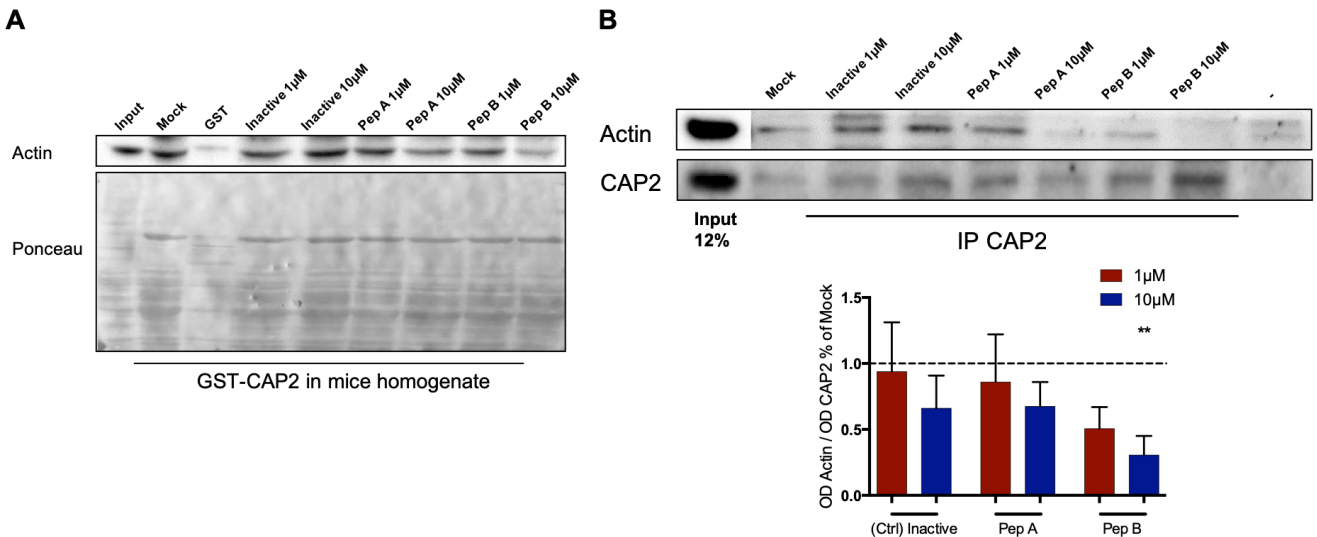


**Figure 27) *In vitro* test of the efficacy of both CPPs designed to interfere with the CAP2 association to actin.**

**A)** To test the efficacy of both CPPs (Pep A and Pep B) designed to disrupt the CAP2-actin complex, we performed a GST-Pull down assay. We used a mice brain homogenate and incubated it with GST-CAP2 fusion protein and different concentrations (1  $\mu$ M or 10  $\mu$ M) of our active or control/inactive peptides. With this in-vitro assay we identified that Pep B, at the concentration of 10  $\mu$ M, showed the biggest efficacy. (No statistical data since  $n = 1$ ).

**B)** To confirm the efficacy in another way, we used primary hippocampal cultures that we treated with 1  $\mu$ M or 10  $\mu$ M of our active or control/inactive peptides and performed Co-IP experiments, precipitating CAP2 with a rabbit anti-CAP2 antibody, and revealing the co-precipitation of actin with a mouse anti-actin antibody, while CAP2 was revealed using a goat anti-CAP2 antibody. A representative WB image is shown, and statistical analysis was done using a One-way ANOVA with a Tukey post-hoc test. The most effective CPP, is again Pep B at a concentration of 10  $\mu$ M, which is the only one that shows a statistical difference. Mock mean = 1 +/- 0.39; Pep B 10  $\mu$ M mean = 0.1688 +/- 0.057; Mock vs. Pep B 10  $\mu$ M \*\* $p = 0,008$ ,  $n = 6$ .

## 6.6.) Uncoupling CAP2/Actin interaction *in vivo*: Acute treatment

### 6.6)1. Testing CCPs efficacy and specificity *in vivo*

According to the results we got in the *in vitro* experiments, we proceeded with a test of the CPPs *in vivo*. We treated 8 weeks old C57BL/6 mice by intraperitoneal injection with either the active CPPs Pep A or Pep B or with the inactive peptide at a dose of 3nmol/gram, or a saline solution alone as a control. 24 hours after the injection, the animals were sacrificed by dislocation and the hippocampal area and cortex were rapidly dissected. We used the total hippocampal homogenate to analyze the

interaction between CAP2 and actin. The homogenate was immunoprecipitated using an anti-CAP2 antibody and the presence of actin was revealed by western blot. As shown in Fig. 28A, Pep B is the CPP that shows significant reduction in the CAP2/actin association and is able to interfere with the binding of CAP2 and actin, while Pep A doesn't affect this interaction. To check whether the CPPs don't interfere with binding of the other member of the CAP family, CAP1, to actin, we performed Co-IP experiments shown in Fig. 28B. Both CPPs show specificity for the interference between CAP2 and actin association, without affecting the binding between CAP1 and actin. These results demonstrate the capability of Pep B to interfere with the CAP2/Actin complex formation *in vivo*, without affecting CAP1.

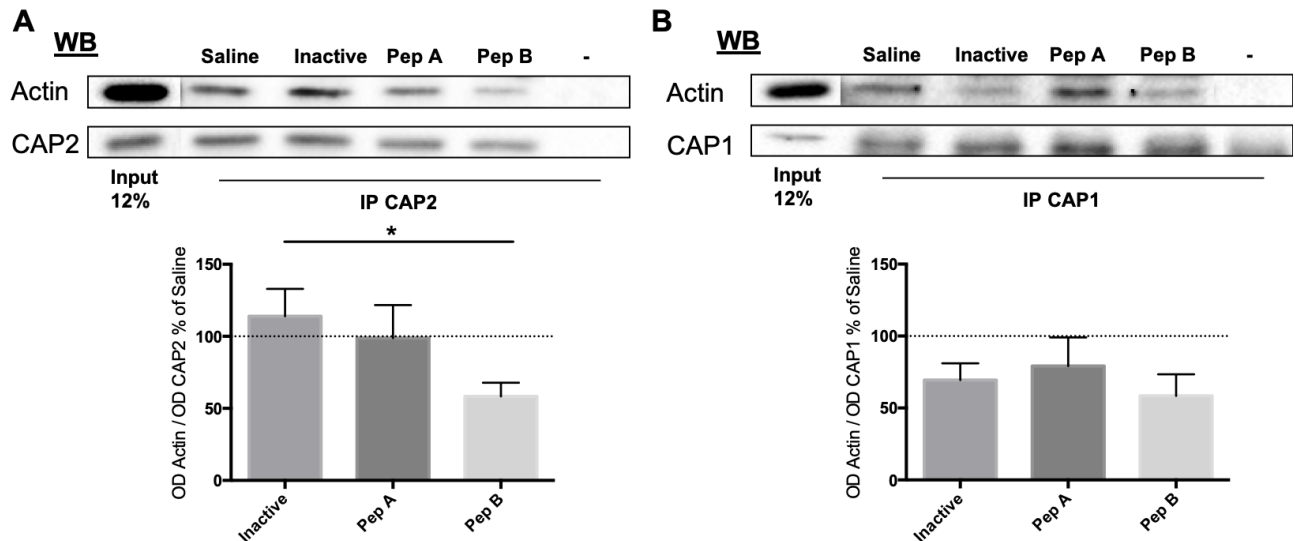


**Figure 28) The efficacy and specificity of both CPPs *in vivo* upon an acute treatment.**

**A)** To test the efficacy of both CPPs (Pep A and Pep B) designed to disrupt the CAP2-actin complex *in-vivo*, we used wild type C57/BL6 mice that we treated with a dose of 3nmol/gram of the active or control/inactive peptides and performed Co-IP experiments from hippocampal homogenates, precipitating CAP2 with a rabbit anti-CAP2 antibody, and revealing the co-precipitation of actin with a mouse anti-actin antibody, while CAP2 was revealed using a goat anti-CAP2 antibody. A representative WB image is shown, and statistical analysis was done using a One-way ANOVA with a Fisher LSD post-hoc test. The most effective CPP, is again Pep B, which is the only one that shows a statistical difference. Saline mean = 100 +/- SEM 16; Inactive mean = 114 +/- SEM 18.9; Pep A mean = 98.81 +/- SEM 22.8; Pep B mean = 58.36 +/- SEM 9.5; saline vs. Pep B \*p = 0.04; inactive pep vs. Pep B \*p = 0.02, n = 6.

**B)** The specificity of the CPPs was tested by investigating the binding between CAP1 (the other homologue belonging to the CAP family) and actin remains intact. Data show no statistical changes upon the acute treatment with the CPPs, n = 6.

### **6.7.) CPPs can modulate ADAM10 synaptic localization and activity towards APP without affecting N-Cadherin shedding**

To verify the effects of the CPPs *in vivo*, we analyzed the ADAM10 synaptic availability and its activity towards substrates as APP and N-Cadherin. To this, we purified the TIF fraction from the hippocampus to determine ADAM10 synaptic levels. Shown in figure 29A/B, Pep B was able to significantly increase the levels of ADAM10 in the synaptic membrane by approximately 50%, indicating that the Pep B is able to modify ADAM10 synaptic availability in the synapse. As far as the activity of ADAM10, we noticed an increase of sAPP $\alpha$  measured by ELISA (Fig. 29D), indicating an increase of ADAM10 activity towards APP. On the other hand, the activity towards N-Cadherin was measured by western blot in the synaptic fraction, and there is no difference in the CTF $\alpha$ -N-Cadherin, the cleavage product of ADAM10, showing us that the activity towards N-Cadherin is not altered (Fig. 29A). Taken the data together, the activity of CPP Pep B could serve as a novel therapeutic strategy, by interfering between the CAP2 binding to actin. By this interference, we can increase ADAM10 synaptic localization, and thereby its cleavage towards substrate APP. This is a mechanism how the toxic A $\beta$  peptide can be decreased in AD pathogenesis. To fully unravel the mechanism of action, we have to understand whether the increased ADAM10 synaptic levels are due to a decrease in endocytosis or an increase of exocytosis of ADAM10.

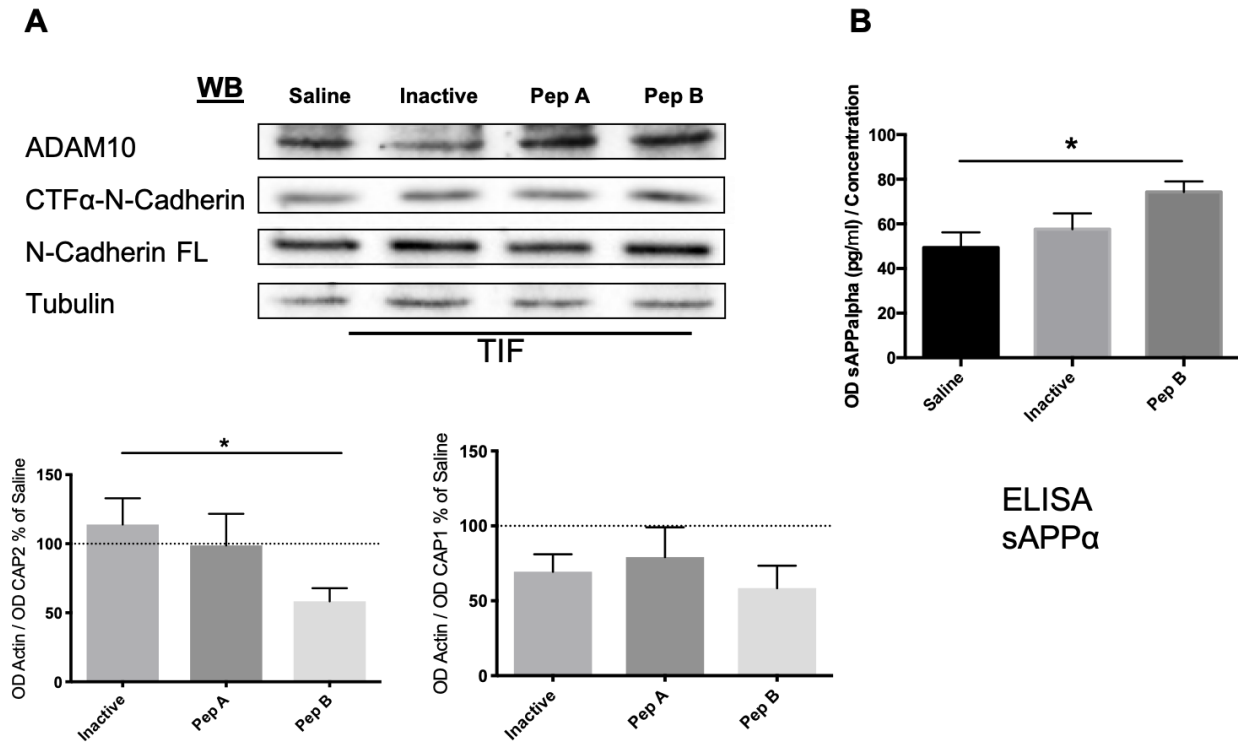


**Figure 29) CPPs influence ADAM10 synaptic localization and its activity towards APP.**

**A)** Representative WB images of the TIF fraction of hippocampal tissue of APP/PS1 mice treated with Saline, Inactive peptide and 2 different active peptides (Pep A and Pep B). Underneath the corresponding graphs, where on the left the OD of ADAM10 was normalized on the OD of Tubulin and then the ratio was made by normalizing them on the Saline condition. On the right the OD of CTF-N-Cadherin is normalized on the OD of total N-Cadherin and the ratio was made by normalizing them on the Saline condition. Data analysis done with a one-way ANOVA and Tukey post-hoc test. The Pep B significantly increases the ADAM10 synaptic availability comparing both with the saline ( $*p = 0,015$  data represented as mean PepB 1,654 +/- SEM 0,23) and inactive/control peptide ( $*p = 0,017$  data represented as mean Inactive 1.01 +/- SEM 0.032),  $n = 6$ . Both CPPs are not able to affect the synaptic levels of N-Cadherin-FL and its C-terminal cleavage product from ADAM10, and therefore not affecting its ratio. data represented as Inactive mean 1,2 +/- SEM 0,236, Pep A mean 0,805 +/- SEM 0,236, Pep B mean 0,88 +/- SEM 0,18,  $n = 6$ .

**B)** To follow up whether the increase of ADAM10 synaptic localization also influences its activity towards APP, we used an ELISA assay of the sAPP $\alpha$  fragment which is the cleavage product released by ADAM10 cleavage. The OD of the sAPP $\alpha$  was normalized on the concentration of the homogenate of the mice treated with either saline/inactive or active Pep B. PepB shows a statistical increase of the sAPP $\alpha$  fragment compared to the saline treated mice ( $*p = 0,038$ ), data represented as mean 74,26 +/- SEM 4,8,  $n = 6$ .

# Discussion

The full molecular mechanism behind AD pathogenesis is still not completely understood, although many studies point out that A $\beta$ , in particular the soluble oligomeric form, is the main driving factor of the disease, by inducing synaptic dysfunction and the cascade of events leading to dementia<sup>5,16,18</sup>. It has been demonstrated that if A $\beta$  is present at high concentrations and in oligomeric forms, it can affect glutamatergic synaptic transmission and eventually cause synapse loss<sup>37-40</sup>. The production of A $\beta$  can be prevented by the cleavage of APP by the  $\alpha$ -secretase ADAM10<sup>34-36</sup>. Additionally, ADAM10 activity can regulate synaptic morphology and synaptic connectivity<sup>213,220</sup>. ADAM10 can only exert its activity towards its substrates when its inserted in the synaptic membrane. The synaptic localization of ADAM10, and thereby its activity, is governed by the interaction with SAP97 and AP2 to the C-terminal domain of ADAM10, which control forward trafficking and endocytosis of ADAM10 respectively<sup>212,213</sup>. Notably, such interactions are altered in AD patients at the earliest stages of the disease<sup>241</sup> and this mechanism is tuned by activity-dependent plasticity, where LTD activates the ADAM10 forward trafficking and LTP fosters ADAM10 endocytosis<sup>213</sup>. In order to understand the complete mechanism controlling ADAM10 in the synapse, and in light of the importance of ADAM10 cytoplasmic domain in the regulation of ADAM10 activity, we performed a two-hybrid screening and that has recently identified a protein called cyclase-associated protein 2 (CAP2) as a novel protein partner of ADAM10. CAP2 is a member of the CAP family, which are evolutionary highly conserved multidomain proteins involved in several processes including regulating changes in actin cytoskeleton, such as cell migration, movement and polarity, vesicle trafficking and endocytosis<sup>117</sup>. Therefore, CAP2 is linking signaling pathways to the actin cytoskeleton. Additionally, CAP2 is a known actin binding protein that can form dimers and has a limited expression, including the brain, indicating unique roles of CAP2 in neuronal cells<sup>245</sup>. Since CAP2 is a novel binding partner of ADAM10 and might have an influence on the regulation of its synaptic localization, it is important to understand the role of CAP2 in this process to unravel its role in AD. Therefore, the first aim of this study was to unravel the binding domains responsible for the association of CAP2 with its binding partners, i.e. ADAM10 and actin, and to



understand their function in ADAM10 synaptic localization. The binding domain to ADAM10 is located in the N-terminal domain of CAP2, where the association to actin takes part in the last 24 amino acids of the C-terminal side of CAP2 (Fig. 1/2). Importantly, ADAM10 and actin don't compete for the binding to CAP2. Additionally, we found that upon interference with association between CAP2 and actin, the synaptic localization of ADAM10 is increased, because of a decrease of ADAM10 endocytosis (Fig. 3)<sup>213</sup>. Since the actin cytoskeleton plays an essential role in endocytosis, where actin assembly can create protrusions that encompass extracellular materials<sup>311,312</sup>, these data suggest that CAP2 is involved in ADAM10 endocytosis. Overall, these data confirm that CAP2 is a novel binding partner of ADAM10, capable of regulating its synaptic localization.

Since there is not much known about the function of CAP2 in the brain<sup>301</sup>, we characterized the physiological role of CAP2 in the brain. We show that CAP2 is expressed in the post-synaptic fraction of the neuron, but not as enriched as ADAM10 (Fig. 4). Then, we produced a mutant lacking the CAP2 dimerization ability by mutating the Cys32 to Gly, and it turned out that CAP2 dimer formation is important for the association of CAP2 to cofilin. Considering the role of cofilin-1 in severing F-actin and maintaining fast actin treadmilling rate in dendritic spines<sup>111,112</sup>, we can hypothesize that CAP2 could be a novel regulator of cofilin activity (Fig. 5).

Then, to go into more detail in unraveling the physiological role of CAP2 in the brain, we took advantage of a CAP2 KO mice model. In the hippocampi of CAP2 KO mice we found a decrease in synaptic levels of ADAM10 and GluN2A, which are absent in the cortex or striatum. Moreover, no alterations in protein expression are found in the total homogenate, indicating that only the ADAM10 localization is affected by the lack of CAP2, and thereby can influence synaptic plasticity and ADAM10 activity (Fig. 6). Additionally, when looking at the spine morphology and density of hippocampal neurons in the brain of these mice, we found a decrease in spine density and a decrease in the spine length and width. The morphology of the spines is also affected, where we found an increased percentage of the more immature stubby spines (Fig. 7). Additionally, the CAP2 KO mice show elevated levels of the toxic A $\beta$ <sub>1-42</sub> variant in the

hippocampal area compared to the WT mice (Fig. 8). These outcomes indicate a possible role of CAP2 in the maturation of spines and in the regulation of ADAM10 localization and A $\beta$  production in the hippocampus (Fig. 30).

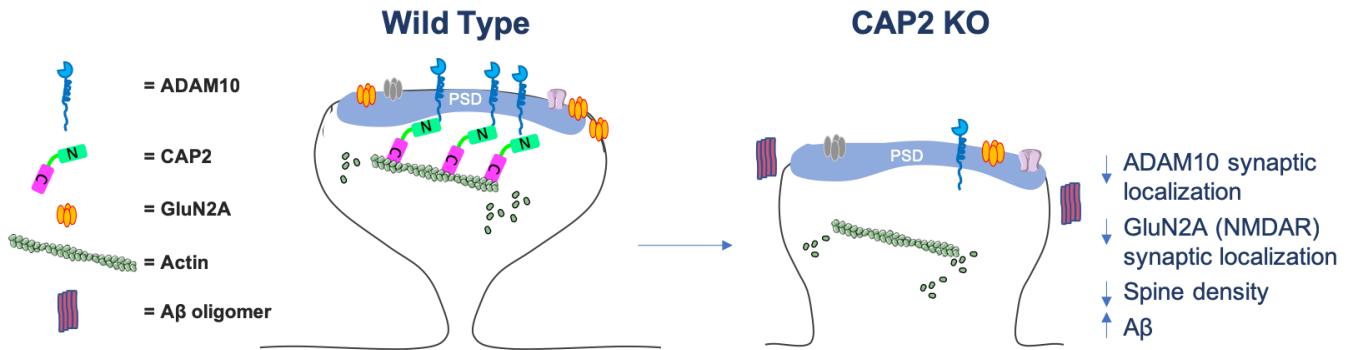


**Figure 30) Schematic overview of the role of CAP2 in hippocampal dendritic spines.** A wild type healthy dendritic spine compared to a spine lacking CAP2 of a CAP2 knock-out (CAP2 KO) mouse. The lack of CAP2 influences the structure of dendritic spines by decreasing the spine density and shifting the morphology towards a more immature spine shape. In addition, the levels of ADAM10 and the NMDAR subunit GluN2A in the synaptic membrane are decreased influencing the functionality of the synapse. Moreover, an increase of the toxic A $\beta_{1-42}$  species is found in the hippocampus.

For future research, to fully elaborate the function of CAP2 in the brain, the CAP2 KO mice should be fully characterized. For instance, electrophysiological recordings and cognitive behavioral tests in the CAP2 KO mice could give a better functional indication about the role of CAP2 in the brain.

In light of the findings regarding the structural alterations detected in the absence of CAP2, we investigated the role of CAP2 upon activity-dependent synaptic plasticity phenomena. Therefore, we induced either LTP or LTD in primary hippocampal neurons by chemically inducing well established cLTP or cLTD protocols (Fig. 9A/10A)<sup>213,314,315</sup>. We found that stimulating neurons with a cLTP treatment, elicited and increased CAP2 synaptic availability and notably, this stimulation also caused an increase in CAP2 dimer levels in the synaptic fraction (Fig. 9B/C). Whereas, upon cLTD induction in primary hippocampal cultures, we did not find any alterations in the CAP2 synaptic localization or dimer formation (Fig. 10). This indicates that CAP2 plays a role in LTP, but not in LTD. Then, to evaluate whether the effects we found upon cLTP stimulation could be ascribed to the CAP2 Cys32-dimerization motif, we transfected primary hippocampal neurons with EGFP-CAP2 and either Myc-CAP2 or Myc-CAP2(C32G) and then we

induced cLTP. Taking advantage of a PLA assay, we found that cLTP increased the dimerization in the EGFP-CAP2/Myc-CAP2 condition, confirming the results obtained by a biochemical approach (Fig. 9D). On the other hand, when we interfered with the dimerization of CAP2 with the CAP2(C32G) mutant, we couldn't detect differences in the PLA signal. These effects are specifically due to LTP, since upon LTD induction we couldn't detect any effects (Fig. 10D). In addition, given the pivotal role of cofilin-mediated actin dynamics in the structural remodeling of spines during activity-dependent synaptic plasticity phenomena<sup>133</sup>, we tested whether cLTP modulates the CAP2 association to cofilin. To address this, we performed PLA assays after cLTP induction and the quantitative analysis revealed a significant increase in the association between endogenous CAP2 and cofilin upon LTP induction (Fig. 9E). These results indicate a role of CAP2 in synaptic plasticity, possibly through an increase in self-association, which affects the binding to cofilin and could enhance the cofilin-mediated actin filament dynamics. This goes hand in hand with previous research, where it has been already shown that CAP proteins promote actin filament dynamics, by cooperating with ADF/cofilin<sup>291,292</sup>. To evaluate if the association between CAP2 and its binding partners ADAM10 and actin is affected by activity-dependent synaptic plasticity, we looked at their interactions upon cLTP and cLTD induction. The CAP2 complex formation with ADAM10 is increased upon cLTP, where the formation of this complex is not triggered by cLTD (Fig. 11A/C). The CAP2/actin interaction is strongly reduced by cLTP, while again cLTD is not affecting their association (Fig. 11B/D). Since CAP2 association to its partners is affected by activity-dependent synaptic plasticity, we wondered whether this pathway could be a target of aberrant plasticity phenomena, as the ones triggered by A $\beta$  oligomers (oA $\beta$ <sub>1-42</sub>). To address this, we used an oA $\beta$ <sub>1-42</sub> preparation which we fully characterized, to trigger aberrant plasticity. Primary hippocampal cultures were treated with a preparation of oA $\beta$ <sub>1-42</sub> which is able to induce synaptic depression within 30 minutes and spine loss in 24 hours, in the absence of cell death. Since several studies show that oA $\beta$ <sub>1-42</sub> affects the phosphorylation of GluA1 serine-845 by decreasing its phosphorylation, which is an event related to LTD<sup>38,132,162</sup>. We also show that our oA $\beta$ <sub>1-42</sub> preparation protocol

induces a decrease in phosphorylation of this site (Fig. 12). In these experimental conditions, the short-term exposure to oA $\beta$ <sub>1-42</sub> results in an increased ADAM10 synaptic availability (Fig. 13A/B). Although it has been shown that LTD fosters SAP97-mediated ADAM10 delivery to the postsynaptic compartment<sup>213,241</sup>, oA $\beta$ <sub>1-42</sub> treatment leads to a decrease in the association between ADAM10 and AP2 complex, which is responsible for the endocytosis of the enzyme, without affecting the binding to SAP97 (Fig. 13D). Accordingly, we found that the short-term exposure of oA $\beta$ <sub>1-42</sub> decreases CAP2 synaptic availability without affecting its expression and dimer formation (Fig. 13B/C). Therefore, we show that the aberrant plasticity by oA $\beta$ <sub>1-42</sub>, but not the physiological LTD, decreases CAP2 availability in the synapse. In addition, we detected an increase in the CAP2 association to actin and a decreased binding between CAP2 and ADAM10 upon the short-term exposure to oA $\beta$ <sub>1-42</sub> (Fig. 14A/B). Since AP2 and CAP2 are involved in the ADAM10 endocytosis pathway, our data suggest that the increase in ADAM10 synaptic localization is due to the impairment of its endocytosis rather than to a stimulation of its forward trafficking, suggesting that the molecular mechanism underlying LTD and regulating ADAM10 are profoundly different from those responsible for oA $\beta$ <sub>1-42</sub>-induced depression. Moreover, these outcomes indicate that CAP2 and its binding to ADAM10 and actin are targets of the acute exposure to oA $\beta$ <sub>1-42</sub>. Taken together, our data indicate that oA $\beta$ <sub>1-42</sub> triggers aberrant plasticity phenomena. Possibly, the increased ADAM10 synaptic levels could be related to a negative feedback mechanism, where the increased levels of toxic A $\beta$  can stimulate the non-amyloidogenic pathways. Overall, here we show that oA $\beta$ <sub>1-42</sub> can trigger aberrant synaptic plasticity pathways related to the amyloid cascade, and thereby affect synaptic plasticity. Since the synapses are considered to be an early site of pathology in AD<sup>318</sup> and loss of synapses is the best pathologic correlate of cognitive impairment in AD patients<sup>150</sup>, understanding the molecular underpinnings leading to synaptic dysfunction will aid in the development of tailored synapse-targeted therapies for AD. Considering that the CAP2 pathway is a target of oA $\beta$ <sub>1-42</sub> and that ADAM10 synaptic localization is reduced in AD patients<sup>241</sup>, the next step focusses on the complex formation of CAP2 with ADAM10 and actin in AD patients' hippocampal tissue and in

animal models at different stages of the disease. For this, we first looked at the CAP2 expression, dimerization and localization in the synapse. We detected a decreased expression of CAP2 in AD patients' hippocampi compared to non-demented controls (Fig. 16) and in AD mice model (APP/PS1 mice) compared to wild-type mice at 6 months of age (Fig. 20). In addition, ADAM10 synaptic levels are also reduced in the hippocampi of 6-month old APP/PS1 mice (Fig. 20). Additionally, the CAP2 dimer total levels are not altered, but the dimer availability in the synaptic membrane was reduced both in AD patients and APP/PS1 mice at early stages of the disease (Fig. 16/21). Furthermore, in AD patients the ADAM10 association to CAP2 is not altered (Fig. 17), while the CAP2 binding to actin is increased (Fig. 18). Since the AD patients are late-stage AD patients, we were interested in figuring out whether the binding between CAP2 and ADAM10 could be altered in earlier stages of the disease. For this we used the 6-month-old APP-PS1 mice, which already show early symptoms of the disease, progressing into the full-blown pathology around 12 months of age (Fig. 19). Surprisingly, in these mice, we found a decreased association between ADAM10 and CAP2 only at the early stages of the disease, where these levels are stabilized and returned to normal at later stages of the disease (Fig. 22). These results suggest a role for the CAP2-ADAM10 complex in the earlier stages of the disease. In the APP/PS1 animals we also detected an increased binding of CAP2 to actin, both in the early and later stages of the disease (Fig. 23). Taken together, these results show an important role of CAP2 in AD pathogenesis, where especially the increased binding between CAP2 and actin seems to play a role in ADAM10 synaptic localization in AD.

In light of these results, we planned two therapeutic approaches to interfere with the CAP2 pathway in AD pathogenesis. According to the decreased expression of CAP2 in AD pathology, we performed an *in-vitro* rescue experiment in APP/PS1 mice hippocampal cultures. We found that the overexpression of CAP2 rescued the reduced PSD-95 levels in the APP/PS1 mice, and restored the ADAM10 synaptic localization, which thereby might stimulate ADAM10 activity towards its substrates (Fig. 25). These results indicate that CAP2 overexpression could stabilize the postsynaptic side of

spines and restore ADAM10 synaptic localization and possibly its activity, thus rebalancing the main pathological features of AD.

The second rescue approach targets the CAP2-actin complex formation, since the results we obtained in AD patients and AD mouse model pointed in the direction that especially the association between CAP2 and actin seems important in controlling the synaptic levels of ADAM10. In collaboration with Prof. Daniele Di Marino (Università Politecnica delle Marche), we designed cell permeable peptides (CPPs) to interfere selectively with the CAP2 complex formation with actin (Fig.31). With this tool we tested *in-vitro* and *in-vivo* whether the interference between the CAP2-actin complex influences ADAM10 synaptic levels, and potentially rescues the synaptic dysfunction and cognitive impairment in AD mice. First, we investigated the efficacy of the designed CPPs towards its target in an *in-vitro* approach. For this, we treated primary hippocampal cultures with our inactive and 2 active (Pep A and Pep B) CPPs, and performed Co-IP experiments. We saw that especially Pep B is able to disrupt the binding between CAP2 and actin (Fig. 27). Then to confirm the Co-IP results, we performed a GST-Pull down using mice brain homogenate incubated with the CPPs. The results confirmed that Pep B shows to be most efficient in disrupting the CAP2-actin association (Fig. 27). In light of the *in-vitro* results, we moved to an acute *in-vivo* model, where we treated 6 months-old wild type (C57/BL6) mice with a 3nmol/g dose of the CPPs and looked at the main 4 outcomes; 1: the efficacy of the CPPs to interfere between CAP2 and actin binding, 2: the specificity of the CPPs, 3: CPP effect on ADAM10 synaptic localization and 4: ADAM10 activity towards its substrates. 24 hours after an intraperitoneal injection, Co-IP assays showed that the Pep B was able to significantly interfere with the CAP2-Actin association (Fig. 28). Since CAP1 and CAP2 are the two homologues from the CAP family and their genes share 64% of amino acid identity in mammals <sup>247,248</sup>, we verified CAP1/actin association is not affected (Fig. 28). These data highlighted that Pep B is effective, but also specific for the interference between CAP2 and actin. Then, we assessed whether ADAM10 levels were increased in the synaptic fraction. Pep B significantly increased ADAM10 availability in the synaptic membrane (Fig. 29A), thus demonstrating that CAP2/actin association is

instrumental in the regulation of ADAM10 synaptic availability, as previously shown in hippocampal cultures (Fig. 3). Since ADAM10 is only active towards its substrates when it is inserted in the synaptic membrane, the increase in ADAM10 synaptic localization should also promote the activity of ADAM10. To address this, we looked at the sAPP $\alpha$  levels in the hippocampal homogenate by ELISA. Pep B was able to significantly increase the neurotrophic factor of APP released by ADAM10 cleavage (Fig. 29B). In order to assess whether the ADAM10 cleavage activity was also altered towards other ADAM10 substrates, we analyzed the metabolism of N-Cadherin. Western blot analysis of the hippocampal synaptic fraction indicates that Pep B treatment is not affecting ADAM10 cleavage of N-Cadherin since there were no changes in the C-terminal cleavage product that ADAM10 produces by shedding N-Cadherin (Fig. 29A). Considering the age of the mice, it might be the case that ADAM10 exerts a preferential activity towards APP instead of N-Cadherin in adult mice.

Together, these results demonstrate that the developed Pep B can interfere with the binding between CAP2 and actin, and that, by this interference, we can increase ADAM10 synaptic levels and activity towards APP. We showed that the CAP2 actin binding domain is relevant for ADAM10 endocytosis, however the mechanism according to which CAP2/actin association control ADAM10 synaptic localization has not been determined yet (Fig. 31).

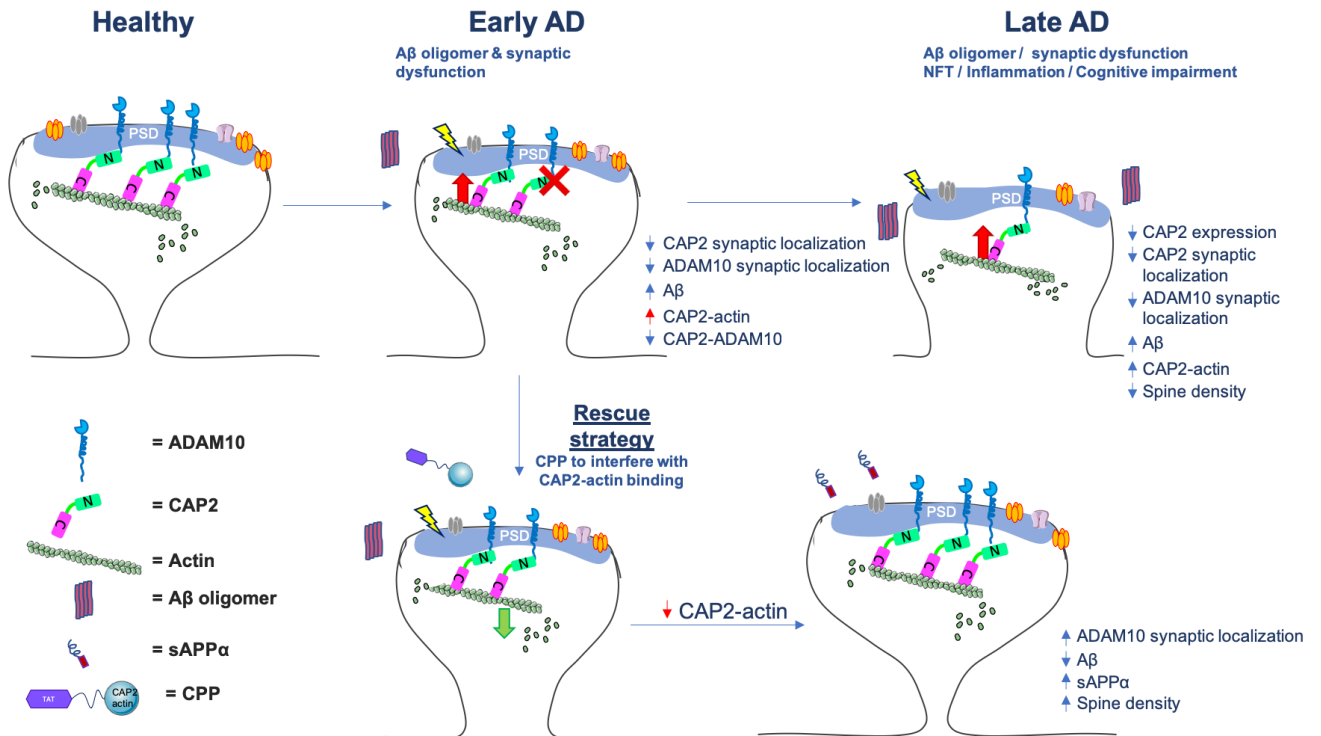


**Figure 31)** Schematic overview of the role of CAP2 in different stages of AD including the potential rescue strategy. Indication of the role of CAP2 and its complex formation to ADAM10 and Actin in healthy neurons compared to early AD and late AD stages are shown in the upper part. The rescue strategy is shown in the lower part. Here we focus on the early stages of AD, where we try to rescue the pathological pathway by interfering with the binding of CAP2 and actin.

A limitation to the use of CPPs is that this sort of peptides are not targeting and penetrating a specific cell type. In order to increase the delivery towards specific targets, the pharmacokinetics of the CPPs could be improved by the design of peptidomimetics, which could be a next step in the use of our CAP2/actin interfering peptide. Another approach could be to design a viral strategy where it is possible to target a specific cell type with the use of a neuron specific promotor controlling the expression of the CAP2-actin binding domain sequence.

For future experiments, we will also use our CAP2-actin CPP in a chronic treatment setup in an AD mice model, to access whether it is possible to rescue the cognitive impairment and synaptic deficits found in the AD mice.

In this framework, we hypothesized that the actin-binding protein CAP2, a newly identified partner of ADAM10, can be positioned at the crossroad of the amyloid



cascade and actin-mediated spine dysmorphogenesis, and can be implicated in brain pathologies, like AD, in which there is an impairment of the localization/activity of ADAM10. According to that, in previous research, microarray analysis of hippocampal gene expression of AD patients, reported a downregulation of CAP2 gene<sup>302-304</sup>. Moreover, the CAP2 gene is present at chromosome 6p22.3 in the human genome. An interstitial 6p22-24 deletion syndrome of the short arm of chromosome 6 was reported where patients with this deletion have a variable phenotype including a developmental delay<sup>299,300</sup>. Since CAP2 could be involved in synaptic failure in both neurodegenerative and neurodevelopmental disorders, it represents a potential pharmacological target for several diseases. Our current data support the fact that CAP2 protein expression levels are altered in AD patients, and that CAP2 is involved in the amyloid related synaptic dysfunction.

In order to identify a disease-modifying strategy for AD, it is fundamental to target the disease as early as possible. Therefore, we focused on the earlier stages of AD and used different *in-vitro* and *ex-vivo* models. First, we took advantage of an *in-vitro* model based on A $\beta$  oligomers synaptotoxicity to investigate the earliest hallmark of AD. The results showed that CAP2 synaptic trafficking is affected by A $\beta$  oligomers, without influencing the CAP2 expression. At the later stages of the disease in AD patients, when also synaptic dysfunction and brain atrophy is found, also the CAP2 expression is decreased. It would be important to address the CAP2 mRNA levels at different stages of the disease in an AD mice model in order to assess whether the decrease of CAP2 protein levels could be ascribed to transcriptional deficits or to an increased degradation.

More importantly, the formation of the CAP2/ADAM10 complex is strictly modified in the early stages of the disease, while the binding between CAP2 and actin is altered along disease progression. This might point at an over-compensatory mechanism for the ADAM10 binding of CAP2 at the later stages of AD, but this hypothesis should be further investigated.

Since we found that the CAP2/actin complex is important for ADAM10 synaptic localization, we focused on trying a rescue strategy targeting CAP2/actin (Fig. 31). To

understand whether uncoupling the CAP2/actin complex can serve as a potential strategy to increase ADAM10 activity and to ameliorate possibly cognitive impairment in AD, future research should aim at a chronic treatment with the CPP B in an AD mice model at different stages of the disease. Here, the dendritic spine morphology and cognitive behavioral tests should give an idea on the structural and functional effects of the peptide in a disease model, where also ADAM10 localization and activity towards its substrates should be investigated.

It's important to keep in mind, is that targeting ADAM10 activity, influences multiple substrates all throughout the body <sup>319</sup>. It is known that ADAM10 expression and its activity are important in several pathologies <sup>319</sup>, affecting the brain <sup>320,321</sup>, but also a number of other diseases including the liver <sup>322</sup> and the immune system <sup>323-325</sup>. Thereby, accelerating ADAM10 activity towards its substrates, could exert, besides the beneficial cleavage of APP and preventing A $\beta$  accumulation, toxic effects in other organs. Therefore, a substrate/cell specific approach should be used to activate ADAM10. It was previously described that ADAM10 activation has a better tolerance compared to its inhibition in both human <sup>326</sup> and mice <sup>320,327</sup>. Besides APP, there are two other examples of pathways that profit from an increased ADAM10 shedding activity, namely Notch and Prion protein. Where the increase of Notch shedding accounts for an increased hippocampal neurogenesis <sup>327-329</sup>, prion protein shedding can reduce the levels of prion protein that acts directly as a receptor for the A $\beta$  oligomers <sup>330</sup>. Hence, when targeting ADAM10, the substrate specificity should be taken into consideration. For this reason, we tried to target ADAM10 activity through CAP2, a protein that has a more specific expression including the brain than ADAM10. In conclusion, we demonstrated that the actin-binding protein CAP2, a confirmed binding partner of ADAM10, can serve as bridge to keep the right balance between ADAM10 synaptic localization and actin regulation, to avoid A $\beta$  accumulation and synaptic dysfunction that is seen in AD patients. Therefore, CAP2 serves as a novel target in the AD pathogenesis that is worth studying in more extensive research.

# References

1. Alzheimer, A. Uber eine eigenartige Erkrankung der Hirnrinde. *Allg Zeitschr f Psychiatr. u Psych-Gerichtl Med* (1907). doi:10.1002/ca.980080612
2. McKhann, G. *et al.* Clinical diagnosis of Alzheimer's disease: Report of the NINCDS-ADRDA Work Group\* under the auspices of Department of Health and Human Services Task Force on Alzheimer's Disease. *Neurology* (1984). doi:10.1212/WNL.34.7.939
3. Braak, H. & Braak, E. Neuropathological staging of Alzheimer-related changes. *Acta Neuropathologica* (1991). doi:10.1007/BF00308809
4. Jack, C. R. *et al.* Tracking pathophysiological processes in Alzheimer's disease: An updated hypothetical model of dynamic biomarkers. *The Lancet Neurology* (2013). doi:10.1016/S1474-4422(12)70291-0
5. Hardy, J. & Selkoe, D. J. The amyloid hypothesis of Alzheimer's disease: Progress and problems on the road to therapeutics. *Science* (2002). doi:10.1126/science.1072994
6. Vassar, R. *et al.*  $\beta$ -Secretase cleavage of Alzheimer's amyloid precursor protein by the transmembrane aspartic protease BACE. *Science* (80-. ). (1999). doi:10.1126/science.286.5440.735
7. Tanzi, R. E. & Bertram, L. Twenty years of the Alzheimer's disease amyloid hypothesis: A genetic perspective. *Cell* (2005). doi:10.1016/j.cell.2005.02.008
8. Braak, H. & Braak, E. Morphological criteria for the recognition of Alzheimer's disease and the distribution pattern of cortical changes related to this disorder. *Neurobiol. Aging* (1994). doi:10.1016/0197-4580(94)90032-9
9. Jack, C. R. *et al.* Hypothetical model of dynamic biomarkers of the Alzheimer's pathological cascade. *Lancet Neurol.* (2010). doi:10.1016/S1474-4422(09)70299-6
10. Tanzi, R. E. The genetics of Alzheimer disease. *Cold Spring Harbor perspectives in medicine* (2012). doi:10.1101/cshperspect.a006296
11. Selkoe, D. J. The molecular pathology of Alzheimer's disease. *Neuron* (1991). doi:10.1016/0896-6273(91)90052-2
12. Ballard, C. *et al.* Alzheimer's disease. *Lancet* (2011). doi:10.1016/S0140-6736(10)61349-9
13. Serretti, A., Olgiati, P. & De Ronchi, D. Genetics of Alzheimer's disease. A rapidly evolving field. in *Journal of Alzheimer's Disease* (2007). doi:10.3233/JAD-2007-12108
14. Bertram, L. *et al.* The genetics of Alzheimer disease: back to the future. *Neuron* (2010). doi:10.1016/j.neuron.2010.10.013
15. Jiang, Q. *et al.* ApoE Promotes the Proteolytic Degradation of A $\beta$ . *Neuron* (2008). doi:10.1016/j.neuron.2008.04.010
16. Hardy, J. A. & Higgins, G. A. Alzheimer's disease: The amyloid cascade hypothesis. *Science* (1992). doi:10.1126/science.1566067
17. Klein, W. L., Krafft, G. A. & Finch, C. E. Targeting small A  $\beta$  oligomers: The solution to an Alzheimer's disease conundrum? *Trends Neurosci.* 24, 219-224

- (2001).
18. Walsh, D. M., Klyubin, I., Fadeeva, J. V., Rowan, M. J. & Selkoe, D. J. Amyloid- $\beta$  oligomers: their production, toxicity and therapeutic inhibition. *Biochem. Soc. Trans.* (2002). doi:10.1042/bst0300552
  19. Selkoe, D. J. Alzheimer ' s Disease : Genes , Proteins , and Therapy. *Perspective* (2001). doi:10.1016/0092-8674(88)90462-x
  20. Oddo, S. *et al.* Triple-transgenic model of Alzheimer's Disease with plaques and tangles: Intracellular A $\beta$  and synaptic dysfunction. *Neuron* (2003). doi:10.1016/S0896-6273(03)00434-3
  21. Selkoe, D. J. & Hardy, J. The amyloid hypothesis of Alzheimer's disease at 25 years. *EMBO Mol. Med.* (2016). doi:10.15252/emmm.201606210
  22. Roßner, S., Sastre, M., Bourne, K. & Lichtenthaler, S. F. Transcriptional and translational regulation of BACE1 expression-Implications for Alzheimer's disease. *Progress in Neurobiology* (2006). doi:10.1016/j.pneurobio.2006.06.001
  23. Cole, S. L. & Vassar, R. BACE1 structure and function in health and Alzheimer's disease. *Curr. Alzheimer Res.* (2008). doi:10.2174/156720508783954758
  24. Steiner, H., Fluhner, R. & Haass, C. Intramembrane proteolysis by gamma-secretase. *J. Biol. Chem.* (2008). doi:10.1074/jbc.R800010200
  25. Nikolaev, A., McLaughlin, T., O'Leary, D. D. M. & Tessier-Lavigne, M. APP binds DR6 to trigger axon pruning and neuron death via distinct caspases. *Nature* (2009). doi:10.1038/nature07767
  26. Haass, C. & Selkoe, D. J. Soluble protein oligomers in neurodegeneration: Lessons from the Alzheimer's amyloid  $\beta$ -peptide. *Nature Reviews Molecular Cell Biology* (2007). doi:10.1038/nrm2101
  27. Zhao, L. N., Long, H., Mu, Y. & Chew, L. Y. The toxicity of amyloid  $\beta$  oligomers. *International Journal of Molecular Sciences* (2012). doi:10.3390/ijms13067303
  28. Bitan, G. *et al.* A Molecular Switch in Amyloid Assembly: Met35 and Amyloid  $\beta$ -Protein Oligomerization. *J. Am. Chem. Soc.* (2003). doi:10.1021/ja0349296
  29. Selkoe, D. J. Translating cell biology into therapeutic advances in Alzheimer's disease. *Nature* (1999). doi:10.1038/399a023
  30. Lichtenthaler, S. F. Alpha-secretase in Alzheimer's disease: Molecular identity, regulation and therapeutic potential. *Journal of Neurochemistry* (2011). doi:10.1111/j.1471-4159.2010.07081.x
  31. Furukawa, K. *et al.* Increased Activity-Regulating and Neuroprotective Efficacy of  $\alpha$ -Secretase-Derived Secreted Amyloid Precursor Protein Conferred by a C-Terminal Heparin-Binding Domain. *J. Neurochem.* (2002). doi:10.1046/j.1471-4159.1996.67051882.x
  32. Meziane, H. *et al.* Memory-enhancing effects of secreted forms of the  $\beta$ -amyloid precursor protein in normal and amnesic mice. *Proc. Natl. Acad. Sci.* (1998). doi:10.1073/pnas.95.21.12683
  33. Stein, T. D. Neutralization of Transthyretin Reverses the Neuroprotective Effects of Secreted Amyloid Precursor Protein (APP) in APPSw Mice Resulting in Tau Phosphorylation and Loss of Hippocampal Neurons: Support for the Amyloid Hypothesis. *J. Neurosci.* 24, 7707-7717 (2004).

34. Lammich, S. *et al.* Constitutive and regulated alpha-secretase cleavage of Alzheimer's amyloid precursor protein by a disintegrin metalloprotease. *Proc. Natl. Acad. Sci. U. S. A.* (1999). doi:10.1073/pnas.96.7.3922
35. Postina, R. *et al.* A disintegrin-metalloproteinase prevents amyloid plaque formation and hippocampal defects in an Alzheimer disease mouse model. *J. Clin. Invest.* (2004). doi:10.1172/JCI20864
36. Kuhn, P.-H. *et al.* ADAM10 is the physiologically relevant, constitutive alpha-secretase of the amyloid precursor protein in primary neurons. *EMBO J.* (2010). doi:10.1038/emboj.2010.167
37. Kamenetz, F. *et al.* APP Processing and Synaptic Function. *Neuron* (2003). doi:10.1016/S0896-6273(03)00124-7
38. Li, S. *et al.* Soluble Oligomers of Amyloid  $\beta$  Protein Facilitate Hippocampal Long-Term Depression by Disrupting Neuronal Glutamate Uptake. *Neuron* (2009). doi:10.1016/j.neuron.2009.05.012
39. Mucke, L. *et al.* High-Level Neuronal Expression of A $\beta$ <sub>1-42</sub> in Wild-Type Human Amyloid Protein Precursor Transgenic Mice: Synaptotoxicity without Plaque Formation. *J. Neurosci.* (2000). doi:10.1523/JNEUROSCI.20-11-04050.2000
40. Shankar, G. M. *et al.* Natural Oligomers of the Alzheimer Amyloid- Protein Induce Reversible Synapse Loss by Modulating an NMDA-Type Glutamate Receptor-Dependent Signaling Pathway. *J. Neurosci.* (2007). doi:10.1523/JNEUROSCI.4970-06.2007
41. Patterson, C. *et al.* Diagnosis and treatment of dementia: 1. Risk assessment and primary prevention of Alzheimer disease. *C. Can. Med. Assoc. J.* (2008). doi:10.1503/cmaj.070796
42. Li, J.-Y., Plomann, M. & Brudin, P. Huntington's disease: a synaptopathy? *Trends Mol. Med.* 9, 414-420 (2003).
43. Lepeta, K. *et al.* Synaptopathies: synaptic dysfunction in neurological disorders - A review from students to students. *Journal of Neurochemistry* (2016). doi:10.1111/jnc.13713
44. Penzes, P., Cahill, M. E., Jones, K. A., Vanleeuwen, J. E. & Woolfrey, K. M. Dendritic spine pathology in neuropsychiatric disorders. *Nature Neuroscience* (2011). doi:10.1038/nn.2741
45. Harris, K. M. & Stevens, J. K. Dendritic spines of CA 1 pyramidal cells in the rat hippocampus: serial electron microscopy with reference to their biophysical characteristics. *J. Neurosci.* (1989). doi:10.1021/la0512603
46. Fiala, J. C., Spacek, J. & Harris, K. M. Dendritic spine pathology: Cause or consequence of neurological disorders? *Brain Research Reviews* (2002). doi:10.1016/S0165-0173(02)00158-3
47. Sorra, K. E. & Harris, K. M. Overview on the structure, composition, function, development, and plasticity of hippocampal dendritic spines. *Hippocampus* (2000). doi:10.1002/1098-1063(2000)10:5<501::AID-HIPO1>3.0.CO;2-T
48. Yuste, R. Dendritic spines and distributed circuits. *Neuron* (2011). doi:10.1016/j.neuron.2011.07.024
49. Jones, E. G. & Powell, T. P. S. Morphological Variations in the Dendritic Spines of the Neocortex. *J. Cell Sci.* s (1969).

50. Peters, A. & Kaiserman-Abramof, I. R. The small pyramidal neuron of the rat cerebral cortex. The perikaryon, dendrites and spines. *Am. J. Anat.* (1970). doi:10.1002/aja.1001270402
51. Harris, K. M., Jensen, F. E. & Tsao, B. Three-dimensional structure of dendritic spines and synapses in rat hippocampus (CA1) at postnatal day 15 and adult ages: implications for the maturation of synaptic physiology and long-term potentiation. *J. Neurosci.* (1992). doi:10.1523/JNEUROSCI.12-07-02685.1992
52. Bourne, J. & Harris, K. M. Do thin spines learn to be mushroom spines that remember? *Current Opinion in Neurobiology* (2007). doi:10.1016/j.conb.2007.04.009
53. Fiala, J. C., Allwardt, B. & Harris, K. M. Dendritic spines do not split during hippocampal LTP or maturation. *Nat. Neurosci.* (2002). doi:10.1038/nn830
54. Berry, K. P. & Nedivi, E. Spine Dynamics: Are They All the Same? *Neuron* 96, 43-55 (2017).
55. Matus, A. The postsynaptic density. *Trends Neurosci.* 4, 51-53 (1981).
56. Marisa K. Baron, Tobias M. Boeckers, Bianca Vaida, Salem Faham, Mari Gingery, Michael R. Sawaya, Danielle Salyer, Eckart D. Gundelfinger, J. U. B. An Architectural Framework That May Lie at the Core of the Postsynaptic Density. *Science* (80-. ). 311, 531-535 (2006).
57. Hering, H. & Sheng, M. Dendritic spines: structure, dynamics and regulation. *Nat. Rev. Neurosci.* (2001). doi:10.1038/35104061
58. Yuste, R. & Bonhoeffer, T. Morphological Changes in Dendritic Spines Associated with Long-Term Synaptic Plasticity. *Annu. Rev. Neurosci.* (2001). doi:10.1146/annurev.neuro.24.1.1071
59. Carlisle, H. J. & Kennedy, M. B. Spine architecture and synaptic plasticity. *Trends in Neurosciences* (2005). doi:10.1016/j.tins.2005.01.008
60. Zuber, B., Nikonenko, I., Klausner, P., Muller, D. & Dubochet, J. The mammalian central nervous synaptic cleft contains a high density of periodically organized complexes. *Proc. Natl. Acad. Sci.* (2005). doi:10.1073/pnas.0509527102
61. Nakanishi, N., Schneider, N. A. & Axel, R. A family of glutamate receptor genes: Evidence for the formation of heteromultimeric receptors with distinct channel properties. *Neuron* (1990). doi:10.1016/0896-6273(90)90212-X
62. Burnashev, N. *et al.* Control by asparagine residues of calcium permeability and magnesium blockade in the NMDA receptor. *Science* (80-. ). (1992). doi:10.1126/science.1382314
63. Martin, L. J., Blackstone, C. D., Levey, A. I., Huganir, R. L. & Price, D. L. AMPA glutamate receptor subunits are differentially distributed in rat brain. *Neuroscience* (1993). doi:10.1016/0306-4522(93)90199-P
64. Nowak, L., Bregestovski, P., Ascher, P., Herbert, A. & Prochiantz, A. Magnesium gates glutamate-activated channels in mouse central neurones. *Nature* (1984). doi:10.1038/307462a0
65. Mayer, M. L., Westbrook, G. L. & Guthrie, P. B. Voltage-dependent block by Mg<sup>2+</sup> of NMDA responses in spinal cord neurones. *Nature* (1984). doi:10.1038/309261a0
66. Kleckner, N. W. & Dingledine, R. Requirement for glycine in activation of NMDA

- receptors expressed in xenopus oocytes. *Science* (80-. ). (1988).  
doi:10.1126/science.2841759
67. Dingledine, R., Borges, K., Bowie, D. & Traynelis, S. F. The glutamate receptor ion channels. *Pharmacol Rev* (1999). doi:10049997
  68. Kuryatov, A., Laube, B., Betz, H. & Kuhse, J. Mutational analysis of the glycine-binding site of the NMDA receptor: Structural similarity with bacterial amino acid-binding proteins. *Neuron* (1994). doi:10.1016/0896-6273(94)90445-6
  69. O'Hara, P. J. *et al.* The ligand-binding domain in metabotropic glutamate receptors is related to bacterial periplasmic binding proteins. *Neuron* (1993). doi:10.1016/0896-6273(93)90269-W
  70. Monyer, H. *et al.* Heteromeric NMDA receptors: Molecular and functional distinction of subtypes. *Science* (80-. ). (1992). doi:10.1126/science.256.5060.1217
  71. Wyllie, D. J. A., Livesey, M. R. & Hardingham, G. E. Influence of GluN2 subunit identity on NMDA receptor function. *Neuropharmacology* (2013). doi:10.1016/j.neuropharm.2013.01.016
  72. Meddows, E. *et al.* Identification of Molecular Determinants That Are Important in the Assembly of N-Methyl-D-aspartate Receptors. *J. Biol. Chem.* (2001). doi:10.1074/jbc.M101382200
  73. Anastasio, N. C., Xia, Y., O'connor, Z. R. & Johnson, K. M. Differential role of N-methyl-D-aspartate receptor subunits 2A and 2B in mediating phencyclidine-induced perinatal neuronal apoptosis and behavioral deficits. *Neuroscience* (2009). doi:10.1016/j.neuroscience.2009.07.058
  74. Chen, M. *et al.* Differential roles of NMDA receptor subtypes in ischemic neuronal cell death and ischemic tolerance. *Stroke* (2008). doi:10.1161/STROKEAHA.108.521898
  75. DeRidder, M. N. *et al.* Traumatic mechanical injury to the hippocampus in vitro causes regional caspase-3 and calpain activation that is influenced by NMDA receptor subunit composition. *Neurobiol. Dis.* (2006). doi:10.1016/j.nbd.2005.10.011
  76. Shan, Y. *et al.* Regulation of PINK1 by NR2B-containing NMDA receptors in ischemic neuronal injury. *J. Neurochem.* (2009). doi:10.1111/j.1471-4159.2009.06398.x
  77. Martel, M. A., Wyllie, D. J. A. & Hardingham, G. E. In developing hippocampal neurons, NR2B-containing N-methyl-d-aspartate receptors (NMDARs) can mediate signaling to neuronal survival and synaptic potentiation, as well as neuronal death. *Neuroscience* (2009). doi:10.1016/j.neuroscience.2008.01.080
  78. Wang, J. Q. *et al.* Glutamate Signaling to Ras-MAPK in Striatal Neurons: Mechanisms for Inducible Gene Expression and Plasticity. *Mol. Neurobiol.* (2004). doi:10.1385/MN:29:1:01
  79. Parameshwaran, K., Dhanasekaran, M. & Suppiramaniam, V. Amyloid beta peptides and glutamatergic synaptic dysregulation. *Experimental Neurology* (2008). doi:10.1016/j.expneurol.2007.10.008
  80. Ferreira, I. L. *et al.* Amyloid beta peptide 1-42 disturbs intracellular calcium homeostasis through activation of GluN2B-containing N-methyl-d-aspartate

- receptors in cortical cultures. *Cell Calcium* (2012). doi:10.1016/j.ceca.2011.11.008
81. Liu, Y. *et al.* NMDA Receptor Subunits Have Differential Roles in Mediating Excitotoxic Neuronal Death Both In Vitro and In Vivo. *J. Neurosci.* (2007). doi:10.1523/JNEUROSCI.0116-07.2007
  82. Liu, J. *et al.* Amyloid- $\beta$  induces caspase-dependent loss of PSD-95 and synaptophysin through NMDA receptors. *J. Alzheimer's Dis.* (2010). doi:10.3233/JAD-2010-100948
  83. Sala, C. & Segal, M. Dendritic Spines: The Locus of Structural and Functional Plasticity. *Physiol. Rev.* (2014). doi:10.1152/physrev.00012.2013
  84. Salinas, P. C. & Price, S. R. Cadherins and catenins in synapse development. *Current Opinion in Neurobiology* (2005). doi:10.1016/j.conb.2005.01.001
  85. Okamura, K. *et al.* Cadherin activity is required for activity-induced spine remodeling. *J. Cell Biol.* (2004). doi:10.1083/jcb.200406030
  86. Dunah, A. W. *et al.* LAR receptor protein tyrosine phosphatases in the development and maintenance of excitatory synapses. *Nat. Neurosci.* (2005). doi:10.1038/nn1416
  87. Saglietti, L. *et al.* Extracellular Interactions between GluR2 and N-Cadherin in Spine Regulation. *Neuron* (2007). doi:10.1016/j.neuron.2007.04.012
  88. Passafaro, M., Nakagawa, T., Sala, C. & Sheng, M. Induction of dendritic spines by an extracellular domain of AMPA receptor subunit GluR2. *Nature* (2003). doi:10.1038/nature01781
  89. Mendez, P., De Roo, M., Poglia, L., Klauser, P. & Muller, D. N-cadherin mediates plasticity-induced long-term spine stabilization. *J. Cell Biol.* (2010). doi:10.1083/jcb.201003007
  90. Boeckers, T. M. *et al.* Proline-rich synapse-associated protein-1/cortactin binding protein 1 (ProSAP1/CortBP1) is a PDZ-domain protein highly enriched in the postsynaptic density. *J. Neurosci.* 19, 6506–6518 (1999).
  91. Garner, C. C., Nash, J. & Huganir, R. L. PDZ domains in synapse assembly and signalling. *Trends in Cell Biology* (2000). doi:10.1016/S0962-8924(00)01783-9
  92. Dunah, A. W. *et al.* Alterations in subunit expression, composition, and phosphorylation of striatal N-methyl-D-aspartate glutamate receptors in a rat 6-hydroxydopamine model of Parkinson's disease. *Mol. Pharmacol.* (2000). doi:10.1080/04416651.1977.9650927
  93. Sheng, M. & Pak, D. T. S. Ligand-Gated Ion Channel Interactions with Cytoskeletal and Signaling Proteins. *Annu. Rev. Physiol.* (2000). doi:10.1146/annurev.physiol.62.1.755
  94. Wyszynski, M. *et al.* Competitive binding of  $\alpha$ -actinin and calmodulin to the NMDA receptor. *Nature* (1997). doi:10.1038/385439a0
  95. Gardoni, F. *et al.* CaMKII-dependent Phosphorylation Regulates SAP97/NR2A Interaction. *J. Biol. Chem.* (2003). doi:10.1074/jbc.M303576200
  96. Elias, G. M., Elias, L. A. B., Apostolides, P. F., Kriegstein, A. R. & Nicoll, R. A. Differential trafficking of AMPA and NMDA receptors by SAP102 and PSD-95 underlies synapse development. *Proc. Natl. Acad. Sci.* (2008). doi:10.1073/pnas.0811025106



97. Howard, M. A., Elias, G. M., Elias, L. A. B., Swat, W. & Nicoll, R. A. The role of SAP97 in synaptic glutamate receptor dynamics. *Proc. Natl. Acad. Sci.* (2010). doi:10.1073/pnas.0914422107
98. Chen, B. S., Thomas, E. V., Sanz-Clemente, A. & Roche, K. W. NMDA Receptor-Dependent Regulation of Dendritic Spine Morphology by SAP102 Splice Variants. *J. Neurosci.* (2011). doi:10.1523/JNEUROSCI.1034-10.2011
99. Landis, D. M. D. & Reese, T. S. Cytoplasmic organization in cerebellar dendritic spines. *J. Cell Biol.* (1983). doi:10.1083/jcb.97.4.1169
100. Allison, D. W., Gelfand, V. I., Spector, I. & Craig, A. M. Role of Actin in Anchoring Postsynaptic Receptors in Cultured Hippocampal Neurons: Differential Attachment of NMDA versus AMPA Receptors. *J. Neurosci.* (1998). doi:10.1038/385439a0
101. Kuriu, T., Inoue, A., Bito, H., Sobue, K. & Okabe, S. Differential Control of Postsynaptic Density Scaffolds via Actin-Dependent and -Independent Mechanisms. *J. Neurosci.* (2006). doi:10.1523/JNEUROSCI.0522-06.2006
102. Fischer, M., Kaech, S., Wagner, U., Brinkhaus, H. & Matus, A. Glutamate receptors regulate actin-based plasticity in dendritic spines. *Nat. Neurosci.* (2000). doi:10.1038/78791
103. Star, E. N., Kwiatkowski, D. J. & Murthy, V. N. Rapid turnover of actin in dendritic spines and its regulation by activity. *Nat. Neurosci.* (2002). doi:10.1038/nn811
104. Wegner, A. Head to tail polymerization of actin. *J. Mol. Biol.* (1976). doi:10.1016/S0022-2836(76)80100-3
105. Winder, S. J. & Ayscough, K. R. Actin-binding proteins. *J. Cell Sci.* 118, 651–654 (2005).
106. Carlier, M. F. & Pantaloni, D. Actin assembly in response to extracellular signals: Role of capping proteins, thymosin  $\beta$ 4 and profilin. *Semin. Cell Dev. Biol.* (1994). doi:10.1006/scel.1994.1023
107. Gieselmann, R. & Mann, K. ASP-56, a new actin sequestering protein from pig platelets with homology to CAP, an adenylate cyclase-associated protein from yeast. *FEBS Lett.* (1992). doi:10.1016/0014-5793(92)80043-G
108. Sohn, R. H. & Goldschmidt-Clermont, P. J. Profilin: At the crossroads of signal transduction and the actin cytoskeleton. *BioEssays* (1994). doi:10.1002/bies.950160705
109. Zigmond, S. H. How WASP regulates actin polymerization. *Journal of Cell Biology* (2000). doi:10.1083/jcb.150.6.F117
110. Yarmola, E. G. & Bubb, M. R. How depolymerization can promote polymerization: The case of actin and profilin. *BioEssays* (2009). doi:10.1002/bies.200900049
111. Bravo-Cordero, J. J., Magalhaes, M. A. O., Eddy, R. J., Hodgson, L. & Condeelis, J. Functions of cofilin in cell locomotion and invasion. *Nature Reviews Molecular Cell Biology* (2013). doi:10.1038/nrm3609
112. Hotulainen, P. Actin-depolymerizing Factor and Cofilin-1 Play Overlapping Roles in Promoting Rapid F-Actin Depolymerization in Mammalian Nonmuscle Cells. *Mol. Biol. Cell* (2004). doi:10.1091/mbc.E04-07-0555
113. Hayashi, K. *et al.* Domain analysis of the actin-binding and actin-remodeling

- activities of drebrin. *Exp. Cell Res.* (1999). doi:10.1006/excr.1999.4663
114. Harigaya, Y., Shoji, M., Shirao, T. & Hirai, S. Disappearance of actin-binding protein, drebrin, from hippocampal synapses in Alzheimer's disease. *J. Neurosci. Res.* (1996). doi:10.1002/jnr.490430111
  115. Hubberstey, A., Yu, G., Loewith, R., Lakusta, C. & Young, D. Mammalian CAP interacts with CAP, CAP2, and actin. *J. Cell. Biochem.* 61, 459-466 (1996).
  116. Kawamukai, M. *et al.* Genetic and biochemical analysis of the adenylyl cyclase-associated protein, cap, in *Schizosaccharomyces pombe*. *Mol. Biol. Cell* (1992). doi:10.1091/mbc.3.2.167
  117. Hubberstey, A. V. & Mortillo, E. P. Cyclase-associated proteins: CAPacity for linking signal transduction and actin polymerization. *FASEB J.* 16, 487-499 (2002).
  118. Koleske, A. J. Molecular mechanisms of dendrite stability. *Nature Reviews Neuroscience* (2013). doi:10.1038/nrn3486
  119. Honkura, N., Matsuzaki, M., Noguchi, J., Ellis-Davies, G. C. R. & Kasai, H. The Subspine Organization of Actin Fibers Regulates the Structure and Plasticity of Dendritic Spines. *Neuron* (2008). doi:10.1016/j.neuron.2008.01.013
  120. Citri, A. & Malenka, R. C. Synaptic plasticity: multiple forms, functions, and mechanisms. *Neuropsychopharmacology* (2008). doi:10.1038/sj.npp.1301559
  121. Hotulainen, P. & Hoogenraad, C. C. Actin in dendritic spines: Connecting dynamics to function. *Journal of Cell Biology* (2010). doi:10.1083/jcb.201003008
  122. Yuste, R. Electrical Compartmentalization in Dendritic Spines. *Annu. Rev. Neurosci.* (2013). doi:10.1146/annurev-neuro-062111-150455
  123. Hebb, D. O. *The Organization of Behavior. A Neuropsychological Theory.* 1949. *Wiley, New York* (1949).
  124. Bliss, T. V. P. & Gardner-Medwin, A. R. Long-lasting potentiation of synaptic transmission in the dentate area of the unanaesthetized rabbit following stimulation of the perforant path. *J. Physiol.* (1973). doi:10.1113/jphysiol.1973.sp010274
  125. Nicoll, R. A., Kauer, J. A. & Malenka, R. C. The current excitement in long term potentiation. *Neuron* (1988). doi:10.1016/0896-6273(88)90193-6
  126. Malenka, R. C. *et al.* Long-Term Potentiation--A Decade of Progress? *Science* (80- ). (1999). doi:10.1126/science.285.5435.1870
  127. Hayashi, Y. *et al.* Driving AMPA receptors into synapses by LTP and CaMKII: Requirement for GluR1 and PDZ domain interaction. *Science* (80- ). (2000). doi:10.1126/science.287.5461.2262
  128. Roche, K. W., O'Brien, R. J., Mammen, A. L., Bernhardt, J. & Huganir, R. L. Characterization of multiple phosphorylation sites on the AMPA receptor GluR1 subunit. *Neuron* (1996). doi:10.1016/S0896-6273(00)80144-0
  129. Barria, A., Muller, D., Derkach, V., Griffith, L. C. & Soderling, T. R. Regulatory phosphorylation of AMPA-type glutamate receptors by CaM-KII during long-term potentiation. *Science* (80- ). (1997). doi:10.1126/science.276.5321.2042
  130. Lee, H. K., Barbarosie, M., Kameyama, K., Bear, M. F. & Huganir, R. L. Regulation of distinct AMPA receptor phosphorylation sites during bidirectional synaptic

- plasticity. *Nature* (2000). doi:10.1038/35016089
131. Esteban, J. A. *et al.* PKA phosphorylation of AMPA receptor subunits controls synaptic trafficking underlying plasticity. *Nat. Neurosci.* (2003). doi:10.1038/nn997
  132. Lee, H. K., Kameyama, K., Huganir, R. L. & Bear, M. F. NMDA induces long-term synaptic depression and dephosphorylation of the GluR1 subunit of AMPA receptors in hippocampus. *Neuron* (1998). doi:10.1016/S0896-6273(00)80632-7
  133. Bosch, M. *et al.* Structural and molecular remodeling of dendritic spine substructures during long-term potentiation. *Neuron* (2014). doi:10.1016/j.neuron.2014.03.021
  134. Matsuzaki, M., Honkura, N., Ellis-Davies, G. C. R. & Kasai, H. Structural basis of long-term potentiation in single dendritic spines. *Nature* (2004). doi:10.1038/nature02617
  135. Toni, N., Buchs, P. A., Nikonenko, I., Bron, C. R. & Muller, D. LTP promotes formation of multiple spine synapses between a single axon terminal and a dendrite. *Nature* (1999). doi:10.1038/46574
  136. Okamoto, K. I., Nagai, T., Miyawaki, A. & Hayashi, Y. Rapid and persistent modulation of actin dynamics regulates postsynaptic reorganization underlying bidirectional plasticity. *Nat. Neurosci.* (2004). doi:10.1038/nn1311
  137. Dudek, S. M. & Bear, M. F. Homosynaptic long-term depression in area CA1 of hippocampus and effects of N-methyl-D-aspartate receptor blockade. *Proc. Natl. Acad. Sci.* (1992). doi:10.1073/pnas.89.10.4363
  138. Mulkey, R. M. & Malenka, R. C. Mechanisms underlying induction of homosynaptic long-term depression in area CA1 of the hippocampus. *Neuron* (1992). doi:10.1016/0896-6273(92)90248-C
  139. Banke, T. G. *et al.* Control of GluR1 AMPA Receptor Function by cAMP-Dependent Protein Kinase. *J. Neurosci.* (2000). doi:10.1523/JNEUROSCI.20-01-00089.2000
  140. Ashby, M. C. Removal of AMPA Receptors (AMPA Rs) from Synapses Is Preceded by Transient Endocytosis of Extrasynaptic AMPARs. *J. Neurosci.* (2004). doi:10.1523/JNEUROSCI.1042-04.2004
  141. Blanpied, T. A., Scott, D. B. & Ehlers, M. D. Dynamics and regulation of clathrin coats at specialized endocytic zones of dendrites and spines. *Neuron* (2002). doi:10.1016/S0896-6273(02)00979-0
  142. Groc, L. *et al.* Differential activity-dependent regulation of the lateral mobilities of AMPA and NMDA receptors. *Nat. Neurosci.* (2004). doi:10.1038/nn1270
  143. Cingolani, L. A. & Goda, Y. Actin in action: The interplay between the actin cytoskeleton and synaptic efficacy. *Nature Reviews Neuroscience* (2008). doi:10.1038/nrn2373
  144. Fukazawa, Y. *et al.* Hippocampal LTP is accompanied by enhanced F-actin content within the dendritic spine that is essential for late LTP maintenance in vivo. *Neuron* (2003). doi:10.1016/S0896-6273(03)00206-X
  145. Ramon y Cajal, S. Degeneration and regeneration of the nervous system. *Oxford Univ. Press. London* (1928).

146. Arendt, T. Synaptic degeneration in Alzheimer's disease. *Acta Neuropathologica* (2009). doi:10.1007/s00401-009-0536-x
147. Selkoe, D. J. Alzheimer's disease is a synaptic failure. *Science* (2002). doi:10.1126/science.1074069
148. Koffie, R. M. *et al.* Alzheimer's disease: synapses gone cold. *Mol. Neurodegener.* (2011). doi:10.1186/1750-1326-6-63
149. Davies, C. A., Mann, D. M. A., Sumpter, P. Q. & Yates, P. O. A quantitative morphometric analysis of the neuronal and synaptic content of the frontal and temporal cortex in patients with Alzheimer's disease. *J. Neurol. Sci.* (1987). doi:10.1016/0022-510X(87)90057-8
150. Terry, R. D. *et al.* Physical basis of cognitive alterations in alzheimer's disease: Synapse loss is the major correlate of cognitive impairment. *Ann. Neurol.* (1991). doi:10.1002/ana.410300410
151. DeKosky, S. T., Scheff, S. W. & Styren, S. D. Structural correlates of cognition in dementia: Quantification and assessment of synapse change. in *Neurodegeneration* (1996). doi:10.1006/neur.1996.0056
152. DeKosky, S. T. & Scheff, S. W. Synapse loss in frontal cortex biopsies in Alzheimer's disease: Correlation with cognitive severity. *Ann. Neurol.* (1990). doi:10.1002/ana.410270502
153. Masliah, E. *et al.* Altered expression of synaptic proteins occurs early during progression of Alzheimer's disease. *Neurology* (2001). doi:10.1212/WNL.56.1.127
154. Scheff, S. W., Price, D. A., Schmitt, F. A., Dekosky, S. T. & Mufson, E. J. Synaptic alterations in CA1 in mild Alzheimer disease and mild cognitive impairment. *Neurology* (2007). doi:10.1212/01.wnl.0000260698.46517.8f
155. Kandel, E. R. & Schwartz, J. H. Molecular biology of learning: Modulation of transmitter release. *Science* (80- ). (1982). doi:10.1126/science.6289442
156. Lynch, G. & Baudry, M. The biochemistry of memory: A new and specific hypothesis. *Science* (80- ). (1984). doi:10.1126/science.6144182
157. Morris, R. G. M. Hippocampal synaptic plasticity: Role in spatial learning or the automatic recording of attended experience? in *Philosophical Transactions of the Royal Society B: Biological Sciences* (1997). doi:10.1098/rstb.1997.0136
158. Reddy, P. H. *et al.* Differential loss of synaptic proteins in Alzheimer's disease: Implications for synaptic dysfunction. *J. Alzheimer's Dis.* (2005). doi:10.3233/JAD-2005-7203
159. Bertoni-Freddari, C., Fattoretti, P., Casoli, T., Caselli, U. & Meier-Ruge, W. Deterioration threshold of synaptic morphology in aging and senile dementia of Alzheimer's type. *Anal. Quant. Cytol. Histol.* (1996). doi:10.1016/j.ajog.2006.12.033
160. Scheff, S. W., Price, D. A., Schmitt, F. A. & Mufson, E. J. Hippocampal synaptic loss in early Alzheimer's disease and mild cognitive impairment. *Neurobiol. Aging* (2006). doi:10.1016/j.neurobiolaging.2005.09.012
161. Walsh, D. M. *et al.* Naturally secreted oligomers of amyloid  $\beta$  protein potently inhibit hippocampal long-term potentiation in vivo. *Nature* (2002). doi:10.1038/416535a

162. Hsieh, H. *et al.* AMPAR Removal Underlies A $\beta$ -Induced Synaptic Depression and Dendritic Spine Loss. *Neuron* (2006). doi:10.1016/j.neuron.2006.10.035
163. Shankar, G. M. & Walsh, D. M. Alzheimer's disease: synaptic dysfunction and A $\beta$ . (2009).
164. Shrestha, B. R. *et al.* Amyloid  $\beta$  peptide adversely affects spine number and motility in hippocampal neurons. *Mol. Cell. Neurosci.* (2006). doi:10.1016/j.mcn.2006.07.011
165. Calabrese, B. *et al.* Rapid, concurrent alterations in pre- and postsynaptic structure induced by naturally-secreted amyloid- $\beta$  protein. *Mol. Cell. Neurosci.* (2007). doi:10.1016/j.mcn.2007.02.006
166. Lacor, P. N. *et al.* A Oligomer-Induced Aberrations in Synapse Composition, Shape, and Density Provide a Molecular Basis for Loss of Connectivity in Alzheimer's Disease. *J. Neurosci.* (2007). doi:10.1523/JNEUROSCI.3501-06.2007
167. Evans, N. A. *et al.* A $\beta$ 1-42 reduces synapse number and inhibits neurite outgrowth in primary cortical and hippocampal neurons: A quantitative analysis. *J. Neurosci. Methods* (2008). doi:10.1016/j.jneumeth.2008.08.001
168. Spires, T. L. Dendritic Spine Abnormalities in Amyloid Precursor Protein Transgenic Mice Demonstrated by Gene Transfer and Intravital Multiphoton Microscopy. *J. Neurosci.* (2005). doi:10.1523/JNEUROSCI.1879-05.2005
169. Jacobsen, J. S. *et al.* Early-onset behavioral and synaptic deficits in a mouse model of Alzheimer's disease. *Proc. Natl. Acad. Sci.* (2006). doi:10.1073/pnas.0600948103
170. Wang, H. Y., Lee, D. H. S., Davis, C. B. & Shank, R. P. Amyloid peptide A $\beta$ 1-42 binds selectively and with picomolar affinity to  $\alpha$ 7 nicotinic acetylcholine receptors. *J. Neurochem.* (2000). doi:10.1046/j.1471-4159.2000.0751155.x
171. Ye, C., Walsh, D. M., Selkoe, D. J. & Hartley, D. M. Amyloid  $\beta$ -protein induced electrophysiological changes are dependent on aggregation state: N-methyl-D-aspartate (NMDA) versus non-NMDA receptor/channel activation. *Neurosci. Lett.* (2004). doi:10.1016/j.neulet.2004.05.060
172. Mishizen-Eberz, A. J. *et al.* Biochemical and molecular studies of NMDA receptor subunits NR1/2A/2B in hippocampal subregions throughout progression of Alzheimer's disease pathology. *Neurobiol. Dis.* (2004). doi:10.1016/j.nbd.2003.09.016
173. Zhang, Y., Li, P., Feng, J. & Wu, M. Dysfunction of NMDA receptors in Alzheimer's disease. *Neurological Sciences* (2016). doi:10.1007/s10072-016-2546-5
174. Snyder, E. M. *et al.* Regulation of NMDA receptor trafficking by amyloid- $\beta$ . *Nat. Neurosci.* (2005). doi:10.1038/nn1503
175. Hall, A. M. & Roberson, E. D. Mouse Models of Alzheimer's Disease. *Brain Res. Bull.* (2010).
176. Harvey, R. J., Skelton-Robinson, M. & Rossor, M. N. The prevalence and causes of dementia in people under the age of 65 years. *J. Neurol. Neurosurg. Psychiatry* (2003). doi:10.1136/jnnp.74.9.1206
177. Landhuis, E. & Stribek, G. Law and Disorder—APPswe Patent Suits Raise Ruckus

- Again. *Alzheimer Research Forum* (2010).
178. Cheng, I. H. *et al.* Aggressive amyloidosis in mice expressing human amyloid peptides with the Arctic mutation. *Nat. Med.* (2004). doi:10.1038/nm1123
  179. Lewis, P. A. *et al.* Expression of BRI-amyloid  $\beta$  peptide fusion proteins: A novel method for specific high-level expression of amyloid  $\beta$  peptides. *Biochim. Biophys. Acta - Mol. Basis Dis.* (2001). doi:10.1016/S0925-4439(01)00054-0
  180. McGowan, E. *et al.* A $\beta$ 42 is essential for parenchymal and vascular amyloid deposition in mice. *Neuron* (2005). doi:10.1016/j.neuron.2005.06.030
  181. Lewis, J. *et al.* Enhanced neurofibrillary degeneration in transgenic mice expressing mutant tau and APP. *Science* (80-. ). (2001). doi:10.1126/science.1058189
  182. Oddo, S., Caccamo, A., Kitazawa, M., Tseng, B. P. & LaFerla, F. M. Amyloid deposition precedes tangle formation in a triple transgenic model of Alzheimer's disease. in *Neurobiology of Aging* (2003). doi:10.1016/j.neurobiolaging.2003.08.012
  183. Oddo, S. *et al.* Triple-transgenic model of Alzheimer's Disease with plaques and tangles: Intracellular A $\beta$  and synaptic dysfunction. *Neuron* (2003). doi:10.1016/S0896-6273(03)00434-3
  184. Andorfer, C. *et al.* Hyperphosphorylation and aggregation of tau in mice expressing normal human tau isoforms. *J. Neurochem.* (2003). doi:10.1046/j.1471-4159.2003.01879.x
  185. Lewis, J. *et al.* Neurofibrillary tangles, amyotrophy and progressive motor disturbance in mice expressing mutant (P301L)tau protein. *Nat. Genet.* (2000). doi:10.1038/78078
  186. Götz, J., Chen, F., Van Dorpe, J. & Nitsch, R. M. Formation of neurofibrillary tangles in P301L tau transgenic mice induced by A $\beta$ 42 fibrils. *Science* (80-. ). (2001). doi:10.1126/science.1062097
  187. Bolmont, T. *et al.* Induction of tau pathology by intracerebral infusion of amyloid- $\beta$ -containing brain extract and by amyloid- $\beta$  deposition in APP x tau transgenic mice. *Am. J. Pathol.* 171, 2012–2020 (2007).
  188. Borchelt, D. R. *et al.* Familial Alzheimer's disease-linked presenilin I variants elevate a $\beta$ 1-42/1-40 ratio in vitro and in vivo. *Neuron* (1996). doi:10.1016/S0896-6273(00)80230-5
  189. Chui, D. H. *et al.* Transgenic mice with Alzheimer presenilin 1 mutations show accelerated neurodegeneration without amyloid plaque formation. *Nat. Med.* (1999). doi:10.1038/8438
  190. Citron, M. *et al.* Mutant presenilins of Alzheimer's disease increase production of 42-residue amyloid  $\beta$ -protein in both transfected cells and transgenic mice. *Nat. Med.* (1997). doi:10.1038/nm0197-67
  191. Dewachter, I. *et al.* Aging increased amyloid peptide and caused amyloid plaques in brain of old APP/V717I transgenic mice by a different mechanism than mutant presenilin1. *J. Neurosci.* (2000). doi:20/17/6452 [pii]
  192. Duff, K. *et al.* Increased amyloid- $\beta$ 42(43) in brains of mice expressing mutant presenilin 1. *Nature* (1996). doi:10.1038/383710a0
  193. Hwang, D. Y. *et al.* Alterations in behavior, amyloid  $\beta$ -42, caspase-3, and Cox-2

- in mutant PS2 transgenic mouse model of Alzheimer's disease. *FASEB J.* (2002). doi:10.1096/fj.01-0732com
194. Leutner, S. *et al.* Reduced antioxidant enzyme activity in brains of mice transgenic for human presenilin-1 with single or multiple mutations. *Neurosci. Lett.* (2000). doi:10.1016/S0304-3940(00)01449-X
  195. Oyama, F. *et al.* Mutant presenilin 2 transgenic mouse: effect on an age-dependent increase of amyloid beta-protein 42 in the brain. *J. Neurochem.* (1998). doi:10.1046/j.1471-4159.1998.71010313.x
  196. Wen, P. H. *et al.* The presenilin-1 familial Alzheimer disease mutant P117L impairs neurogenesis in the hippocampus of adult mice. *Exp. Neurol.* (2004). doi:10.1016/j.expneurol.2004.04.002
  197. Dewachter, I. *et al.* Modulation of synaptic plasticity and Tau phosphorylation by wild-type and mutant presenilin1. *Neurobiol. Aging* (2008). doi:10.1016/j.neurobiolaging.2006.11.019
  198. Holcomb, L. A. *et al.* Behavioral changes in transgenic mice expressing both amyloid precursor protein and presenilin-1 mutations: Lack of association with amyloid deposits. *Behav. Genet.* (1999). doi:10.1023/A:1021691918517
  199. Huang, X. G., Yee, B. K., Nag, S., Chan, S. T. H. & Tang, F. Behavioral and neurochemical characterization of transgenic mice carrying the human presenilin-1 gene with or without the leucine-to-proline mutation at codon 235. *Exp. Neurol.* (2003). doi:10.1016/S0014-4886(03)00242-5
  200. Janus, C. *et al.* Spatial learning in transgenic mice expressing human presenilin 1 (PS1) transgenes. *Neurobiol. Aging* (2000). doi:10.1016/S0197-4580(00)00107-X
  201. Lalonde, R., Qian, S. & Strazielle, C. Transgenic mice expressing the PS1-A246E mutation: Effects on spatial learning, exploration, anxiety, and motor coordination. *Behav. Brain Res.* (2003). doi:10.1016/S0166-4328(02)00230-9
  202. Selkoe, D. J. Biochemistry of altered brain proteins in Alzheimer's Disease. *Annu. Rev. Neurosci.* 12, 463-490 (1989).
  203. Jankowsky, J. L. *et al.* Mutant presenilins specifically elevate the levels of the 42 residue  $\beta$ -amyloid peptide in vivo: Evidence for augmentation of a 42-specific  $\gamma$  secretase. *Hum. Mol. Genet.* 13, 159-170 (2004).
  204. Reiss, K. & Saftig, P. The 'A Disintegrin And Metalloprotease' (ADAM) family of sheddases: Physiological and cellular functions. *Seminars in Cell and Developmental Biology* (2009). doi:10.1016/j.semcd.2008.11.002
  205. Seegar, T. C. M. *et al.* Structural Basis for Regulated Proteolysis by the  $\alpha$ -Secretase ADAM10. *Cell* 171, 1638-1648.e7 (2017).
  206. Huovila, A. P. J., Turner, A. J., Pelto-Huikko, M., Kärkkäinen, I. & Ortiz, R. M. Shedding light on ADAM metalloproteinases. *Trends in Biochemical Sciences* (2005). doi:10.1016/j.tibs.2005.05.006
  207. Janes, P. W. *et al.* Adam meets Eph: An ADAM substrate recognition module acts as a molecular switch for ephrin cleavage in trans. *Cell* (2005). doi:10.1016/j.cell.2005.08.014
  208. Duojia, P. & Rubin, G. M. Kuzbanian controls proteolytic processing of Notch and mediates lateral inhibition during *Drosophila* and vertebrate neurogenesis.

- Cell* (1997). doi:10.1016/S0092-8674(00)80335-9
209. Stawikowska, R. et al. Activity of ADAM17 (a disintegrin and metalloprotease 17) is regulated by its noncatalytic domains and secondary structure of its substrates. *J. Biol. Chem.* (2013). doi:10.1074/jbc.M113.462267
  210. Tape, C. J. et al. Cross-domain inhibition of TACE ectodomain. *Proc. Natl. Acad. Sci.* (2011). doi:10.1073/pnas.1017067108
  211. Sundberg, C. et al. Regulation of ADAM12 cell-surface expression by protein kinase C  $\epsilon$ . *J. Biol. Chem.* (2004). doi:10.1074/jbc.M403753200
  212. Marcello, E. et al. Synapse-Associated Protein-97 Mediates  $\gamma$ -Secretase ADAM10 Trafficking and Promotes Its Activity. *J. Neurosci.* 27, 1682-1691 (2007).
  213. Marcello, E. et al. Endocytosis of synaptic ADAM10 in neuronal plasticity and Alzheimer's disease. *J. Clin. Invest.* 123, 2523-2538 (2013).
  214. Endres, K. et al. Tumor necrosis factor- $\alpha$  converting enzyme is processed by proprotein-convertases to its mature form which is degraded upon phorbol ester stimulation. *Eur. J. Biochem.* (2003). doi:10.1046/j.1432-1033.2003.03606.x
  215. Schlöndorff, J., Becherer, J. D. & Blobel, C. P. Intracellular maturation and localization of the tumour necrosis factor  $\alpha$  convertase (TACE). *Biochem. J.* (2000). doi:10.1042/0264-6021:3470131
  216. Kuhn, P. H. et al. Systematic substrate identification indicates a central role for the metalloprotease ADAM10 in axon targeting and synapse function. *Elife* (2016). doi:10.7554/eLife.12748.001
  217. Hattori, M., Osterfield, M. & Flanagan, J. G. Regulated cleavage of a contact-mediated axon repellent. *Science* (80-. ). (2000). doi:10.1126/science.289.5483.1360
  218. Nakagawa, S. & Takeichi, M. Neural crest emigration from the neural tube depends on regulated cadherin expression. *Development* (1998). doi:10.1039/c7ay01244f
  219. Paradies, N. E. & Grunwald, G. B. Purification and characterization of NCAD90, a Soluble endogenous form of N-cadherin, which is generated by proteolysis during retinal development and retains adhesive and neurite-promoting function. *Journal of Neuroscience Research* (1993). doi:10.1002/jnr.490360105
  220. Malinverno, M. et al. Synaptic Localization and Activity of ADAM10 Regulate Excitatory Synapses through N-Cadherin Cleavage. *J. Neurosci.* (2010). doi:10.1523/JNEUROSCI.1984-10.2010
  221. Reiss, K. et al. ADAM10 cleavage of N-cadherin and regulation of cell-cell adhesion and  $\beta$ -catenin nuclear signalling. *EMBO J.* (2005). doi:10.1038/sj.emboj.7600548
  222. Reiss, K. et al. Regulated ADAM10-dependent ectodomain shedding of gamma-protocadherin C3 modulates cell-cell adhesion. *J. Biol. Chem.* 281, 21735-21744 (2006).
  223. Parkin, E. T., Watt, N. T., Turner, A. J. & Hooper, N. M. Dual Mechanisms for Shedding of the Cellular Prion Protein. *J. Biol. Chem.* (2004). doi:10.1074/jbc.M312105200
  224. Vincent, B. ADAM Proteases: Protective Role in Alzheimer's and Prion



- Diseases? *Curr. Alz. Res.* (2004). doi:http://dx.doi:10.2174/1567205043332072
225. Bray, S. J. Notch signalling: A simple pathway becomes complex. *Nature Reviews Molecular Cell Biology* (2006). doi:10.1038/nrm2009
  226. Hartmann, D. *et al.* The disintegrin/metalloprotease ADAM 10 is essential for Notch signalling but not for alpha-secretase activity in fibroblasts. *Hum. Mol. Genet.* 11, 2615-2624 (2002).
  227. De Strooper, B. *et al.* A presenilin-1-dependent  $\gamma$ -secretase-like protease mediates release of notch intracellular domain. *Nature* (1999). doi:10.1038/19083
  228. Young-Pearse, T. L. *et al.* A Critical Function for  $\gamma$ -Amyloid Precursor Protein in Neuronal Migration Revealed by In Utero RNA Interference. *J. Neurosci.* (2007). doi:10.1207/s15324796abm2903\_1
  229. Young-Pearse, T. L., Chen, A. C., Chang, R., Marquez, C. & Selkoe, D. J. Secreted APP regulates the function of full-length APP in neurite outgrowth through interaction with integrin beta1. *Neural Dev.* (2008). doi:10.1186/1749-8104-3-15
  230. Bittner, T. *et al.* Amyloid plaque formation precedes dendritic spine loss. *Acta Neuropathol.* (2012). doi:10.1007/s00401-012-1047-8
  231. Cousins, S. L., Kenny, A. V. & Stephenson, F. A. Delineation of additional PSD-95 binding domains within NMDA receptor NR2 subunits reveals differences between NR2A/PSD-95 and NR2B/PSD-95 association. *Neuroscience* (2009). doi:10.1016/j.neuroscience.2007.12.051
  232. Allinson, T. M. J., Parkin, E. T., Turner, A. J. & Hooper, N. M. ADAMs Family Members As Amyloid Precursor Protein  $\alpha$ -Secretases. *Journal of Neuroscience Research* (2003). doi:10.1002/jnr.10737
  233. Asai, M. *et al.* Putative function of ADAM9, ADAM10, and ADAM17 as APP  $\alpha$ -secretase. *Biochem. Biophys. Res. Commun.* (2003). doi:10.1016/S0006-291X(02)02999-6
  234. Jorissen, E. *et al.* The Disintegrin/Metalloproteinase ADAM10 Is Essential for the Establishment of the Brain Cortex. *J. Neurosci.* 30, 4833-4844 (2010).
  235. Saraceno, C. *et al.* SAP97-mediated ADAM10 trafficking from Golgi outposts depends on PKC phosphorylation. *Cell Death Dis.* (2014). doi:10.1038/cddis.2014.492
  236. Mauceri, D., Cattabeni, F., Di Luca, M. & Gardoni, F. Calmodulin-dependent protein kinase II phosphorylation drives synapse-associated protein 97 into spines. *J. Biol. Chem.* (2004). doi:10.1074/jbc.M402796200
  237. Wan, X.-Z. *et al.* Activation of NMDA Receptors Upregulates A Disintegrin and Metalloproteinase 10 via a Wnt/MAPK Signaling Pathway. *J. Neurosci.* 32, 3910-3916 (2012).
  238. Colciaghi, F. *et al.*  $\alpha$ -Secretase ADAM10 as well as  $\alpha$ APPs is reduced in platelets and CSF of Alzheimer disease patients. *Mol. Med.* (2002). doi:S1528365802200671 [pii]
  239. Sogorb-Esteve, A. *et al.* Levels of ADAM10 are reduced in Alzheimer's disease CSF. *J. Neuroinflammation* (2018). doi:10.1186/s12974-018-1255-9
  240. Gatta, L. B., Albertini, A., Ravid, R. & Finazzi, D. Levels of  $\beta$ -secretase BACE and

- $\alpha$ -secretase ADAM10 mRNAs in Alzheimer hippocampus. *Neuroreport* (2002). doi:10.1097/00001756-200211150-00008
241. Marcello, E. *et al.* SAP97-mediated local trafficking is altered in Alzheimer disease patients' hippocampus. *Neurobiol. Aging* 33, 422.e1-422.e10 (2012).
  242. Epis, R. *et al.* Blocking ADAM10 synaptic trafficking generates a model of sporadic Alzheimer's disease. *Brain* (2010). doi:10.1093/brain/awq217
  243. Gerst, J. E., Ferguson, K., Vojtek, A., Wigler, M. & Field, J. CAP is a bifunctional component of the *Saccharomyces cerevisiae* adenylyl cyclase complex. *Mol. Cell. Biol.* (1991). doi:10.1128/MCB.11.3.1248.Updated
  244. Hubberstey, A. V. & Mortillo, E. P. Cyclase-associated proteins: CAPacity for linking signal transduction and actin polymerization. *FASEB J.* (2002). doi:10.1096/fj.01-0659rev
  245. Bertling, E. *et al.* Cyclase-associated Protein 1 (CAP1) Promotes Cofilin-induced Actin Dynamics in Mammalian Nonmuscle Cells. *Mol. Biol. Cell* (2004). doi:10.1091/mbc.E04-01-0048
  246. Peche, V. *et al.* CAP2, cyclase-associated protein 2, is a dual compartment protein. *Cell. Mol. Life Sci.* (2007). doi:10.1007/s00018-007-7316-3
  247. Swiston, J., Hubberstey, A., Yu, G. & Young, D. Differential expression of CAP and CAP2 in adult rat tissues. *Gene* (1995). doi:10.1016/0378-1119(95)00522-8
  248. Yu, G., Swiston, J. & Young, D. Comparison of human CAP and CAP2, homologs of the yeast adenylyl cyclase-associated proteins. *J. Cell Sci.* (1994).
  249. Wang, C., Zhou, G.-L., Vedantam, S., Li, P. & Field, J. Mitochondrial shuttling of CAP1 promotes actin- and cofilin-dependent apoptosis. *J. Cell Sci.* (2008). doi:10.1242/jcs.023911
  250. Ono, S. The role of cyclase-associated protein in regulating actin filament dynamics - more than a monomer-sequestration factor. *J. Cell Sci.* (2013). doi:10.1242/jcs.128231
  251. Vojtek, A. *et al.* Evidence for a functional link between profilin and CAP in the yeast *S. cerevisiae*. *Cell* (1991). doi:10.1016/0092-8674(81)90013-1
  252. Nishida, Y. *et al.* Coiled-coil interaction of N-terminal 36 residues of cyclase-associated protein with adenylyl cyclase is sufficient for its function in *Saccharomyces cerevisiae* Ras pathway. *J. Biol. Chem.* (1998). doi:10.1074/jbc.273.43.28019
  253. Burkhard, P., Stetefeld, J. & Strelkov, S. V. Coiled coils: A highly versatile protein folding motif. *Trends in Cell Biology* (2001). doi:10.1016/S0962-8924(00)01898-5
  254. Ksiazek, D. *et al.* Structure of the N-terminal domain of the adenylyl cyclase-associated protein (CAP) from *Dictyostelium discoideum*. *Structure* (2003). doi:10.1016/S0969-2126(03)00180-1
  255. Moriyama, K. & Yahara, I. Human CAP1 is a key factor in the recycling of cofilin and actin for rapid actin turnover. *J. Cell Sci.* (2002). doi:10.1080/13668250802291606
  256. Quintero-Monzon, O. *et al.* Reconstitution and dissection of the 600-kDa Srv2/CAP complex: Roles for oligomerization and cofilin-actin binding in driving actin turnover. *J. Biol. Chem.* 284, 10923-10934 (2009).

257. Chaudhry, F. *et al.* Srv2/cyclase-associated protein forms hexameric shurikens that directly catalyze actin filament severing by cofilin. *Mol. Biol. Cell* (2013). doi:10.1091/mbc.E12-08-0589
258. Lila, T. & Drubin, D. G. Evidence for physical and functional interactions among two *Saccharomyces cerevisiae* SH3 domain proteins, an adenyl cyclase-associated protein and the actin cytoskeleton. *Mol. Biol. Cell* (1997). doi:10.1091/mbc.8.2.367
259. Bertling, E., Quintero-Monzon, O., Mattila, P., Goode, B. L. & Lappalainen, P. Mechanism and biological role of profilin-Srv2/CAP interaction. *J. Cell Sci.* 120, 1225-1234 (2007).
260. Vaduva, G., Martin, N. C. & Hopper, A. K. Actin-binding verprolin is a polarity development protein required for the morphogenesis and function of the yeast actin cytoskeleton. *J. Cell Biol.* (1997). doi:10.1083/jcb.139.7.1821
261. Paunola, E., Mattila, P. K. & Lappalainen, P. WH2 domain: A small, versatile adapter for actin monomers. *FEBS Letters* (2002). doi:10.1016/S0014-5793(01)03242-2
262. Chaudhry, F., Little, K., Talarico, L., Quintero-Monzon, O. & Goode, B. L. A central role for the WH2 domain of Srv2/CAP in recharging actin monomers to drive actin turnover in vitro and in vivo. *Cytoskeleton* (2010). doi:10.1002/cm.20429
263. Dodatko, T. *et al.* Crystal structure of the actin binding domain of the cyclase-associated protein. *Biochemistry* (2004). doi:10.1021/bi049071r
264. Amberg, D. C., Basart, E. & Botstein, D. Defining protein interactions with yeast actin in vivo. *Nat. Struct. Biol.* (1995). doi:10.1038/nsb0195-28
265. Zelicof, A. *et al.* Two separate functions are encoded by the carboxyl-terminal domains of the yeast cyclase-associated protein and its mammalian homologs. Dimerization and actin binding. *J. Biol. Chem.* (1996). doi:10.1074/jbc.271.30.18243
266. Ono, S. The role of cyclase-associated protein in regulating actin filament dynamics - more than a monomer-sequestration factor. *J. Cell Sci.* 126, 3249-3258 (2013).
267. Balcer, H. I. *et al.* Coordinated Regulation of Actin Filament Turnover by a High-Molecular- Weight Srv2/CAP Complex, Cofilin, Profilin, and Aip1. *Curr. Biol.* (2003). doi:10.1016/j.cub.2003.11.051
268. Yang, S., Cope, M. J. & Drubin, D. G. Sla2p is associated with the yeast cortical actin cytoskeleton via redundant localization signals. *Mol. Biol. Cell* (1999). doi:10.1091/mbc.10.7.2265
269. Yu, J., Wang, C., Palmieri, S. J., Haarer, B. K. & Field, J. A cytoskeletal localizing domain in the cyclase-associated protein, CAP/Srv2p, regulates access to a distant SH3-binding site. *J. Biol. Chem.* (1999). doi:10.1074/jbc.274.28.19985
270. Yusof, A. M., Hu, N. J., Wlodawer, A. & Hofmann, A. Structural evidence for variable oligomerization of the N-terminal domain of cyclase-associated protein (CAP). *Proteins Struct. Funct. Genet.* (2005). doi:10.1002/prot.20314
271. Yusof, A. M. *et al.* Mechanism of Oligomerisation of Cyclase-associated Protein from *Dictyostelium discoideum* in Solution. *J. Mol. Biol.* (2006).

- doi:10.1016/j.jmb.2006.08.008
272. Freeman, N. L., Chen, Z., Horenstein, J., Weber, A. & Field, J. An actin monomer binding activity localizes to the carboxyl-terminal half of the *Saccharomyces cerevisiae* cyclase-associated protein. *J. Biol. Chem.* (1995). doi:10.1074/jbc.270.10.5680
  273. Peche, V. S. *et al.* Ablation of cyclase-associated protein 2 (CAP2) leads to cardiomyopathy. *Cell. Mol. Life Sci.* (2013). doi:10.1007/s00018-012-1142-y
  274. Mattila, P. K. A High-affinity Interaction with ADP-Actin Monomers Underlies the Mechanism and In Vivo Function of Srv2/cyclase-associated Protein. *Mol. Biol. Cell* (2004). doi:10.1091/mbc.E04-06-0444
  275. Bugyi, B. & Carlier, M.-F. Control of Actin Filament Treadmilling in Cell Motility. *Annu. Rev. Biophys.* (2010). doi:10.1146/annurev-biophys-051309-103849
  276. De La Cruz, E. M. & Pollard, T. D. Structural biology. Actin' up. *Science* (80-. ). 293, 616-618 (2001).
  277. Kinosian, H. J., Selden, L. A., Estes, J. E. & Gershman, L. C. Nucleotide binding to actin. Cation dependence of nucleotide dissociation and exchange rates. *J. Biol. Chem.* (1993). doi:10.3390/ijerph120708448
  278. Pollard, T. D. Rate constants for the reactions of ATP- and ADP-actin with the ends of actin filaments. *J. Cell Biol.* (1986). doi:10.1083/jcb.103.6.2747
  279. Pollard, T. D., Goldberg, I. & Schwarz, W. H. Nucleotide exchange, structure, and mechanical properties of filaments assembled from ATP-actin and ADP-actin. *J. Biol. Chem.* (1992).
  280. Nishida, E. Opposite Effects of Cofilin and Profilin from Porcine Brain on Rate of Exchange of Actin-Bound Adenosine 5'-Triphosphate. *Biochemistry* (1985). doi:10.1021/bi00326a015
  281. Goldschmidt-Clermont, P. J. *et al.* The control of actin nucleotide exchange by thymosin beta 4 and profilin. A potential regulatory mechanism for actin polymerization in cells. *Mol. Biol. Cell* (1992). doi:10.1091/mbc.3.9.1015
  282. Goldschmidt-Clermont, P. J., Machesky, L. M., Doberstein, S. K. & Pollard, T. D. Mechanism of the interaction of human platelet profilin with actin. *J. Cell Biol.* (1991). doi:10.1083/jcb.113.5.1081
  283. Mockrin, S. C. & Korn, E. D. *Acanthamoeba* Profilin Interacts with G-Actin to Increase the Rate of Exchange of Actin-Bound Adenosine 5'-Triphosphate. *Biochemistry* (1980). doi:10.1021/bi00564a033
  284. Chaudhry, F., Guerin, C., von Witsch, M., Blanchoin, L. & Staiger, C. J. Identification of Arabidopsis Cyclase-associated Protein 1 as the First Nucleotide Exchange Factor for Plant Actin. *Mol. Biol. Cell* (2007). doi:10.1109/23.221048
  285. Nomura, K., Ono, K. & Ono, S. CAS-1, a *C. elegans* cyclase-associated protein, is required for sarcomeric actin assembly in striated muscle. *J. Cell Sci.* (2012). doi:10.1242/jcs.104950
  286. Carlier, M.-F., Jean, C., Riegert, K. J., Lenfant, M. & Pantaloni, D. Modulation of the interaction between G-actin and thymosin I4 by the ATP/ADP ratio: Possible implication in the regulation of actin dynamics. *Biochemistry* 90, 5034-5038 (1993).

287. Pantaloni, D. & Carlier, M. F. How profilin promotes actin filament assembly in the presence of thymosin  $\beta$ 4. *Cell* (1993). doi:10.1016/0092-8674(93)90544-Z
288. Blanchoin, L. & Pollard, T. D. Interaction of Actin Monomers with Acanthamoeba Actophorin (ADF/cofilin) and profilin. *J. Biol. Chem.* 273, 25106–25111 (1998).
289. Didry, D., Carlier, M.-F. & Pantaloni, D. Synergy between Actin Depolymerizing Factor/Cofilin and Profilin in Increasing Actin Filament Turnover. *J. Biol. Chem.* 273, 25602–25611 (1998).
290. Makkonen, M., Bertling, E., Chebotareva, N. A., Baump, J. & Lappalainen, P. Mammalian and malaria parasite cyclase-associated proteins catalyze nucleotide exchange on G-actin through a conserved mechanism. *J. Biol. Chem.* (2013). doi:10.1074/jbc.M112.435719
291. Nomura, K. & Ono, S. ATP-dependent regulation of actin monomer-filament equilibrium by cyclase-associated protein and ADF/cofilin. *Biochem. J.* (2013). doi:10.1042/BJ20130491
292. Normoyle, K. P. M. & Briehner, W. M. Cyclase-associated protein (CAP) acts directly on F-actin to accelerate cofilin-mediated actin severing across the range of physiological pH. *J. Biol. Chem.* (2012). doi:10.1074/jbc.M112.396051
293. Hawkins, M., Pope, B., Maciver, S. K. & Weeds, A. G. Human Actin Depolymerizing Factor Mediates a pH-Sensitive Destruction of Actin Filaments. *Biochemistry* (1993). doi:10.1021/bi00089a014
294. Hayden, S. M., Miller, P. S., Brauweiler, A. & Bamburg, J. R. Analysis of the Interactions of Actin Depolymerizing Factor with G- and F-Actin. *Biochemistry* (1993). doi:10.1021/bi00089a015
295. Yonezawa, N., Nishida, E. & Sakai, H. pH control of actin polymerization by cofilin. *J. Biol. Chem.* 260, 14410–14412 (1985).
296. Field, J. *et al.* CAP2 in cardiac conduction, sudden cardiac death and eye development. *Sci. Rep.* (2015). doi:10.1038/srep17256
297. Stöckigt, F. *et al.* Deficiency of cyclase-associated protein 2 promotes arrhythmias associated with connexin43 maldistribution and fibrosis. *Arch. Med. Sci.* (2016). doi:10.5114/aoms.2015.54146
298. Kosmas, K. *et al.* CAP2 is a regulator of the actin cytoskeleton and its absence changes infiltration of inflammatory cells and contraction of wounds. *Eur. J. Cell Biol.* (2015). doi:10.1016/j.ejcb.2014.10.004
299. Bremer, A., Schoumans, J., Nordenskjöld, M., Anderlid, B. M. & Giacobini, M. An interstitial deletion of 7.1 Mb in chromosome band 6p22.3 associated with developmental delay and dysmorphic features including heart defects, short neck, and eye abnormalities. *Eur. J. Med. Genet.* (2009). doi:10.1016/j.ejmg.2009.06.002
300. Davies, A. F. *et al.* Delineation of two distinct 6p deletion syndromes. *Hum. Genet.* (1999). doi:10.1007/s004390050911
301. Kumar, A. *et al.* Neuronal Actin Dynamics, Spine Density and Neuronal Dendritic Complexity Are Regulated by CAP2. *Front. Cell. Neurosci.* 10, 1–17 (2016).
302. Saetre, P., Jazin, E. & Emilsson, L. Age-related changes in gene expression are accelerated in Alzheimer's disease. *Synapse* (2011). doi:10.1002/syn.20933

303. Emilsson, L., Saetre, P. & Jazin, E. Alzheimer's disease: mRNA expression profiles of multiple patients show alterations of genes involved with calcium signaling. *Neurobiol. Dis.* (2006). doi:10.1016/j.nbd.2005.09.004
304. Blalock, E. M. *et al.* Incipient Alzheimer's disease: Microarray correlation analyses reveal major transcriptional and tumor suppressor responses. *Proc. Natl. Acad. Sci.* (2004). doi:10.1108/PM-08-2016-0044
305. Kuhn, P. H. *et al.* Systematic substrate identification indicates a central role for the metalloprotease ADAM10 in axon targeting and synapse function. *Elife* 5, (2016).
306. Marcello, E., Gardoni, F., Di Luca, M. & Pérez-Otan, I. An arginine stretch limits ADAM10 exit from the endoplasmic reticulum. *J. Biol. Chem.* 285, 10376-10384 (2010).
307. Kim, B. G., Dai, H. N., McAtee, M., Vicini, S. & Bregman, B. S. Labeling of dendritic spines with the carbocyanine dye Dil for confocal microscopic imaging in lightly fixed cortical slices. *J. Neurosci. Methods* (2007). doi:10.1016/j.jneumeth.2007.01.016
308. Stine, W. B., Dahlgren, K. N., Krafft, G. A. & LaDu, M. J. In vitro characterization of conditions for amyloid- $\beta$  peptide oligomerization and fibrillogenesis. *J. Biol. Chem.* (2003). doi:10.1074/jbc.M210207200
309. Ruben, S. *et al.* Structural and functional characterization of human immunodeficiency virus tat protein. *J. Virol.* (1989). doi:10.1353/ccj.2006.0049
310. Saraceno, C. *et al.* SAP97-mediated ADAM10 trafficking from Golgi outposts depends on PKC phosphorylation. *Cell Death Dis.* 5, e1547-13 (2014).
311. Galletta, B. J., Mooren, O. L. & Cooper, J. A. Actin dynamics and endocytosis in yeast and mammals. *Current Opinion in Biotechnology* (2010). doi:10.1016/j.copbio.2010.06.006
312. Mooren, O. L., Galletta, B. J. & Cooper, J. A. Roles for Actin Assembly in Endocytosis. *Annu. Rev. Biochem.* (2012). doi:10.1146/annurev-biochem-060910-094416
313. Liu, Y., Xiao, W., Shinde, M., Field, J. & Templeton, D. M. Cadmium favors F-actin depolymerization in rat renal mesangial cells by site-specific, disulfide-based dimerization of the CAP1 protein. *Arch. Toxicol.* (2018). doi:10.1007/s00204-017-2142-3
314. Lu, W. Y. *et al.* Activation of synaptic NMDA receptors induces membrane insertion of new AMPA receptors and LTP in cultured hippocampal neurons. *Neuron* (2001). doi:10.1016/S0896-6273(01)00194-5
315. Beattie, E. C. *et al.* Regulation of AMPA receptor endocytosis by a signaling mechanism shared with LTD. *Nat. Neurosci.* (2000). doi:10.1038/81823
316. Chapman, P. F. *et al.* Impaired synaptic plasticity and learning in aged amyloid precursor protein transgenic mice. *Nat. Neurosci.* (1999). doi:10.1038/6374
317. He, K., Lee, A., Song, L., Kanold, P. O. & Lee, H.-K. AMPA receptor subunit GluR1 (GluA1) serine-845 site is involved in synaptic depression but not in spine shrinkage associated with chemical long-term depression. *J. Neurophysiol.* (2011). doi:10.1152/jn.00913.2010
318. Selkoe, D. J. Alzheimers Disease. *Cold Spring Harb. Perspect. Biol.* 3, 387-403

- (2011).
319. Wetzel, S., Seipold, L. & Saftig, P. The metalloproteinase ADAM10: A useful therapeutic target? *Biochimica et Biophysica Acta - Molecular Cell Research* (2017). doi:10.1016/j.bbamcr.2017.06.005
  320. Postina, R. *et al.* A disintegrin-metalloproteinase prevents amyloid plaque formation and hippocampal defects in an Alzheimer disease mouse model. *J. Clin. Invest.* (2004). doi:10.1172/JCI20864
  321. Pasciuto, E. *et al.* Dysregulated ADAM10-Mediated Processing of APP during a Critical Time Window Leads to Synaptic Deficits in Fragile X Syndrome. *Neuron* (2015). doi:10.1016/j.neuron.2015.06.032
  322. Müller, M. *et al.* A disintegrin and metalloprotease 10 (ADAM10) is a central regulator of murine liver tissue homeostasis. *Oncotarget* (2016). doi:10.18632/oncotarget.7836
  323. Orme, J. J. *et al.* Heightened cleavage of Axl receptor tyrosine kinase by ADAM metalloproteases may contribute to disease pathogenesis in SLE. *Clin. Immunol.* (2016). doi:10.1016/j.clim.2016.05.011
  324. Hoffmann, F. S. *et al.* The Immunoregulator Soluble TACI Is Released by ADAM10 and Reflects B Cell Activation in Autoimmunity. *J. Immunol.* (2014). doi:10.4049/jimmunol.1402070
  325. Li, D., Xiao, Z., Wang, G. & Song, X. Knockdown of ADAM10 inhibits migration and invasion of fibroblast-like synoviocytes in rheumatoid arthritis. *Mol. Med. Rep.* (2015). doi:10.3892/mmr.2015.4011
  326. Endres, K. *et al.* Increased CSF APPs-a levels in patients with Alzheimer disease treated with acitretin. *Neurology* (2014). doi:10.1212/WNL.0000000000001017
  327. Suh, J. *et al.* ADAM10 Missense Mutations Potentiate  $\beta$ -Amyloid Accumulation by Impairing Prodomain Chaperone Function. *Neuron* (2013). doi:10.1016/j.neuron.2013.08.035
  328. Caille, I. Soluble form of amyloid precursor protein regulates proliferation of progenitors in the adult subventricular zone. *Development* (2004). doi:10.1242/dev.01103
  329. Ables, J. L. *et al.* Notch1 Is Required for Maintenance of the Reservoir of Adult Hippocampal Stem Cells. *J. Neurosci.* (2010). doi:10.1523/jneurosci.4721-09.2010
  330. Um, J. W. *et al.* Alzheimer amyloid beta oligomer bound to postsynaptic prion protein activates Fyn to impair neurons. *Nat. Neurosci.* (2012). doi:10.1038/nn.3178

# Acknowledgements



*This thesis has been made possible by the work and support of many people. I would like to thank all of you -each in their own way- for making this an unforgettable period for me!*

*I would like to start by thanking my promotor and supervisor Monica for all the professional and personal advice you gave me. Upon my arrival I felt a very warm welcome, and I was included into your Italian "Di Luca lab" family. This feeling was maintained over the years I spend in here and this will always stay with me. Thank you for listening to my work, giving me critical advice and thereby making me grow as a scientist, but also as a person. I am very thankful and proud to have been able to do my PhD under your supervision*

*Then, I would like to thank my co-promotor and supervisor Elena. Thanks for always being around and making the time to listen to my day-to-day "lab struggles", and of course always giving me the proper advice to survive. You made me feel at ease and welcome at all times, and partly because of you, I was able to grow as a person and as a scientist. You gave me the opportunity to handle multiple projects at the same time, which helped me with the planning and organization of my work, to be able to handle everything at the same time. Without your supervision I would have been nowhere, so your presence has been priceless to me. Thanks for including me in the "blonde CAP2 team"!*

*Then a very special thanks to my colleague, and luckily now I can say close friend Silvia! The little Calimero that made me feel included and was always there for me when I was having a hard time. Thanks for always listening and advising me on "how to survive in Italy", but also in how to proceed in my project. I am more than grateful for your presence and to be part of the "blonde CAP2 team" together with you. I couldn't have wished for a better person around! We survived because of each other's existence and I saw us growing together. I wish you all the best in your future path and I'm sure you'll be able to follow your dreams and I hope to stay in touch with you forever.*

*Another special thanks to two of my colleagues that became close friends during these years, Nic and Luca! Because you were around in the lab, I felt at ease and could always come to you to share my difficulties. Thanks for all the Sbagliato's we shared after work and the bitching around, which always ended up in fun evenings and bursting into tears laughs we had. Luckily, we could share our PhD adventures that we could share together including the trips to Gargnano and Chiesa in Valmalenco, which will be part of my memories forever. Good luck finishing your PhD's and the path that will follow after.*

*I would like to thank Ana and Seb, which I shared the Italian experience with together. At least we had each other to understand some of the Italian culture and language barrier. Good luck in the future!*

*Then I would like to thank all the other members of the "Di Luca lab", Fabrizio, Elisa, Annalisa, Francesca, Elena Jr., Laura, Manuela and Luana. Thanks for always trying to make the effort to switch to English when I was around. You were always there for advice and helping me during crazy busy days by offering a hand. Fabrizio, I would like to thank you for your advice along the way, to give more structure to my work. Elisa, Zianni thanks for your technical support and extra hands if it was necessary, and the laughs we shared. Annalisa, thanks for the technical help you gave me. Francesca, thanks for the fun in the lab and the "white elephant" evening you organized, good luck in San Francisco. Elena jr. and Laura, good luck with your pathways in the lab. Manuela, thanks for the tips and tricks you taught me and your critical view. Good luck in the future! Luana, thanks for always making our lives easier and helping out. In addition, a special thanks to my students Camilla, Silvia and Alessia for their hard work and helping me with my project, and Marta for all the good times in the lab.*

*Grazie milleeeee tutti!*

*Another very special thanks to my schatje Alberto. Although we are not living in the same country, it always felt like you were close to me. You were always there listening to my struggles and made me see the light at the end of the tunnel. Because of you I*

*was always able to put everything in perspective. I'm grateful we've met along our PhD journey and thanks for putting a smile on my face every day!*

*Een hele grote dank gaat uit naar mijn familie. Lieve Leo, Ines en Judie, het was niet altijd makkelijk voor mij om zo ver weg te zijn van de vertrouwde thuishaven in Amsterdam, maar ondanks dit hebben jullie mij altijd gesteund in mijn beslissingen. Alle keren facetimen en de maandelijkse tripjes hebben ervoor gezorgd dat we elkaar gelukkig vaak hebben kunnen zien. Bedankt voor alle steun en lieve woorden voor als ik er doorheen zat. Jullie zijn heel erg belangrijk voor mij en wil graag dat jullie dat nooit vergeten!*

*Dan wil ik natuurlijk ook al mijn fantastische vriendinnetjes bedanken! Wat een fijn idee en gevoel om nu te weten dat afstand geen limiet is in vriendschap. Een waardevolle ervaring die ik voor altijd koester. Bedankt voor jullie steun en alle tripjes die jullie hebben gemaakt naar Milaan om mij op te zoeken. Gelukkig hebben jullie mijn "la vita bella" in Italië ook een klein beetje kunnen proeven, en de Spritz blijft er vanaf nu altijd in! Lieve kippies, bedankt voor het vertrouwen dat jullie in mij hebben en de fantastische bezoeken die jullie mij hebben gebracht. Stuk voor stuk zijn jullie heel belangrijk voor mij, en ben trots op wat iedereen deze jaren heeft bereikt! Ondanks de afstand is er zo'n sterke band ontstaan die alleen maar verder is gegroeid. Lieve gouden jaren van Aquilae, zo fijn om jullie in mijn leven te hebben. Alle adviezen en diepe gesprekken die we met elkaar delen zijn me erg dierbaar. Iedereen heeft zo'n eigen persoonlijkheid en kijk op het leven, wat mij heeft geleerd om overal met een open blik naar te kijken en kritisch te zijn. Bedankt voor mijn studievrienden waarmee ik samen aan de Neuroscience weg begonnen ben. Iedereen heeft zijn eigen pad bewandeld, en we zijn beland in verschillende landen en vakgebieden. Ben trots op wat iedereen heeft bereikt!*

*Then last but not least, thanks for the people I've been able to call friends after I've met them along my Milan experience. In het bijzonder Anahita, omdat we samen in hetzelfde schuitje zaten en er mede dankzij elkaar samen doorheen zijn gekomen. Ik*

*ben blij dat wij elkaar hebben ontmoet en dat we zoveel leuke momenten gedeeld hebben. Hoop dat we elkaar in de toekomst zullen blijven tegenkomen! Then, Megan, Alisa and Alex, three girls that I can truly say, became very special and close to me and were invaluable for my experience here. All the fun moments we shared, discovering together the cultural differences and growing to understand how things work differently over here. Thanks for all the happy moments we had!*

*To end, the SyDAD program, which gave me so many great opportunities to explore the Alzheimer field together with the great people that were part of this program. All the important and great people that were part of this program, and the experiences I had because of this, made me grow as a scientist.*



# Research Activity

- **Attended Conference without abstract:**

- Alzheimer's disease/Parkinson's disease conference, March 2017, Vienna, Austria

- **Attended Conferences with poster/abstract:**

- **European Synapse Meeting, December 2017, Milan, Italy**

**Title:** Linking actin-dependent dendritic spine remodeling and ADAM10 activity in Alzheimer's Disease: the role of CAP2

L. Vandermeulen, S. Pelucchi, M. Rust, M. DiLuca, E. Marcello

- **Federation of European Neuroscience conference, July 2018, Berlin, Germany**

**Title:** Linking actin-dependent dendritic spine remodeling and ADAM10 activity in Alzheimer's Disease: the role of CAP2

L. Vandermeulen, S. Pelucchi, M. Rust, S. Frykman, M. DiLuca, E. Marcello

- **Society for Neuroscience, November 2018, San Diego, USA**

**Title:** Linking actin-dependent dendritic spine remodeling and ADAM10 activity in Alzheimer's Disease: the role of CAP2

L. Vandermeulen, S. Pelucchi, M. Rust, S. Frykman, M. Di Luca, E. Marcello

- **Oral presentations:**

- PhD spring school, April 2017, Gargnano Italy

- Annual meeting SyDAD (Marie Curie PhD project), May 2017, Bonn, Germany

- PhD spring school, April 2018, Chiesa in Valmalenco, Italy

- Annual meeting SyDAD (Marie Curie PhD project), May 2018, Milan, Italy

- Next step, June 2018, Milan, Italy

- Annual meeting SyDAD (Marie Curie PhD project), March 2019, Bordeaux, France

- **Period abroad:**

- PhD Secondment at Karolinska Institute, September - December 2017, Stockholm, Sweden

- **Publications:**

- "Amyloid- $\beta$  oligomers regulate ADAM10 synaptic localization through aberrant plasticity phenomena" E. Marcello, S. Musardo, **L. Vandermeulen**, S. Pelucchi, F. Gardoni, N. Santo, F. Antonucci, M. Di Luca (Molecular Neurobiology April 2019, PMID: 30989630 DOI: 10.1007/s12035-019-1583-5)

- "Similar pre- and postsynaptic distribution of ADAM10 and BACE1 in rat and human adult brain" J. Lundgren, L. Vandermeulen, A. Sandebring-Matton, S. Ahmed, B. Winblad, M. Di Luca, L. Tjernberg, E. Marcello, S. Frykman (Manuscript in revision, Neurochemical Research) 2019

- "CAP2 dimer as a novel regulator of cofilin in spines" S. Pelucchi, L. Vandermeulen, F. Antonucci, D. Mauceri, E. Marcello, M. Di Luca (Manuscript in preparation)

- "CAP2 links ADAM10 activity to the actin-mediated synaptic dysfunction in Alzheimer's disease" L. Vandermeulen, S. Pelucchi, M. Rust, S. Frykman, E. Marcello, M. Di Luca (Manuscript in preparation)

- "PCSK9, a novel protein involved in hippocampal related cognitive function" L. Vandermeulen, L. Da Dalt, S. Musardo, G. Norata, E. Marcello, M. Di Luca (Manuscript in preparation)

- **Attended courses:**

- Innovation Workshops, Serendipity Innovations and Axon Neuroscience, Karolinska Institute, April 23th, 2016
- Alzheimer Disease Course, Karolinska Institute, April 25-29th 2016
- Neuropsychopharmacology course, Milan, 6-10 June 2016
- Innovative techniques in pharmacology research, Milan, 20-24 June 2016
- Transversal competence course A; Open access, Milan, September 26th 2016
- Transversal competence course B; Evaluation of research, Milan, October 3th 2016
- Alzheimer Methodology course, Bordeaux, January 18-26th, 2017
- Drug Discovery Course, Axon Neuroscience, Bratislava, March 26-28th 2017
- Molecular Biology course, Milan, June-July 2017
- Stem cells in experimental and clinical pharmacology, Milan, June-July 2017
- Animal welfare, Milan, June 2018
- Molecular Pharmacology and Applied statistics, Milan, June 2018
- Nutraceutica, Milan, July 2018

- **Other activities:**

- Supervisor of 2 master students and 1 bachelor student during their experimental master thesis project
- Supervisor of 2 master students during their literature master thesis project
- Instructor during a 7 day-course of advanced methods for preclinical Alzheimer research (Bordeaux, France)
- Instructor during multiple didactical laboratory classes in the course "cellular and molecular pharmacology" for Chemistry and Pharmaceutical Technology master students
- Outreach activity: - Controlling website SyDAD

- Help in organizing "Next step" meeting, DiSFeB
- Help in preparation "meet me tonight", European researcher night
- Article on the ricercamix website of DiSFeB